

DOKUZ EYLÜL UNIVERSITY
GRADUATE SCHOOL OF NATURAL AND APPLIED SCIENCES

**MULTIVARIATE STATISTICAL PROCESS
CONTROL AND MONITORING WITH CHANGE
POINT ANALYSIS**

by
Eralp DOĞU

October, 2011
İZMİR

**MULTIVARIATE STATISTICAL PROCESS
CONTROL AND MONITORING WITH CHANGE
POINT ANALYSIS**

**A Thesis Submitted to the
Graduate School of Natural and Applied Sciences of Dokuz Eylül University
In Partial Fulfilment of the Requirements for the Degree of Doctor of
Philosophy in Statistics Program**

**by
Eralp DOĞU**

**October, 2011
İZMİR**

Ph.D. THESIS EXAMINATION RESULT FORM

We have read the thesis entitled “**MULTIVARIATE STATISTICAL PROCESS CONTROL AND MONITORING WITH CHANGE POINT ANALYSIS**” completed by **ERALP DOĞU** under supervision of **DR. İPEK DEVECİ-KOCAKOÇ** and we certify that in our opinion it is fully adequate, in scope and in quality, as a thesis for the degree of Doctor of Philosophy.

Assoc. Prof. Dr. İpek DEVECİ-KOCAKOÇ
.....

Supervisor

Assist. Prof. Dr. Ali Rıza FİRUZAN
.....

Assoc. Prof. Dr. Cenk ÖZLER
.....

Thesis Committee Member

Thesis Committee Member

.....

Examining Committee Member

.....

Examining Committee Member

Prof. Dr. Mustafa SABUNCU
Director
Graduate School of Natural and Applied Sciences

ACKNOWLEDGEMENTS

I owe appreciation to many people for their help and support which made this work possible and existing.

Professionally, there are people I respect and would like to express my deepest appreciation for their support and guidance. Firstly, I would like to thank my advisor Dr. İpek Deveci-Kocakoç. She was just right there for me when I needed. Her encouragement, mentoring and instructions helped me a lot to finalize this work. Furthermore, I would like to thank my committee members Dr. Cenk Özler and Dr. Ali Rıza Firuzan for their support and feedbacks throughout the research process. Lastly, I will always be grateful to Dr. Harriet B. Nembhard for her support and feedback about the general flow of this work. I also really appreciate the financial support of the Scientific and Technological Research Council of Turkey (TUBITAK) during my research.

Personally, I wish to give a very special thanks to my wife Zeynep for her ongoing morale, patience, support and encouragement. We traveled together from the very beginning to the end of this journey. I am grateful to my beloved daughter Ela Ceren for the luck and cheer she brought to my life. Special thanks to my family for their constant support and understanding.

Eralp DOGU

MULTIVARIATE STATISTICAL PROCESS CONTROL AND MONITORING WITH CHANGE POINT ANALYSIS

ABSTRACT

Multivariate statistical process control (MSPC) efforts are widely used in order to detect changes in processes where more than one inter-related quality characteristic is considered. The existing monitoring methods like Hotelling's T^2 control chart are capable of generating signals to show the existence of the change. However, this certain signal does not always mean that the change occurred at that particular time. Because of this obstacle, the process professionals need to look for a special cause after a signal and for many cases it is quite difficult to identify the time of a change with only this information.

Change point methods help Statistical Process Control (SPC) practitioners to identify the time of a change after a control chart generates a signal. Using change point estimation with the monitoring tool surely improves the special cause detection ability of the monitoring system.

In this study, change point procedures for multivariate processes are proposed. Firstly, the change point model for monitoring covariance matrices is discussed. The simulation results showed that this model accurately and precisely estimated the change point after a generalize variance control chart issued a signal. Secondly, a change point procedure for simultaneously monitoring the mean vector and covariance matrix is proposed. This procedure is shown to be successful to find the change point for multivariate joint estimation of a step change. The research also includes a comparative study for multivariate single control charts via change point estimation performance.

Keywords: Change Point Estimation, Multivariate Statistical Process Control (MSPC), Generalized Variance Control Chart, Multivariate Combination Control Chart, Multivariate Single Control Charts.

DEĞİŞİM NOKTASI ANALİZİ İLE ÇOK DEĞİŞKENLİ İSTATİSTİKSEL SÜREÇ KONTROLÜ VE İZLENMESİ

ÖZ

Birden fazla kalite karakteristiğinin birlikte incelenmesinin gerektiği durumlarda çok değişkenli istatistiksel süreç kontrol çalışmaları yaygın olarak yapılmaktadır. Hotelling's T^2 kontrol kartı gibi mevcut metotlar bir değişimin ortaya çıktığını ürettikleri sinyal ile gösterebilirler. Ancak bu sinyal her zaman değişimin sinyalin üretildiği zamanda ortaya çıktığını göstermez. Bu zorluktan dolayı süreç uzmanları sinyalden sonra özel nedenin ortaya çıktığı zamanı araştırmak zorundadır. Bu bilgi ile değişimin zamanını tespit etmek çoğu durum için oldukça zordur.

Değişim noktası metotları İstatistiksel Süreç Kontrolü (İSK) uygulayıcılarına kontrol kartı sinyal verdikten sonra değişimin zamanını belirlemede yardımcı olurlar. Değişim noktası tahmini yardımıyla yapılan izleme faaliyeti, şüphesiz izleme sisteminin özel neden tespit etme yeteneğini artırır.

Bu çalışmada, çok değişkenli süreçler için değişim noktası yöntemleri önerilmektedir. İlk olarak, kovaryans matrisinin izlenmesinde kullanılan bir değişim noktası metodu tartışılmıştır. Simülasyon sonuçları önerilen yöntemin genelleştirilmiş varyans kontrol kartı sinyal verdikten sonra doğrulukla ve kesinlikle tahmin yapabildiğini göstermiştir. İkinci olarak, ortalama vektörü ve kovaryans matrisinin eşanlı izlenmesini sağlayacak bir değişim noktası prosedürü önerilmiştir. Bu prosedürün bileşik değişim noktası tahmininin başarı ile gerçekleştirdiği gösterilmiştir. Bu araştırmada ayrıca çok değişkenli tek kontrol kartları için değişim noktası tahmin performansları bakımından bir karşılaştırmalı çalışma da bulunmaktadır.

Anahtar Kelimeler: Değişim Noktası Tahmini, Çok Değişkenli İstatistiksel Süreç Kontrolü (ÇDİSK), Genelleştirilmiş Varyans Kontrol Kartı, Çok Değişkenli Kombinasyon Kontrol Kartı, Çok Değişkenli Tek Kontrol Kartları.

CONTENTS

	Page
THESIS EXAMINATION RESULT FORM.....	ii
ACKNOWLEDGMENTS	iii
ABSTRACT	iv
ÖZ.....	v
CHAPTER ONE-INTRODUCTION.....	1
1.1 Introduction	1
1.2 Multivariate Statistical Process Control	2
1.3 $\chi^2 - S $ Control Charts	4
1.4 Change Point Model for SPC	7
1.5 Change Point Estimation for χ^2 Control Chart.....	10
1.5.1 Illustrative Example.....	12
1.6 Objective of the Dissertation	14
CHAPTER TWO – ESTIMATION OF CHANGE POINT IN GENERALIZED VARIANCE CONTROL CHART	17
2.1 Introduction	17
2.2 Process Model Assumption	21
2.3 Estimation of the Change Point.....	22
2.4 Performance Evaluation of the Proposed Estimator.....	24
2.4.1 Accuracy Evaluation	26

2.4.2 Precision Evaluation	32
2.5 Illustrative example	39
2.6 Conclusions	41

CHAPTER THREE- A MULTIVARIATE CHANGE POINT PROCEDURE FOR MONITORING MEAN AND COVARIANCE SIMULTANEOUSLY ... 43

3.1 Introduction	43
3.2 Process Model Assumptions.....	46
3.3 Estimation of the Change Point.....	46
3.4 Performance Assessment of the Proposed Estimator	49
3.4.1 Accuracy Evaluation	50
3.4.2 Precision Evaluation.....	53
3.4.3 Comparison with Other Change Point Estimators.....	60
3.4.4 Confidence Sets Based on the Change Likelihood Function	64
3.5 Illustrative Example.....	69
3.6 Conclusions	71

CHAPTER FOUR – CHANGE POINT ESTIMATION FOR MULTIVARIATE SINGLE CONTROL CHARTS 73

4.1 Introduction	73
4.2 Maximum Multivariate Exponentially Weighted Moving Average (MAX-MEWMA) and Multivariate Exponentially Weighted Likelihood Ratio Charts (MELR)	76
4.3 Multivariate Joint Change Point Estimation for Single Control Charts	78
4.4 Performance Assessment.....	79

4.4.1 Accuracy Evaluation.....	81
4.4.2 Precision Evaluation.....	85
4.4.3 Confidence Sets Based on the Change Likelihood Function	90
4.4.2 Comparison with Generalized Likelihood Ratio Test Based Change	
Point Estimator	93
4.5 Illustrative Example.....	97
4.6 Conclusions	101
CHAPTER FIVE – CONCLUSIONS.....	104
REFERENCES	110

LIST OF TABLES

1. Subgroup averages, reverse cumulative averages, M_i and χ^2 statistics.....	13
2. Average of the change point estimates and their standard errors when quality characteristics increase from σ_x to $\delta_1 \times \sigma_x$ and σ_y to $\delta_2 \times \sigma_y$ ($\delta_1 = \delta_2 = \delta > 1$).....	29
3. Average of the change point estimates and their standard errors when quality characteristics decrease from σ_x to $\delta_1 \times \sigma_x$ and σ_y to $\delta_2 \times \sigma_y$ ($\delta_1 = \delta_2 = \delta < 1$).....	29
4. Average of the change point estimates and their standard errors when one quality characteristic increase from σ_x to $\delta_1 \times \sigma_x$ (or σ_y to $\delta_2 \times \sigma_y$) (δ_1 (or δ_2) = $\delta > 1$).....	30
5. Average of the change point estimates and their standard errors when one quality characteristic decrease from σ_x to $\delta_1 \times \sigma_x$ (or σ_y to $\delta_2 \times \sigma_y$) (δ_1 (or δ_2) = $\delta < 1$).....	30
6. Average of the change point estimates and their standard errors when one of the quality characteristics increases from σ_x to $\delta_1 \times \sigma_x$ ($\delta_1 > 1$) while the other decreases from σ_y to $\delta_2 \times \sigma_y$ b ($\delta_2 < 1$).....	31
7. Empirical distribution of $\hat{\tau}$ around τ when σ_x increases to $\delta_1 \times \sigma_x$ and σ_y increases to $\delta_2 \times \sigma_y$ ($\delta_1 = \delta_2 = \delta > 1$)	34
8. Empirical distribution of $\hat{\tau}$ around τ when σ_x decreases to $\delta_1 \times \sigma_x$ and σ_y decreases to $\delta_2 \times \sigma_y$ ($\delta_1 = \delta_2 = \delta < 1$).....	35
9. Empirical distribution of $\hat{\tau}$ around τ when σ_x increases to $\delta_1 \times \sigma_x$ to (or σ_y increases to $\delta_2 \times \sigma_y$) (δ_1 (or δ_2) = $\delta > 1$).....	36
10. Empirical distribution of $\hat{\tau}$ around τ when σ_x decreases to $\delta_1 \times \sigma_x$ (or σ_y decreases to $\delta_2 \times \sigma_y$) (δ_1 (or δ_2) = $\delta < 1$).....	37

11. Empirical distribution of $\hat{\tau}$ around τ when σ_x increases to $\delta_1 \times \sigma_x$ ($\delta_1 > 1$) while σ_y decreases to $\delta_2 \times \sigma_y$ ($\delta_2 < 1$).....	38
12. Subgroup average vectors, generalized variances and C statistics.....	40
13. Expected time of a signal, average change point estimates and their standard errors after a combination chart signals; $\tau = 50$, $\rho = 0.0$ and 10,000 independent simulation runs	51
14. Expected time of a signal, average change point estimates and their standard errors after a combination chart signals; $\tau = 50$, $\rho = 0.5$ and 10,000 independent simulation runs	52
15. Expected time of a signal, average change point estimates and their standard errors after a combination chart signals; $\tau = 50$, $\rho = 0.9$ and 10,000 independent simulation runs	52
16. Empirical distribution of $\hat{\tau}$ around τ after a combination chart signals; $\tau = 50$, $\rho = 0.0$ and 10,000 independent simulation runs	56
17. Empirical distribution of $\hat{\tau}$ around τ after a combination chart signals; $\tau = 50$, $\rho = 0.5$ and 10,000 independent simulation runs	57
18. Empirical distribution of $\hat{\tau}$ around τ after a combination chart signals; $\tau = 50$, $\rho = 0.9$ and 10,000 independent simulation runs	58
19. Exact detection probabilities of the change point estimator and the combination chart; $\tau = 50$ and 10,000 independent simulation runs	59
20. Expected time of a signal, averages of proposed and combination change point estimates after a combination chart signals; $\tau = 50$, $\rho = 0.5$ and 10,000 independent simulation runs	62
21. Precision evaluation for proposed and combination change point estimates after a combination chart signals; $\tau = 50$, $\rho = 0.5$ and 10,000 independent simulation runs	63
22. Average cardinality and coverage probability values obtained using different critical values (D) after a combination chart signal; $\tau = 50$ and 10,000 independent simulation runs	67

23. Average cardinality and coverage probability values various change points; $\tau = 50$ and 10,000 independent simulation runs	68
24. Spring data, chi-squares, generalized variances, M_t , C_t and MC_t statistics.....	70
25. Expected time of a signal, average change point estimates and their standard errors after $\chi^2 - \mathbf{S} $, Max-MEWMA and MELR control charts signal; $\tau = 50$, $\rho_1 = 0.0$ and 10,000 independent simulation runs.....	82
26. Expected time of a signal, average change point estimates and their standard errors after $\chi^2 - \mathbf{S} $, Max-MEWMA and MELR control charts signal; $\tau = 50$, $\rho_1 = 0.5$ and 10,000 independent simulation runs.....	83
27. Expected time of a signal, average change point estimates and their standard errors after $\chi^2 - \mathbf{S} $, Max-MEWMA and MELR control charts signal; $\tau = 50$, $\rho_1 = 0.9$ and 10,000 independent simulation runs.....	84
28. Empirical distribution of $\hat{\tau}$ around τ after $\chi^2 - \mathbf{S} $, Max-MEWMA and MELR control charts signal; $\tau = 50$, $\rho_1 = 0.0$ and 10,000 independent simulation runs.....	87
29. Empirical distribution of $\hat{\tau}$ around τ after $\chi^2 - \mathbf{S} $, Max-MEWMA and MELR control charts signal; $\tau = 50$, $\rho_1 = 0.5$ and 10,000 independent simulation runs.....	88
30. Empirical distribution of $\hat{\tau}$ around τ after $\chi^2 - \mathbf{S} $, Max-MEWMA and MELR control charts signal; $\tau = 50$, $\rho_1 = 0.9$ and 10,000 independent simulation runs.....	89
31. Average cardinality and coverage probability values obtained using different critical Values (D) after $\chi^2 - \mathbf{S} $, Max-MEWMA and MELR control charts signal; $\tau = 50$, mean shift setting 3 and 4 and 10,000 independent simulation runs.....	92
32. Average Cardinality and Coverage Probability Values Obtained Using Different Critical Values (D) after $\chi^2 - \mathbf{S} $, Max-MEWMA and MELR	

control charts signal; $\tau = 50$, mean shift setting 5 and 6 and 10,000 independent simulation runs.....	93
33. Expected time of a signal, average change point estimates for MLE and GLR and their standard errors after MELR control charts signal; $\tau = 50$, $\rho_1 = 0.0$ and 0.5, 10,000 independent simulation runs.....	95
34. Empirical distributions of $\bar{\tau}_{MC}$ and $\bar{\tau}_{GLR}$ around τ after MELR chart signals; $\tau = 50$, $\rho_1 = 0.0$ and 0.5, 10,000 independent simulation runs.....	97

LIST OF FIGURES

1. Univariate control charts for bivariate standard normal process readings.....	5
2. Scatter plot for bivariate standard normal process readings.....	6
3. Multivariate control charts for bivariate standard normal process readings.....	7
4. A control chart with a step change in the mean; the signal issued at 70 th process reading while the change was introduced after 50 th process reading.....	8
5. Plot of change point likelihoods and χ^2 control chart for steel sleeve example.....	14
6. Plots of precision measures versus various mean-dispersion shift settings when $ \hat{\tau} - \tau \leq 5$; $\tau = 50$, $\rho = 0.0, 0.5$ and 0.9 and 10,000 independent simulation runs.....	54
7. Plots of exact detection probabilities for change point estimator and combination chart versus various mean-dispersion shift settings; $\tau = 50$, $\rho = 0.0, 0.5$ and 0.9 and 10,000 independent simulation runs.....	55
8. Plots of $E(T)$, $\bar{\tau}_{MC}$ and $\bar{\tau}_{Comb}$ versus various mean-dispersion shift settings; $\tau = 50$, $\rho = 0.5$ and 10,000 independent simulation runs.....	61
9. Plot of coverage probabilities versus estimated cardinality of confidence sets for various magnitudes of shift following a signal from a combination chart using different critical values of D; $\tau = 50$ and 10,000 independent simulation runs.....	65
10. Plots of coverage probabilities and average cardinalities versus various change points; $\tau = 50$ and 10,000 independent simulation runs.....	66
11. Plot of likelihood values at possible change points and the threshold for spring data.....	71
12. $\chi^2 - \mathbf{S} $ combination charts for the illustrative example.....	98

13. The Max-MEWMA control chart, mean shift and covariance shift monitoring statistics for the illustrative example.....	99
14. The MELR control chart, mean shift and covariance shift monitoring statistics for the illustrative example.....	100
15. Plots of likelihood values at possible change points $\chi^2 - \mathbf{S} $ combination chart, the Max- MEWMA and the MELR control charts.....	101
16. Plots of coverage probabilities and average cardinalities versus various references (D) for mean shift setting $\lambda = (0.25, 0.5)$; $\tau = 50$, $\rho = 0.5$ and 10,000 independent simulation runs.....	106
17. Plots of coverage probabilities and average cardinalities versus various references (D) for mean shift setting $\lambda = (1, 1)$; $\tau = 50$, $\rho = 0.5$ and 10,000 independent simulation runs.....	106

CHAPTER ONE

INTRODUCTION

1.1 Introduction

Statistical Process Control (SPC) as a sub-area of Statistical Quality Control has been an essential tool in industry and service for quality improvement. Understanding the causes of variation is in great importance for these efforts. Generally, the causes of variation are classified into two classes: common causes and assignable (or special) causes. The common causes are considered to stem from inherent nature of the process and they are hard to eliminate without changing the process itself. The other class is the assignable causes of variation and they interfere to the process. They are easy to detect respectively and should be eliminated.

Control charts which were first developed by Shewhart is widely used in order to detect the causes of variability. Since their development, this tool set has been a principle statistical tool in industry and service. A control chart basically checks the measures and tries to detect whether the underlying probability distribution remains constant over time. This stable situation is defined as 'in-control' situation. If there is some change in the probability distribution, then this situation is defined as 'out-of-control'. The effectiveness of the control charts also attracts practitioners by its visual representation. Figure 1.1 and 1.3 shows examples of control charts. The checks for each time slot are recorded on a graph and this series is compared with a threshold to define the in-control situation. The threshold is considered to be a specific value which is achieved by a significance level.

The estimation of the parameters is a major concern of SPC. If the parameters are unknown, then in order to estimate them a calibration exercise is performed and this is called a Phase I study. The aim of Phase I is to check if a process has been in-control with a set of historical readings. After this calibration step, the samples are

taken sequentially and used to detect departures from in-control parameters and this is called a Phase II study. Woodall (2000) concluded that much effort; process knowledge and process improvement is needed for a transition from Phase I to Phase II.

1.2 Multivariate Statistical Process Control

The increasing practice of SPC in industry creates demand to use more effective methods that are able to detect changes of quality level quickly. The literature is rich in univariate checks of the processes to ensure the parameters are in-control. However, many processes are capable of producing multiple process readings. Therefore, there are many situations in which simultaneous monitoring of two or more inter-related quality characteristics. Following examples of multiple process reading cases are provided by Hawkins and Olwell (1998) as follows:

- Measuring different properties on each unit produced: In manufacturing roller bearings the process professional may measure the length, maximum diameter, and minimum diameter of each sampled bearings.
- Measuring a number of different but connected processes: The measurements can be made on the different processes but connected processes. For instance, in semiconductor wafer fabrication, chips go through sequences of processing steps. The quality of a chip depends on the current process step and the outcomes of all previous process steps. Thus the causes of poor quality may stem from the current process step and also the problems created previously.
- Measuring a number of different processes some of which cannot be controlled: For instance, in a coal washing plant, the yield and ash content of the washed coal are important quality characteristics of the washing process. These characteristics are highly connected to the quality of raw coal entered to the plant. The causes of variability are likely to occur by the internal and external processes.

The multivariate approach deals with a vector of different but possibly correlated process readings rather than a single process reading at each time point. Montgomery (2009) presented two ways of managing this situation. The first way is ignoring the correlation and treating the measurements as separate univariate quality characteristics. If we use this setting as a monitoring tool for related quality metrics, the ignorance of correlation may yield to a point which is in-control for each univariate control chart and out-of-control when the variables are monitored simultaneously. Moreover, the Type I error and probability of a point correctly plotting in control are not equal to their specified levels. For example, in bivariate case the Type I error for each control chart is α and the Type I error of using separate control chart for multivariate readings is $1-(1-\alpha)^2$ which is not equal to α .

The other way of dealing with multivariate process readings is thinking about the collection of measures as a multivariate measure and control this measures with multivariate methods. A major benefit is that the monitoring may be much more sensitive compared to the first approach. Another benefit may be the increased diagnostic aids. Hawkins and Olwell (1998) gave an example to explain this benefit. If we do not monitor the incoming coal quality then an increase in the ash content of the washed coal could be attributed to the problems of washing while in fact, the reason may be the incoming coal quality.

In our study we will assume that the process readings follow a p -variate multivariate normal distribution. \mathbf{X}_{ij} is a $p \times 1$ vector which represents the p -component on the j^{th} observation in the i^{th} sample of size n . The multivariate normal distribution can be described as the vectors \mathbf{X}_{ij} follow a common multivariate normal distribution with some mean vector $\boldsymbol{\mu}_0$ and some covariance matrix $\boldsymbol{\Sigma}_0$. This can be abbreviated to $\mathbf{X}_{ij} \sim N_p(\boldsymbol{\mu}_0, \boldsymbol{\Sigma}_0)$. The covariance matrix represents the relationship between the measures and if the off-diagonal elements are different from zero, then the practitioner would have maximum benefit from thinking a multivariate approach.

1.3 $\chi^2 - |\mathbf{S}|$ Control Charts

In the MSPC literature, there are several multivariate control charts proposed. The most popular among them is the T^2 control chart proposed by Hotelling(1947). It is considered as the multivariate analog of the univariate \bar{X} chart.

Consider p -variate vector $\mathbf{X}_{ij} \sim N_p(\boldsymbol{\mu}_0, \boldsymbol{\Sigma}_0)$. If we want to test the following hypothesis; $H_0 : \boldsymbol{\mu} = \boldsymbol{\mu}_0$, $H_1 : \boldsymbol{\mu} \neq \boldsymbol{\mu}_0$ then the most powerful test statistic is $T_i^2 = n(\bar{\mathbf{X}}_i - \boldsymbol{\mu}_0)' \boldsymbol{\Sigma}_0^{-1} (\bar{\mathbf{X}}_i - \boldsymbol{\mu}_0)$ where n is the sample size and $\bar{\mathbf{X}}_i$ is the sample mean vector for the i^{th} process readings. When the process parameters are known or can be estimated, this chart plots $n(\bar{\mathbf{X}}_i - \boldsymbol{\mu}_0)' \boldsymbol{\Sigma}_0^{-1} (\bar{\mathbf{X}}_i - \boldsymbol{\mu}_0)$; where $\mathbf{X}_{ij} \sim N_p(\boldsymbol{\mu}_0, \boldsymbol{\Sigma}_0)$, $j=1, 2, \dots, n$. If a point falls beyond the upper control limit $UCL = \chi_{p,1-\alpha}^2$, the process is considered to be out of control. This control chart is also called Phase II X^2 chart or χ^2 chart (Bersimis et al., 2007).

As monitoring only the mean vector is not an effective way of controlling the process, many authors focused on developing the methods to monitor dispersion. Alt (1985) and Alt and Smith (1988) proposed different procedures of carrying out multivariate dispersion control and monitoring. They proposed the multivariate analogue of the univariate S -chart and named it as generalized variance ($|\mathbf{S}|$) control chart. $|\mathbf{S}_i|^{1/2}$ values are plotted when the control limits are:

$$\begin{aligned} UCL &= |\boldsymbol{\Sigma}_0| (\chi_{2n-4, \alpha/2}^2)^2 / [4(n-1)^2], \\ LCL &= |\boldsymbol{\Sigma}_0| (\chi_{2n-4, 1-(\alpha/2)}^2)^2 / [4(n-1)^2] \end{aligned} \quad (1.1)$$

where \mathbf{S}_i is a $p \times p$ matrix,

$$\mathbf{S}_i = \sum_{j=1}^n (\mathbf{x}_{ij} - \bar{\mathbf{x}}_i) (\mathbf{x}_{ij} - \bar{\mathbf{x}}_i)' / (n-1) \quad (1.2)$$

$$\text{and } \bar{\mathbf{X}}_i = \sum_{j=1}^n \mathbf{X}_{ij} / n. \quad (1.3)$$

When several characteristics of a manufactured component are to be monitored simultaneously, multivariate Shewhart-type χ^2 and $|\mathbf{S}|$ control charts can be used. As long as the points plotted on the χ^2 and $|\mathbf{S}|$ control charts fall below the upper control limits (UCL) of the charts, the process is assumed to operate under a stable system of common causes and, hence, in a state of control. When one or more points exceed the UCL, the process is deemed out of control due to one or more special causes and an investigation is carried out to detect these special causes (Nedumaran et al., 2000).

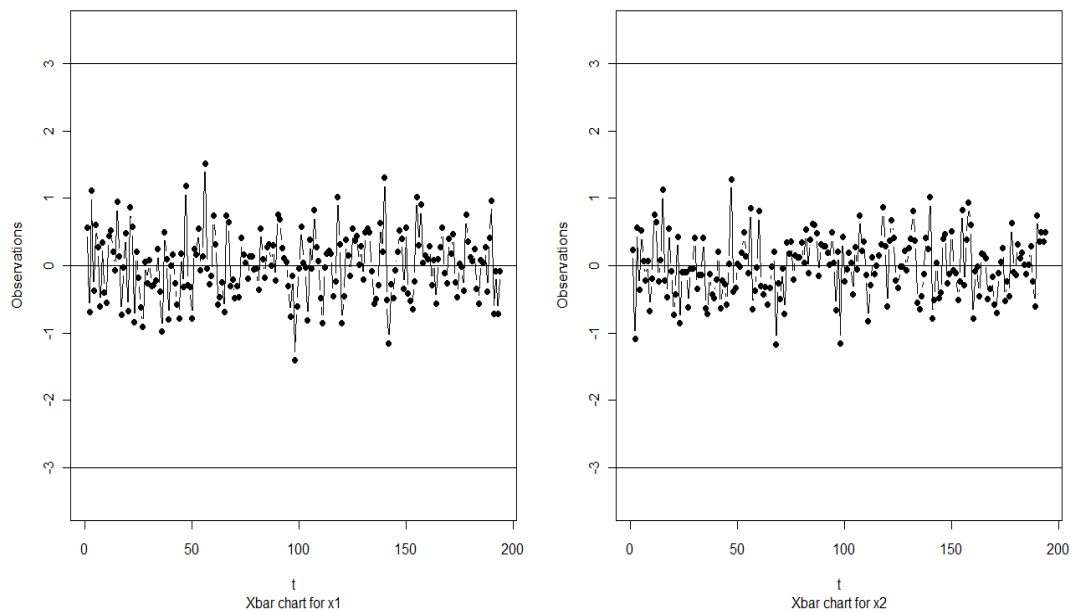


Figure 1.1 Univariate control charts for bivariate standard normal process readings.

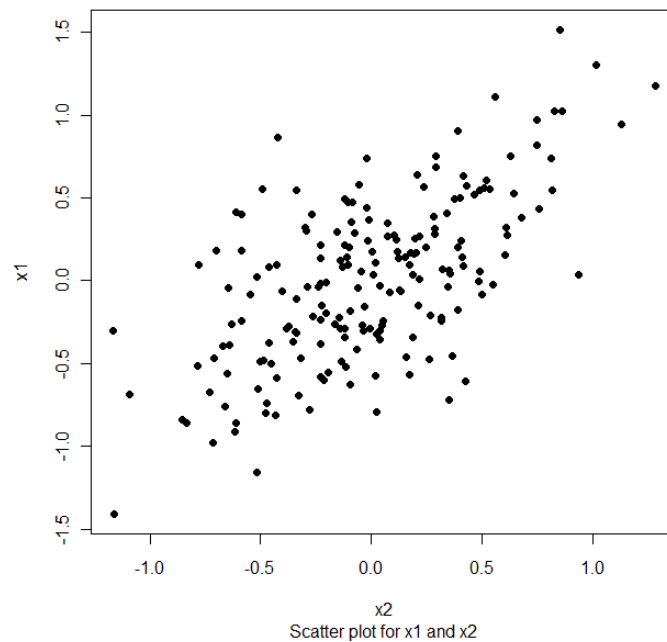


Figure 1.2 Scatter plot for bivariate standard normal process readings.

Figure 1.1 and 1.3 shows the univariate and multivariate control charts for related quality characteristics, respectively. The data was generated from multivariate standard normal distribution with $\rho=0.7$ which can be expressed as a strong positive correlation where ρ is the Pearson correlation coefficient. Figure 1.2 shows this relationship between the quality characteristics. When the control charts set to the same Type I error rate ($\alpha=0.0027$), \bar{X} charts do not generate any signal and look almost perfect. On the other hand, χ^2 chart generates a signal around twentieth observation vector. Moreover, $|S|$ issued another signal at around hundred nineteenth observation vector. These signals are not apparent in Figure 1.1. For discussions and reviews of multivariate mean and dispersion control charts, see, for example, Lowry and Montgomery (1995), Montgomery (2009), Tracy et al. (1997), Hawkins and Olwell (1998), Fuch and Benjamini (1998), Alt (1985), Alt and Smith (1988), Surtihadi et al. (2004), Khoo and Quah (2004), Bersimis et al. (2007) and Vargas and Lagos (2007).

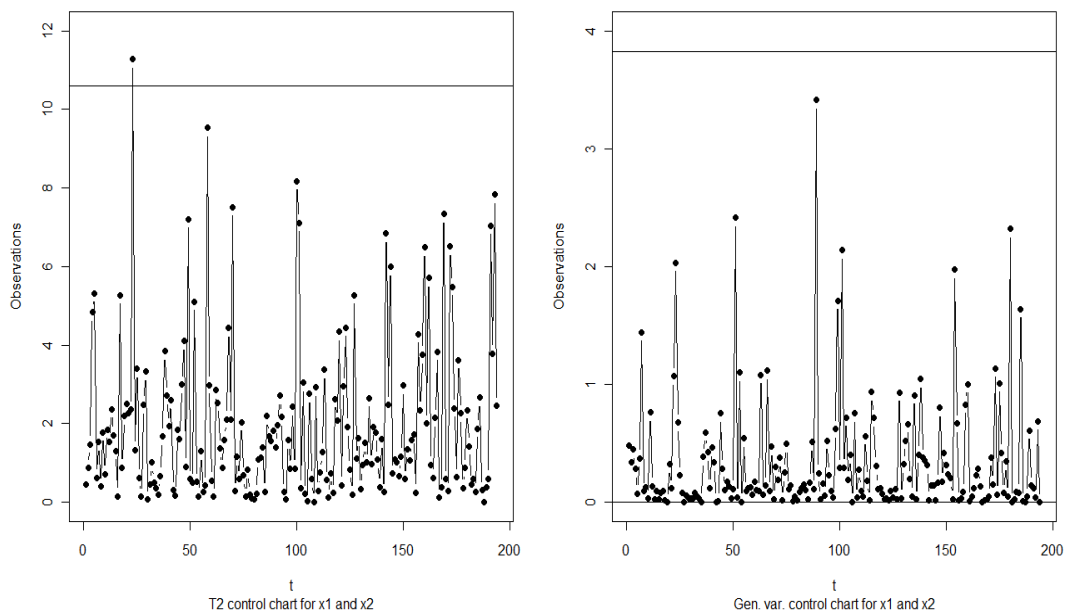


Figure 1.3 Multivariate control charts for bivariate standard normal process readings.

1.4 Change Point Model for SPC

Control charts are widely used tools for detecting changes of a process and identifying special causes. A change in the process distribution leads the control chart to generate an out-of-control signal. The time in which the signal issued is considered as the stopping time and at this point of time process professionals start searching for assignable causes of the change. The signal does not always indicate that a special cause actually occurred at that particular point of time. A typical illustration of a control chart is given in Figure 1.4. The control chart aims to monitor the mean of the process with a step change and the observations are standardized normal readings. Thus, the center line is '0', the upper control limit is '+3' and the lower control limit is '-3'. It is well known that the process has altered to its new level after the 50th observation for this process. The vertical line represents the actual time of this step change. However, the control chart generated its first signal at the 70th observation. The practitioners need some additional run rules in order to identify the time of the change, but this approach may not always provide realistic change point estimation.

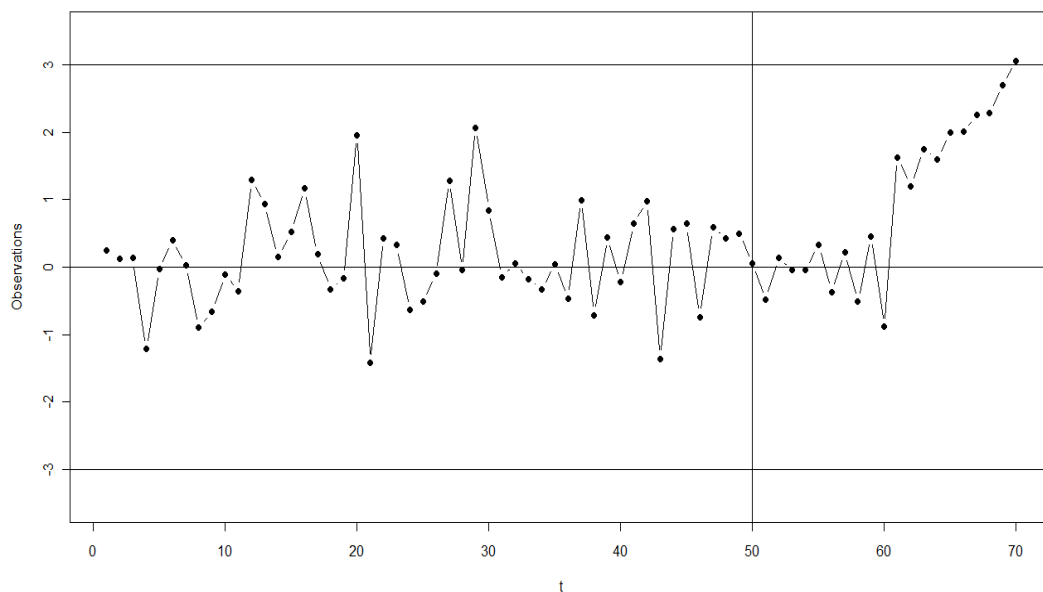


Figure 1.4 A control chart with a step change in the mean; the signal issued at 70th process reading while the change was introduced after 50th process reading.

From the SPC point of view, it is possible to employ change point models to control charts. A change-point model focuses on finding the point in time where the underlying model generating a series of observation has changed in some manner (Montgomery, 2009). In order to summarize the procedure, two distributions are used to model the quality characteristic of a process.

$$x_i \sim f(X, \theta_0), \quad i = 1, 2, \dots, \tau.$$

$$x_i \sim f(X, \theta_1), \quad i = \tau + 1, \dots, T.$$

where x_i is the i^{th} observation of the process and τ at which the process parameter shifts from θ_0 to θ_1 is referred to be the process change-point. The process follows the distribution $f(X, \theta_0)$ up to the change point τ in time and then follows another distribution such as $f(X, \theta_1)$ after the change is occurred.

Many researchers studied the integration of statistical process control and change point applications for various distributions of the quality characteristics. Samuel et

al. (1998a, 1998b) proposed estimators to find the most likely location of the change for normally distributed quality characteristics. They considered step changes in the mean and the variance of a normal distribution, respectively. They compared performances of the estimators with \bar{X} and S control charts, respectively. Samuel and Pignatiello (2001) showed the superiority of the performance of the maximum likelihood estimator (MLE) when compared to the built-in change point estimators of exponentially weighted moving average (EWMA) and cumulative sum (CUSUM) for a normal process mean. Pignatiello and Simpson (2002) proposed a magnitude-robust control chart to monitor a normal process mean and obtained useful change point statistics. Perry and Pignatiello (2006) investigated the linear trend disturbance in the mean for normally distributed quality characteristics. Timmer and Pignatiello (2003) investigated change point estimates for the parameters of an AR(1) process.

Samuel and Pignatiello (1998c) proposed a change-point estimator based on the maximum likelihood function of a Poisson random variable. They investigated the performance of their estimator on a Shewhart c-chart for step changes in the rate parameter. Perry et al. (2005, 2007) also presented maximum likelihood estimators for the change-point of a Poisson rate parameter with a linear trend disturbance and monotonically changing rates, respectively. Perry et al. (2007) provided a change point estimation procedure for a process fraction nonconforming with a monotonic change disturbance. Perry and Pignatiello (2005) showed that the performance of the MLE based change point estimator is superior to the built-in change point estimators of EWMA and CUSUM to identify the change point of a binomial process. The change point estimation procedures were also proposed for high quality processes. Noorossana et al. (2009) provided a maximum likelihood estimator in order to identify the time of a step change in high-yield processes. They studied the change point estimation for a geometric process as the number of items until the occurrence of the first non-conforming item can be modeled by a geometric distribution. The add-on procedure was used with the geometric chart and provided accurate and precise estimations for different magnitudes of shifts in p , the process non-conformity proportion.

Some authors investigated the change point for multivariate processes. Nedumaran et al. (2000) proposed a change point estimator for a multivariate process mean vector when the observations follow a multivariate normal distribution. The estimator is considered as a follow-up procedure for χ^2 chart under the assumption of constant covariance structure. Dogu and Deveci-Kocakoc (2011a) proposed a change point estimator to identify the step change in generalized variance control charts. Another approach is proposing sequential generalized likelihood ratio (GLR) test statistic based control charts. These charts can provide a change point estimator along with the control chart statistics. Sullivan and Woodall (2000) proposed a single multivariate control chart based on GLR for multivariate individual process readings. Zamba and Hawkins (2009) proposed a multivariate unknown parameter change point model through GLR statistics for estimating the change in mean vector and/or covariance structure.

1.5 Change Point Estimation for χ^2 Control Chart

This part focuses on the change point procedure for a typical χ^2 control chart. This estimation was based on the likelihood functions and proposed by Nedumaran et al. (2000) and we will follow a similar approach for jointly monitoring the mean vector and covariance matrix changes in this text. This follow-up approach for homoscedastic case is summarized as follows:

- The process readings are monitored with a χ^2 control chart. When the control chart generates a signal, the reason for this signal is assumed to be a step change.
- The change point estimation procedure starts to find the most likely location of the change and provides an estimation of the time of the step change.
- The point where the log-likelihood function attains its maximum is considered as the change point.
- The process professionals start looking for the special cause at that particular point of time or in a search window of possible change points.

Let $\mathbf{X}_{ij} = (X_{ij1}, X_{ij2}, \dots, X_{ijp})'$ be a $p \times 1$ vector which represents the p characteristics on the j^{th} observation ($j = 1, 2, \dots, n$) in the i^{th} subgroup of size n . Suppose further that when the process is in control, the \mathbf{X}_{ij} 's are independent and identically distributed (iid) and follow a p -variate Normal distribution with mean vector $\boldsymbol{\mu}_0$ and covariance matrix $\boldsymbol{\Sigma}_0$ that is, the \mathbf{X}_{ij} 's are iid $N_p(\boldsymbol{\mu}_0, \boldsymbol{\Sigma}_0)$ when the process is in control. We let n denote the subgroup size and we let $\bar{\mathbf{X}}_i$ denote the average vector of the i^{th} sub grouping and can be calculated with (1.3).

When the i th subgroup is observed, the statistic $\chi_i^2 = n(\bar{\mathbf{X}}_i - \boldsymbol{\mu}_0)' \boldsymbol{\Sigma}_0^{-1} (\bar{\mathbf{X}}_i - \boldsymbol{\mu}_0)$ has a chi-square distribution with p degrees of freedom. This statistic is plotted on a χ^2 control chart with UCL set at $\chi_{p,\alpha}^2$, where $\chi_{p,\alpha}^2$ is the $(1-\alpha)$ th percentile point of the chi-square distribution with p degrees of freedom and α is the probability of a false alarm for each subgroup plotted on the chart.

It is assumed that when the multivariate process mean changes, there has been a step-change from its in-control value of $\boldsymbol{\mu} = \boldsymbol{\mu}_0$ to an unknown value $\boldsymbol{\mu} = \boldsymbol{\mu}_1$ where $\boldsymbol{\mu}_0 \neq \boldsymbol{\mu}_1$. If χ_T^2 exceeds the UCL of the χ^2 control chart, it is concluded that the step-change in the process mean occurred after some unknown time τ , where $0 \leq \tau \leq T-1$. Hence, we assume that the subgroup averages $\bar{\mathbf{X}}_1, \bar{\mathbf{X}}_2, \dots, \bar{\mathbf{X}}_\tau$ came from in-control process and the subgroup averages $\bar{\mathbf{X}}_{\tau+1}, \bar{\mathbf{X}}_{\tau+2}, \dots, \bar{\mathbf{X}}_T$ came from the out-of-control process. It is further assumed that the process mean remains at the new level $\boldsymbol{\mu}_1$ until the special cause has been identified. The maximum likelihood estimator of τ can be the value of t for which the statistic M_t attains its maximum; that is,

$$\hat{\tau} = \arg \max_t (M_t), \quad t = 0, 1, \dots, T-1 \quad (1.4)$$

$$\text{where } M_t = (T-t)(\bar{\bar{\mathbf{X}}}_{t,T} - \boldsymbol{\mu}_0)' \boldsymbol{\Sigma}_0^{-1} (\bar{\bar{\mathbf{X}}}_{t,T} - \boldsymbol{\mu}_0) \quad (1.5)$$

and $\bar{\bar{\mathbf{X}}}_{t,T} = \frac{1}{T-t} \sum_{i=t+1}^T \bar{\mathbf{X}}_i$ is the average of the $(T-t)$ most recent subgroup averages.

1.5.1 Illustrative Example

A hypothetical example was considered by Nedumaran et al. (2000) for the machining of steel sleeves in which the inside diameter, the outside diameter, and the length are the $p = 3$ important quality characteristics. A χ^2 control chart is used to monitor these characteristics. Based on historical data, the process is known to be stable and in control, and observations are as follows:

$$\boldsymbol{\mu}_0 = \begin{bmatrix} 105.0 \\ 150.0 \\ 120.0 \end{bmatrix} \text{ and } \boldsymbol{\Sigma}_0 = \begin{bmatrix} 9.0 & 9.6 & 5.4 \\ 9.6 & 16.0 & 4.8 \\ 5.4 & 4.8 & 12.0 \end{bmatrix}.$$

For $n = 5$ subgroups χ^2 statistics are calculated periodically and plotted on the chart. The probability of a false alarm is set at $\alpha = 0.0027$. The UCL of the χ^2 control chart is then $UCL_{\chi^2} = \chi_{3,0.0027}^2 = 14.157$. The sample averages of 21 subgroups and the corresponding χ^2 statistics are shown in Table 1.1. The control chart has issued an alarm for the twenty-first subgroup. Thus, $T = 21$. The proposed estimator can now be applied to estimate the change point. $\bar{\bar{\mathbf{X}}}_{t,21} = 1/(21-t) \sum_{i=t+1}^{21} \bar{\mathbf{X}}_i$

for $t = 0, 1, 2, \dots, T-1$. M_t values can be calculated easily from

$$M_t = (21-t)(\bar{\bar{\mathbf{X}}}_{t,T} - \boldsymbol{\mu}_0)' \boldsymbol{\Sigma}_0^{-1} (\bar{\bar{\mathbf{X}}}_{t,T} - \boldsymbol{\mu}_0).$$

Table 1.1 Subgroup averages, reverse cumulative averages, M_t and χ^2 statistics

i	t	\bar{X}_i			Reverse cumulative averages			M_t	χ^2
1	0	104.757	150.151	119.243	105.404	150.012	119.988	1.27	0.35
2	1	105.432	150.252	122.584	105.436	150.005	120.026	1.38	3.19
3	2	104.449	151.325	120.496	105.436	149.993	119.891	1.58	4.11
4	3	101.822	146.074	118.236	105.491	149.919	119.857	2.23	5.86
5	4	106.986	150.596	121.009	105.707	150.145	119.887	2.69	4.31
6	5	106.887	153.377	118.408	105.627	150.117	119.887	2.17	7.22
7	6	104.486	148.822	119.61	105.543	149.899	119.985	2.05	0.51
8	7	104.314	147.559	120.316	105.618	149.976	120.012	2.09	2.91
9	8	103.76	149.237	118.594	105.719	150.162	119.989	2.02	1.32
10	9	104.488	149.475	119.524	105.882	150.239	120.105	2.47	0.16
11	10	104.638	150.276	120.708	106.009	150.309	120.158	2.79	1.08
12	11	102.711	147.623	119.969	106.146	150.312	120.103	3.53	3.98
13	12	107.061	152.098	122.726	106.528	150.611	120.118	4.94	3.63
14	13	103.276	148.987	119.682	106.461	150.425	119.792	5.19	2.67
15	14	105.761	151.890	120.036	106.916	150.630	119.807	7.31	1.36
16	15	108.153	151.391	120.350	107.108	150.420	119.769	8.71	10.93
17	16	104.841	147.558	119.485	106.899	150.226	119.653	6.67	4.87
18	17	104.956	147.410	118.942	107.414	150.893	119.694	6.48	6.82
19	18	108.306	151.819	119.715	108.236	152.054	119.951	6.24	12.40
20	19	106.464	150.938	118.532	108.202	152.172	120.069	3.80	5.02
21	20	109.940	153.406	121.605	109.940	153.406	121.605	3.64	18.19

From Table 1.1, it is concluded that, the estimated change point is $\hat{\tau} = 15$. Hence, it is estimated that the process mean has changed during the time between the formation of subgroup 15 and 16. The process engineers may look up their process records for especially at $t = 15$ and $t = 16$ that a special cause would occur.

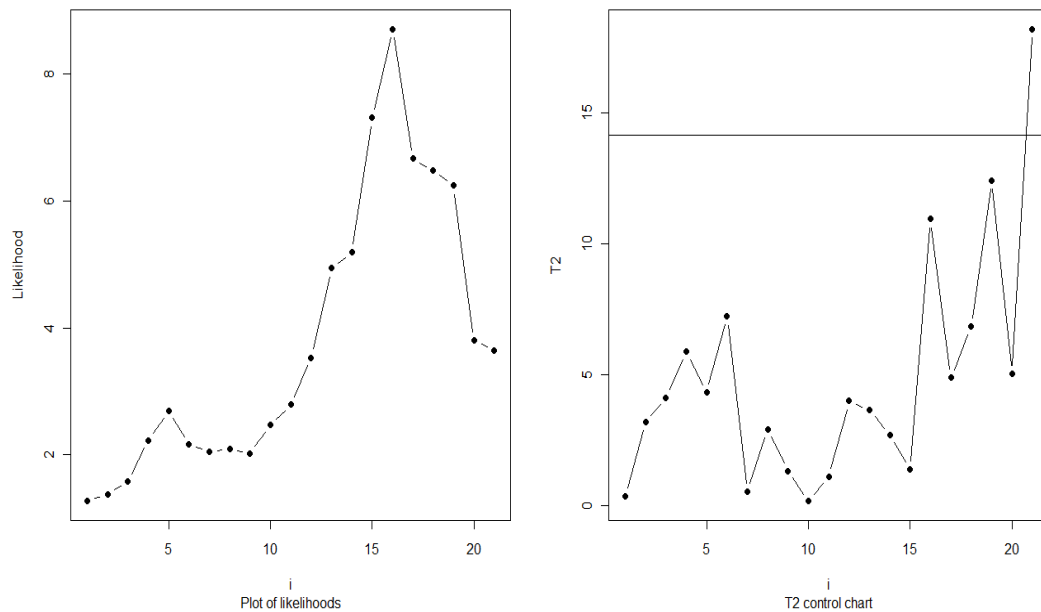


Figure 1.5 Plot of change point likelihoods and χ^2 control chart for steel sleeve example.

Figure 1.5 shows the likelihoods of the change point and χ^2 control chart for this example. Traditionally, the process engineers could have started examining their records at the time of signal and searched backward until a special cause was found. However, using this estimator is a more efficient way of inspecting special causes.

1.6 Objective of the Dissertation

The primary objective of this research is to develop new change point procedures for multivariate processes. This research is motivated by the works of Pignatiello and Samuel et al. (1998a, 1998b), Nedumaran et al. (2000) and Samuel (2001). A signal generated from the monitoring procedure does not always mean that the assignable cause actually occurred at that point. Finding the actual change point has been in great importance for many industries. Nedumaran et al. (2000) focused on the procedure which is capable of identifying the step change in mean vector when the process was monitored with a χ^2 control chart.

Controlling and monitoring only the multivariate normal mean vector is not always sufficient because multivariate normal process dispersion does not remain constant for many industrial applications. The need to control multivariate normal process dispersion led several different extensions to control and monitor process dispersion to appear. The approaches proposed by Alt (1985) and Alt and Smith (1988) are the most commonly used control charts. These schemes do not provide a built-in change point estimator. Our first target is to propose a change point estimation procedure which is capable of detecting step changes when the process is monitored with a $|\mathbf{S}|$ control chart.

Since a successful monitoring program requires monitoring both mean vector and covariance shifts, the importance of simultaneously monitoring process mean and variability has been increased. The traditional way of simultaneous monitoring is constructing two charts: one for the mean and one for the variability. In other words, χ^2 and $|\mathbf{S}|$ control charts are used simultaneously and if any of them or both of them generates a signal the process is considered to be out-of-control. Our second objective is to develop a change point estimation procedure for simultaneous monitoring of mean vector and covariance matrix. Our assumption here is that the monitoring tool is a combination of χ^2 and $|\mathbf{S}|$ control charts.

Cheng and Thaga (2006) concluded that this practice of combining two charts needs more resources such as quality professionals and time. Alt (1985) also noted the importance of the need to develop single control chart for the simultaneous monitoring of both mean and dispersion. There are some single control charts such as Max- MEWMA (Chen et al., 2005) and MELR (Zhang et al., 2010) charts in the literature. Since these control charts have better performance than the traditional combination chart, another concern is the performance of the joint estimation procedure under the assumption that the process is being monitored with a multivariate single control chart.

The remainder of this research is as follows: the following chapter gives the details for the change point estimation in the $|\mathbf{S}|$ control chart, the third chapter includes the joint change point estimation procedure for χ^2 and $|\mathbf{S}|$ combination chart, the fourth chapter is a research paper on the performance of the joint estimation procedure with multivariate single control charts. Each chapter is organized to include its own literature review, statistical model, simulation details and assessment of the estimators. This manuscript also provides a final chapter for conclusions which includes total results and future research directions.

CHAPTER TWO
ESTIMATION OF CHANGE POINT IN
GENERALIZED VARIANCE CONTROL CHART

2.1 Introduction

In many industrial implementations of control charting, dealing with several interrelated quality characteristics is unavoidable. Controlling and monitoring multivariate normal mean vector is not sufficient because multivariate normal process dispersion does not remain constant for many industrial applications. The need to control multivariate normal process dispersion led several different extensions to control and monitor process dispersion to appear.

Alt (1985) and Alt and Smith (1988) proposed different procedures of carrying out multivariate dispersion control and monitoring. The first approach is a direct extension of the univariate S^2 control chart. In this procedure, the following statistic to be charted is calculated based on a modification of the generalized likelihood ratio test.

$$W_i = -pn + pn \log(n) - n \log(|\mathbf{A}_i|/|\boldsymbol{\Sigma}_0|) + tr(\boldsymbol{\Sigma}_0^{-1} \times \mathbf{A}_i),$$

where $\mathbf{A}_i = (n-1)\mathbf{S}_i$, \mathbf{S}_i is the sample variance covariance matrix for sample i and can be calculated using (1.2), n is the sample size, and tr is the trace operator. If W_i statistic is plotted above the $UCL = \chi_{\alpha, p(p+1)/2}^2$, where p refers to the number of quality characteristics to be controlled, then the process is out of control.

The second approach for monitoring $|\mathbf{S}|$ is constructed using only the first two moments of $|\mathbf{S}|$ and the property that the most of the probability distribution of $|\mathbf{S}|$ is contained in the interval $E(|\mathbf{S}|) \pm 3\sqrt{V(|\mathbf{S}|)}$ where $E(|\mathbf{S}|) = b_1|\Sigma_0|$ and, $V(|\mathbf{S}|) = |\Sigma_0|^2 b_2$. Here;

$$b_1 = (n-1)^p \prod_{i=1}^p (n-i), \text{ and}$$

$$b_2 = (n-1)^{-2p} \prod_{i=1}^p (n-i) \times \left[\prod_{j=1}^p (n-j+2) - \prod_{j=1}^p (n-j) \right].$$

If the plotted statistics are within UCL and LCL, then the process is evaluated to be statistically in-control. When the LCL is negative, it is set to zero. The limits for this approach are as follows;

$$UCL = |\Sigma_0| (b_1 + 3b_2^{1/2}),$$

$$CL = b_1 |\Sigma_0|, \text{ and}$$

$$LCL = |\Sigma_0| (b_1 - 3b_2^{1/2}).$$

The third approach is considered to be the multivariate analogue of the univariate S-chart. In this approach, the distributional properties of $|\mathbf{S}|^{1/2}$ are used. Hence, when two quality characteristics are considered to be monitored, then $2(n-1)|\mathbf{S}|^{1/2}/|\Sigma_0|^{1/2}$ is distributed as χ_{2n-4}^2 . To calculate the UCL and LCL, the distribution of $|\mathbf{S}|$ is used.

$$\alpha = P(LCL > |\mathbf{S}| > UCL) = P\left(\sqrt{\frac{LCL \times 2 \times (n-1)}{|\Sigma_0|}} > \chi_{2n-4}^2 > \sqrt{\frac{UCL \times 2 \times (n-1)}{|\Sigma_0|}}\right)$$

$$= P(\chi_{2n-4, 1-(\alpha/2)}^2 > \chi_{2n-4}^2 > \chi_{2n-4, \alpha/2}^2)$$

Hence,

$$\begin{aligned}
 UCL &= |\Sigma_0| (\chi_{2n-4, \alpha/2}^2)^2 / [4(n-1)^2], \text{ and} \\
 LCL &= |\Sigma_0| (\chi_{2n-4, 1-(\alpha/2)}^2)^2 / [4(n-1)^2].
 \end{aligned}
 \tag{2.1}$$

Aparisi et al. (1999, 2001) studied the statistical properties of the $|\mathbf{S}|$ -chart. The control limits and power of the generalized variance control chart with its distributional properties are considered in these studies. There are several comparative studies on which approach to be selected. For discussions and reviews of multivariate dispersion control charts designed for process control, see, Lowry and Montgomery (1995), Alt (1985) and Alt and Smith (1988), and Bersimis et al. (2007). Surtihadi et al. (2004) discussed different cases of covariance matrix shifts and proposed effective control charts for each case of structured shift.

Khoo and Quah (2004) discussed the use of run rules in multivariate variability control. Vargas and Lagos (2007) compared four multivariate control charts for process dispersion, discussed robust estimation of covariance matrix and proposed RG chart which is a modification of G chart (Levinson et al., 2002). Djauhari (2005) and Djauhari et al. (2008) discussed the Improved Generalized Variance (GV) chart and Vector Variance (VV) chart to solve the problems about the estimation and interpretation of generalized variance. Costa and Machado (2009) proposed a new multivariate control chart for process dispersion. They proposed VMAX statistic which is based on the standardized sample variance of p quality characteristics to construct the VMAX chart.

Beside the fact that, charting is a reliable way of controlling and monitoring multivariate dispersion of a process, in many situations, knowing when a change occurred is vital for special cause identification. With control efforts, if the exact time of change of the process dispersion is determined, practitioners can easily solve the root causes of variability. Samuel et al. (1998a, 1998b) considered finding the time of a permanent change for a univariate normal process mean and variance and

proposed maximum likelihood estimators used when the related control charts issue a signal. Park and Park (2004) proposed a maximum likelihood estimator for identifying the time of the simultaneous change of univariate mean and variance. When a change occurs in controlling several quality characteristics of a manufactured product; in other words, for multivariate cases, Nedumaran et al. (2000) proposed a maximum likelihood estimator to detect the time of the mean vector shifts. This change point detection procedure which is a follow up procedure for χ^2 control chart is based on the assumption of normality and constant covariance structure.

Zamba and Hawkins (2006, 2009) proposed multivariate change point estimation procedures using the unknown (or not fully known) - parameter likelihood ratio test for a change in mean vector and/or covariance matrix. When compared to the procedures proposed by Zamba and Hawkins, our estimator serves to Phase II applications following the work of Samuel et al. (1998a, 1998b), Nedumaran et al. (2000) and Pignatiello and Samuel (2001) and our estimator is a complementary procedure of the $|\mathbf{S}|$ -chart. Our proposed estimator focuses on estimating the most likely location of the step change in the parameter of variation after a signal has been issued by the $|\mathbf{S}|$ -chart. This retrospective procedure allows process engineers and professionals to search for the causes of change in the variability. The proposed 'add-on' procedure is very useful in practice while many industrial professionals prefer to apply $|\mathbf{S}|$ -chart for their control and monitoring activities of covariance matrix. When they encounter an out of control situation, they can easily practice the further action with the proposed estimator and find the estimated change point using the information provided by the chart.

Sullivan et al. (2007) extended the step-down technique to apply the parameters in the covariance matrix and to the other parameters in addition to those making up the mean vector. They assume that other methods have been used to detect a shift and estimate the time of the change. So as a retrospective application, step down analysis can be applied with the proposed change point estimation procedure.

Some other alternative multivariate variability charting techniques including multivariate cumulative sum (MCUSUM) and multivariate exponentially weighted moving average (MEWMA) procedures can be applied to this procedure, but our study focuses on the change point estimation for $|\mathbf{S}|$ -chart which is the most frequently used in industrial practice.

In this study, we consider the use of the change point estimator of the multivariate dispersion once the sample generalized variance, $|\mathbf{S}|$ -chart, in which the required statistics are calculated based on its distributional properties, issues a signal. In the next section, the process model assumptions are given. The derivation of the maximum likelihood estimator (MLE) of the proposed change point estimator is based on Hinkley (1970) and its performance measurements-including accuracy and precision- are investigated for different magnitudes of shift and sample sizes. An illustrative example is given to indicate the practical use of the proposed estimator.

2.2 Process model assumption

Assume that \mathbf{X}_{ij} follows a p – dimensional normal distribution, and there are m samples of size $n > 1$ available from the process. Just as it is important to monitor the process mean vector $\boldsymbol{\mu}$ in the multivariate case, it is also important to monitor process variability. Process variability is summarized in the $p \times p$ covariance matrix, $\boldsymbol{\Sigma}$ (Lowry and Montgomery, 1995).

In this study, it is assumed that p correlated quality characteristics monitored with generalized variance control chart are distributed multivariate normal with known mean vector of $\boldsymbol{\mu} = (\mu_{0,1}, \mu_{0,2}, \dots, \mu_{0,p})'$ and a known variance-covariance matrix, $\boldsymbol{\Sigma}_0$. Let $\mathbf{X}_{ij} = (X_{ij1}, X_{ij2}, \dots, X_{ijp})'$ be a $p \times 1$ vector which represents the p characteristics on the j^{th} observation ($j = 1, 2, \dots, n$) in the i^{th} subgroup of size n .

Suppose further that when the process is in control, the \mathbf{X}_{ij} 's are independent and identically distributed (iid) and follow a p -variate Normal distribution with mean vector $\boldsymbol{\mu}_0$ and covariance matrix $\boldsymbol{\Sigma}_0$; that is, the \mathbf{X}_{ij} 's are iid $N_p(\boldsymbol{\mu}_0, \boldsymbol{\Sigma}_0)$ when the process is in control. And let the process be statistically in control until the process parameters change from $(\boldsymbol{\mu}_0, \boldsymbol{\Sigma}_0)$ to $(\boldsymbol{\mu}_0, \boldsymbol{\Sigma}_1)$ at an unknown change point in time denoted by τ where $\boldsymbol{\Sigma}_0 \neq \boldsymbol{\Sigma}_1$ with unknown change magnitudes in variances, respectively. The step change in process covariance matrix remains at the new level until the special cause is identified and eliminated.

We let n denote the subgroup size and we let $\bar{\mathbf{X}}_i$ denote the average vector of the i^{th} subgroup; calculated with (1.3), and, \mathbf{S}_i is sample covariance matrix for sample i ; calculated with (1.2). Thus, let T be the time of the signal of the generalized variance control chart. Hence, we assume that the subgroup covariances $\mathbf{S}_1, \mathbf{S}_2, \dots, \mathbf{S}_\tau$ came from in-control process and the subgroup covariances $\mathbf{S}_{\tau+1}, \mathbf{S}_{\tau+2}, \dots, \mathbf{S}_T$ came from the out-of-control process. It is further assumed that the process mean remains the same and covariance remains the same at the new level $\boldsymbol{\Sigma}_1$ until the special cause has been issued by the generalized variance control chart.

2.3 Estimation of the change point

After determining the process model assumptions, we consider the derivation of the maximum likelihood estimator (MLE) of the change point τ when a step change occurs in the process covariance matrix. It is assumed that the process covariance has changed at an unknown time, τ . The change is detected at the time T by the generalized variance control chart.

Given the observations $\mathbf{X}_{ij} = (X_{ij1}, X_{ij2}, \dots, X_{ijp})'$, derivation of the maximum likelihood estimator (MLE) of τ , the multivariate process dispersion change point, is as follows:

$$\begin{aligned} \log_e L(\tau, \Sigma_1) &= \log_e \left(\frac{1}{(2\pi)^{np/2} |\Sigma_0|^{n/2}} \right)^\tau + \log_e \left(\frac{1}{(2\pi)^{np/2} |\Sigma_1|^{n/2}} \right)^{T-\tau} \\ &\quad - \frac{1}{2} \left[\sum_{i=1}^{\tau} \sum_{j=1}^n (\mathbf{X}_{ij} - \boldsymbol{\mu}_0)' \Sigma_0^{-1} (\mathbf{X}_{ij} - \boldsymbol{\mu}_0) \right] - \frac{1}{2} \left[\sum_{i=\tau+1}^T \sum_{j=1}^n (\mathbf{X}_{ij} - \boldsymbol{\mu}_0)' \Sigma_1^{-1} (\mathbf{X}_{ij} - \boldsymbol{\mu}_0) \right]. \end{aligned}$$

The first part of the function can be written as:

$$-\frac{n\tau}{2} \log_e \left((2\pi) |\Sigma_0| \right) - \frac{n(T-\tau)}{2} \log_e \left((2\pi) |\Sigma_1| \right).$$

There are two unknowns in the likelihood function; τ and Σ_1 . If the time of the step change were known, the MLE of Σ_1 , namely the covariance matrix of the $(T-t)$ most recent subgroup averages would be:

$$\hat{\Sigma}_1 = \frac{1}{n(T-t)} \sum_{i=t+1}^T \sum_{j=1}^n (\mathbf{X}_{ij} - \boldsymbol{\mu}_0) (\mathbf{X}_{ij} - \boldsymbol{\mu}_0)'.$$

Substituting the MLE of Σ_1 back into the log-likelihood function, we obtain

$$\begin{aligned} \log_e L(\tau, \Sigma_1) &= \frac{1}{2} \sum_{i=t+1}^T \sum_{j=1}^n (\mathbf{X}_{ij} - \boldsymbol{\mu}_0)' \Sigma_0^{-1} (\mathbf{X}_{ij} - \boldsymbol{\mu}_0) \\ &\quad - \frac{n(T-t)}{2} \log_e \left(\left| \frac{\sum_{i=t+1}^T \sum_{j=1}^n (\mathbf{X}_{ij} - \boldsymbol{\mu}_0) (\mathbf{X}_{ij} - \boldsymbol{\mu}_0)'}{n(T-t)} \right| \div |\Sigma_0| \right) - \frac{np(T-t)}{2}. \end{aligned}$$

The MLE of τ , denoted by $\hat{\tau}$ is the value of t that maximizes the log-likelihood function, or $\hat{\tau}$ is the maximum value of C statistics. So;

$$\hat{\tau} = \arg \max_{0 < \tau < T-1} (C_\tau) \quad \tau=0, 1, \dots, T-1, \quad (2.2)$$

where

$$C_t = \frac{1}{2} \left(tr \left(\Sigma_0^{-1} \sum_{i=t+1}^T \sum_{j=1}^n (\mathbf{X}_{ij} - \boldsymbol{\mu}_0)' (\mathbf{X}_{ij} - \boldsymbol{\mu}_0) \right) \right) - \frac{n(T-t)}{2} \log_e \left(\frac{\sum_{i=t+1}^T \sum_{j=1}^n (\mathbf{X}_{ij} - \boldsymbol{\mu}_0) (\mathbf{X}_{ij} - \boldsymbol{\mu}_0)' \Sigma_0^{-1}}{n(T-t)} \right) - \frac{np(T-t)}{2}. \quad (2.3)$$

Note that Samuel et al. (1998b) proposed the MLE estimator of τ for univariate processes is as follows and when $p=1$, then our proposed multivariate process dispersion estimator turns into the univariate form:

$$\hat{\tau} = \arg \max_{0 < t < T-1} \left[\frac{\sum_{i=\tau+1}^T \sum_{j=1}^n (x_{ij} - \mu_0)^2}{2\sigma_0^2} - \frac{n(T-\tau)}{2} \log_e \frac{\sum_{i=\tau+1}^T \sum_{j=1}^n (x_{ij} - \mu_0)^2}{n(T-\tau)\sigma_0^2} - \frac{n(T-\tau)}{2} \right].$$

2.4 Performance evaluation of the proposed estimator

In this part of the study, the performance of our proposed estimator is investigated and evaluated by using Monte Carlo simulation. The simulation study is focused on Phase II performance of the proposed estimator. In the literature, change point estimators are proposed by Samuel et al. (1998a, 1998b), Nedumaran et al. (2000) and Park and Park (2004) for different types of control charts. These studies used two major performance indicator of the estimator, namely, ‘‘average change point estimate’’ and ‘‘the empirical distribution of the estimated change point around the actual change point’’. During the simulation study, although our proposed estimator can be applied for all cases of multivariate implementations, for simplifying the forms of the alternatives to be studied the bivariate case ($p=2$) was considered. Matlab® is used to carry out the simulation study.

Observations were randomly generated from a $N_p(\boldsymbol{\mu}_0, \boldsymbol{\Sigma}_0)$ distribution when $i \leq 100$, the on-target mean vector was $\boldsymbol{\mu}_0 = (0,0)'$ and the in-control covariance matrix was selected as follows:

$$\boldsymbol{\Sigma}_0 = \begin{bmatrix} 1 & \rho \\ \rho & 1 \end{bmatrix},$$

where $0 \leq \rho \leq 1$ is the correlation coefficient between two quality characteristics. In this study, the correlation coefficient was set to 0.5 and Type I error probability was set to 0.0027. For the first hundred runs it is assumed to be no false alarms. Starting with subgroup 101, the observations are randomly generated from $N_p(\boldsymbol{\mu}_0, \boldsymbol{\Sigma}_1)$ until the generalized variance control chart issued a signal. The structure of the changed variance-covariance matrix is given as:

$$\boldsymbol{\Sigma}_1 = \begin{pmatrix} \delta_1^2 \times \sigma_x^2 & \rho \times \delta_1 \times \delta_2 \times \sigma_x \times \sigma_y \\ \rho \times \delta_1 \times \delta_2 \times \sigma_x \times \sigma_y & \delta_2^2 \times \sigma_y^2 \end{pmatrix}.$$

In order to simulate the changes in the variance-covariance matrix the following cases are considered as in Vargas and Lagos (2007):

- The standard deviation of one of the quality characteristics increases from σ_x to $\delta_1 \times \sigma_x$ (or σ_y to $\delta_2 \times \sigma_y$) for $\delta_1 > 1$ (or $\delta_2 > 1$), or decreases from σ_x to $\delta_1 \times \sigma_x$ (or σ_y to $\delta_2 \times \sigma_y$) for $\delta_1 < 1$ (or $\delta_2 < 1$), while the others remains the same.
- The standard deviations of both quality characteristics increase from σ_x to $\delta_1 \times \sigma_x$ and σ_y to $\delta_2 \times \sigma_y$ for $\delta_1 > 1$ and $\delta_2 > 1$, or decrease from σ_x to $\delta_1 \times \sigma_x$ and σ_y to $\delta_2 \times \sigma_y$ for $\delta_1 < 1$ and $\delta_2 < 1$, by the same magnitude.

- The standard deviation of one of the quality characteristics increases from σ_x to $\delta_1 \times \sigma_x$ for $\delta_1 > 1$ while the other decreases from σ_y to $\delta_2 \times \sigma_y$ for $\delta_2 < 1$.

For every run, when the control chart issued a signal, the time of the change was calculated with the proposed estimator. This procedure was repeated a total of 10,000 times for each of the case and different magnitudes, denoted by δ , and three subgroup sizes $n = 4, n = 10$, and $n = 15$. The average of change point estimates for every simulation run was computed along with its standard error to investigate the accuracy of our estimator. Additionally, the empirical distributions of the estimated change point around the actual change point for all cases, sample sizes and magnitudes of shift were considered in order to evaluate the precision of the estimator.

2.4.1 Accuracy Evaluation

For a control chart, the average run length (ARL) is the expected number of required sub-groups to be controlled to detect a change in the process distribution or parameters. To measure the power of the control charts ARL is frequently used. For the control chart designed from generalized variance sample distribution, the power is defined when the covariance matrix changes to Σ_1 ($\Sigma_0 \neq \Sigma_1$). Aparisi et al. (1999, 2001) gave the control limits and power of generalized variance control chart. The power of generalized variance control chart with upper and lower control limits is defined as follows where β is the Type II error probability and $1 - \beta$ is the power:

$$1 - \beta = P(LCL \geq |\mathbf{S}| \geq UCL / \Sigma = \Sigma_1)$$

$$= P\left(\frac{\chi_{2n-4, (1-\alpha/2)}^2 \times |\Sigma_0|}{4 \times (n-1)^2} \geq |\mathbf{S}| \geq \frac{\chi_{2n-4, (\alpha/2)}^2 \times |\Sigma_0|}{4 \times (n-1)^2} / \Sigma = \Sigma_1\right).$$

If determinant ratio (DR) is $|\Sigma_1|/|\Sigma_0|$, it gives:

$$1 - \beta = P\left(\frac{\chi_{2n-4, (1-\alpha/2)}^2}{\sqrt{DR}} \geq \chi_{2n-4}^2 \geq \frac{\chi_{2n-4, (\alpha/2)}^2}{\sqrt{DR}} \mid \Sigma = \Sigma_1\right).$$

The out of control ARL, as the reverse of power is then found as follows:

$$ARL(DR) = \frac{1}{P\left(\frac{\chi_{2n-4, (1-\alpha/2)}^2}{\sqrt{DR}} \geq \chi_{2n-4}^2 \geq \frac{\chi_{2n-4, (\alpha/2)}^2}{\sqrt{DR}}\right)}.$$

For instance, considering the equal increasing shift ($\delta = \delta_1 = \delta_2 = 1.2$) for both of the quality characteristics, where $\alpha = 0.0027$ and $n = 10$, Σ_1 is calculated as follows. The ARL calculation is also illustrated in Table 1.1 for this case.

For $i \leq 100$, $\Sigma_0 = \begin{bmatrix} 1.0 & 0.5 \\ 0.5 & 1.0 \end{bmatrix}$, and then for $i > 100$,

$$\Sigma_1 = \begin{pmatrix} \delta_1^2 \times \sigma_x^2 & \rho \times \delta_1 \times \delta_2 \times \sigma_x \times \sigma_y \\ \rho \times \delta_1 \times \delta_2 \times \sigma_x \times \sigma_y & \delta_2^2 \times \sigma_y^2 \end{pmatrix}.$$

$$\text{Hence, } \Sigma_1 = \begin{pmatrix} 1.44 \times 1 & 0.5 \times 1.2 \times 1.2 \times 1 \times 1 \\ 0.5 \times 1.2 \times 1.2 \times 1 \times 1 & 1.44 \times 1 \end{pmatrix} = \begin{pmatrix} 1.44 & 0.72 \\ 0.72 & 1.44 \end{pmatrix}.$$

Using the aforementioned ARL calculation,

$$ARL(DR) = \frac{1}{P(0.04 \geq \chi_{2n-4}^2 \geq 2.87)} = 21.8, \text{ and}$$

$$E(T) = 100 + ARL(DR) = 100 + 21.8 = 121.8.$$

Using the fact that the exact change point of the simulation process for all sample sizes and magnitudes is $\tau = 100$, the change point estimates are expected to be close to the exact change point. Analyzing the average of change point estimations ($\bar{\hat{\tau}}$), for all sample sizes and magnitudes, the outputs are fairly close to the actual change point. In general, our proposed change point estimator can be evaluated to be close to the actual change point without considering different sample sizes and magnitudes of shift in covariance matrix. In Table 2.1-2.5, $\bar{\hat{\tau}}$, standard errors and $E(T)$ are summarized.

For instance, the results for the Case 1 when $\delta > 1$ are given in Table 2.1, and that of $\delta < 1$ are given in Table 2.2. The results indicate that, even small shifts in standard deviations of the quality characteristics, the average change point estimates are quite close to 100. When $\delta = 1.1$ for both quality characteristics, the average change point estimates are 107.83, 101.71, and 100.41 for sample sizes $n = 4, 10, 15$. When compared to the expected times of the signals, the values are fairly close to the actual change point for all sample sizes. For example, when $n = 10$, $E(T)$ is 188.66 and $\bar{\hat{\tau}}$ is 101.71. For the small magnitudes of shift, we realized that $E(T)$ values are very far from 100. Even we take 15 measurements for each subgroup, $E(T)$ is 308.13 when $\delta = 0.9$, on the other hand, $\bar{\hat{\tau}} = 100.66$. That means our estimator has good detection potential for all magnitudes of shifts; on the other hand, generalized variance control chart has not for especially small shifts.

Table 2.1 Average of the change point estimates and their standard errors when quality characteristics increase from σ_x to $\delta_1 \times \sigma_x$ and σ_y to $\delta_2 \times \sigma_y$ ($\delta_1 = \delta_2 = \delta > 1$).

		δ					
		1.1	1.2	1.3	1.4	1.5	2.0
n=4	$E(T)$	255.53	166.23	130.65	117.1	110.42	102.85
	$\bar{\hat{\tau}}$	107.83	100.00	99.31	99.32	99.23	99.32
	Std. error	0.364	0.147	0.104	0.085	0.078	0.059
n=10	$E(T)$	188.66	121.80	108.22	104.2	104.15	101.12
	$\bar{\hat{\tau}}$	101.71	99.33	99.13	98.97	98.86	99.61
	Std. error	0.185	0.093	0.079	0.076	0.079	0.043
n=15	$E(T)$	199.05	121.98	106.86	103.29	102.07	101.05
	$\bar{\hat{\tau}}$	100.41	99.24	99.43	99.28	99.39	99.93
	Std. error	0.13	0.096	0.052	0.062	0.053	0.012

Table 2.2 Average of the change point estimates and their standard errors when quality characteristics decrease from σ_x to $\delta_1 \times \sigma_x$ and σ_y to $\delta_2 \times \sigma_y$ ($\delta_1 = \delta_2 = \delta < 1$).

		δ					
		0.9	0.8	0.7	0.6	0.5	0.25
n=4	$E(T)$	537.85	411.98	285.82	203.24	151.09	104.76
	$\bar{\hat{\tau}}$	102.77	99.24	99.67	99.76	99.81	99.92
	Std. error	0.343	0.087	0.04	0.028	0.028	0.017
n=10	$E(T)$	305.62	157.19	115.6	104.53	101.72	101.00
	$\bar{\hat{\tau}}$	100.50	99.83	99.71	99.64	99.57	99.99
	Std. error	0.140	0.047	0.038	0.039	0.042	0.000
n=15	$E(T)$	308.13	156.91	103.63	101.49	101.71	101.00
	$\bar{\hat{\tau}}$	100.66	99.76	98.92	99.20	99.58	100.00
	Std. error	0.151	0.051	0.074	0.058	0.044	0.000

Table 2.3 Average of the change point estimates and their standard errors when one quality characteristic increase from σ_x to $\delta_1 \times \sigma_x$ (or σ_y to $\delta_2 \times \sigma_y$) (δ_1 (or δ_2) = $\delta > 1$).

		δ					
		1.1	1.2	1.3	1.4	1.5	2.0
n=4	$E(T)$	354.4	265.88	209.41	174.73	152.67	115.61
	$\bar{\hat{t}}$	116.73	101.84	100.37	100.06	100.06	99.87
	Std. error	0.570	0.201	0.117	0.080	0.064	0.040
n=10	$E(T)$	304.02	194.98	146.99	126.4	116.39	103.81
	$\bar{\hat{t}}$	104.00	100.31	99.97	99.79	99.82	99.85
	Std. error	0.276	0.096	0.063	0.053	0.041	0.030
n=15	$E(T)$	305.75	195.73	151.47	126.29	115.18	103.06
	$\bar{\hat{t}}$	104.22	100.20	99.89	99.96	99.89	99.94
	Std. error	0.272	0.099	0.046	0.030	0.031	0.019

Table 2.4 Average of the change point estimates and their standard errors when one quality characteristic decrease from σ_x to $\delta_1 \times \sigma_x$ (or σ_y to $\delta_2 \times \sigma_y$) (δ_1 (or δ_2) = $\delta < 1$).

		δ					
		0.9	0.8	0.7	0.6	0.5	0.25
n=4	$E(T)$	546.01	541.85	457.86	371.00	291.06	151.4
	$\bar{\hat{t}}$	108.98	98.71	99.16	99.54	99.71	99.96
	Std. error	0.547	0.140	0.061	0.035	0.027	0.011
n=10	$E(T)$	443.04	290.46	192.21	140.02	116.64	101.69
	$\bar{\hat{t}}$	101.39	99.63	99.79	99.91	99.87	99.95
	Std. error	0.243	0.061	0.030	0.016	0.023	0.015
n=15	$E(T)$	294.36	292.34	119.99	108.64	116.54	101.71
	$\bar{\hat{t}}$	100.53	99.61	99.50	99.54	99.90	99.96
	Std. error	0.185	0.065	0.052	0.048	0.021	0.01

Table 2.5 Average of the change point estimates and their standard errors when one of the quality characteristics increases from σ_x to $\delta_1 \times \sigma_x$ ($\delta_1 > 1$) while the other decreases from σ_y to $\delta_2 \times \sigma_y$ ($\delta_2 < 1$).

		δ_1					
		1.1	1.2	1.3	1.4	1.5	2.0
		δ_2					
		0.9	0.8	0.7	0.6	0.5	0.25
n=4	$E(T)$	475.26	504.28	543.65	556.39	509.63	291.36
	$\bar{\hat{\tau}}$	101.01	99.57	99.73	99.84	99.91	99.98
	Std. error	0.270	0.074	0.036	0.021	0.014	0.004
n=10	$E(T)$	480.92	490.19	458.27	345.47	234.15	116.95
	$\bar{\hat{\tau}}$	99.93	99.88	99.97	99.97	99.98	100.00
	Std. error	0.118	0.312	0.104	0.008	0.004	0.000
n=15	$E(T)$	263.35	240.39	200.35	159.84	129.54	103.82
	$\bar{\hat{\tau}}$	99.42	99.84	99.94	99.95	99.99	100.00
	Std. error	0.097	0.029	0.013	0.015	0.004	0.000

Our proposed estimator also successfully yields for the Case 2 when both $\delta > 1$ and $\delta < 1$. For the different magnitudes of shift and sample sizes, $\bar{\hat{\tau}}$ values are close to 100. In Tables 2.3 and 2.4, the $\bar{\hat{\tau}}$ and $E(T)$ results are given. When the change is intentionally structured in only one quality characteristic, the accuracy of the estimator is not influenced. For instance, when $\delta = 0.7$, the estimates are 99.16, 99.79 and 99.50 for different sample sizes. Table 2.5 is given for the Case 3 when $\delta_1 > 1$ and $\delta_2 < 1$. As it is indicated in the Table 2.5, the average estimates are very close to the 100, regardless of the sample size and magnitude of shift. Even though, generalized variance control chart showed good detection performance for increases in the standard deviations of the variables, the proposed estimator showed better detection performance for all cases.

2.4.2 Precision Evaluation

For the three cases, empirical distribution of $\hat{\tau}$ around τ are given in Tables 2.6-2.10. Each table is constructed to show the estimated probability of being in the k^{th} neighborhood of the actual change point. In other words, the observed frequency which our proposed estimator of the time of the step change was within k subgroups of the actual time of the change is summarized in these tables. The results for Case 1 are summarized in Tables 2.6 and 2.7.

For example, when $\delta = 1.3$ and $n = 15$, in 60.4% of the runs, the proposed estimator correctly identified the change point. When $\delta = 0.6$ and $n = 10$, then, the change point is estimated to be within ± 5 subgroups of the actual change point in 98.9% of the 10,000 simulation runs. From Table 2.7 while $n = 4$, it can be seen that for a 50% decrease in both quality characteristics, our proposed estimator identified the change point correctly in 76.7% of the trials. Our estimate was within four subgroups of the true change point in 99.4% of the trials. When $n = 15$ and $\delta = 0.25$ then 99.9% of the trials the estimator identified the true change point.

Tables 2.8 and 2.9 give the results for Case 2 when $\delta > 1$ or $\delta < 1$ for one of the quality characteristics. When $n = 4$, for a 40% increase in the standard deviations of one of the quality characteristics, simulation study resulted correct identification in 26.7% of the trials. The change point was estimated to be within ± 3 subgroup of the actual change point in 70.1% of the trials and be within ± 10 subgroup of the actual change point in 92.7% of the trials. Also, any decrease in standard deviation of one of the quality characteristics are very well determined by our proposed estimator. For example, when $n = 10$, for a 20% decrease in one of the standard deviations, our estimator correctly identified the true change point in 28.4% of the trials. The change point was estimated to be within ± 1 subgroup of the actual change point in 51.2% of the trials and be within ± 7 subgroup of the actual change point in almost 89.3% of the trials. It is a very important property of our proposed estimator to be efficient even in small magnitudes of shift.

Table 2.10 gives the results for Case 3 when $\delta_1 > 1$ and $\delta_2 < 1$, respectively. As an example from the table, when $n = 15$ for a 20% increase in the standard deviation of the first quality characteristic and 20% decrease in the standard deviation of the second characteristic resulted in correct identification in 57% of the simulation runs. Moreover, in 99% of the trials, the estimated change points are within ± 7 subgroup. While $n = 4$, for 50% increase in the first standard deviation and 50% decrease in the second standard deviation, the estimator correctly identified the true change point in 73.1% of the trials and, in 99.2% of the trials, the estimated change points are within ± 3 subgroup.

Table 2.6 Empirical distribution of $\hat{\tau}$ around τ when σ_x increases to $\delta_1 \times \sigma_x$ and σ_y increases to $\delta_2 \times \sigma_y$ ($\delta_1 = \delta_2 = \delta > 1$).

	P/δ	1.1	1.2	1.3	1.4	1.5	2.0
$n=4$	$\hat{P}(\hat{\tau} = \tau)$	0.051	0.154	0.270	0.388	0.474	0.762
	$\hat{P}(\hat{\tau} - \tau \leq 1)$	0.117	0.314	0.488	0.626	0.714	0.916
	$\hat{P}(\hat{\tau} - \tau \leq 2)$	0.174	0.420	0.615	0.751	0.827	0.951
	$\hat{P}(\hat{\tau} - \tau \leq 3)$	0.223	0.502	0.699	0.820	0.885	0.965
	$\hat{P}(\hat{\tau} - \tau \leq 4)$	0.266	0.566	0.764	0.868	0.921	0.972
	$\hat{P}(\hat{\tau} - \tau \leq 5)$	0.302	0.622	0.809	0.902	0.940	0.976
	$\hat{P}(\hat{\tau} - \tau \leq 6)$	0.336	0.663	0.842	0.920	0.953	0.978
	$\hat{P}(\hat{\tau} - \tau \leq 7)$	0.364	0.700	0.868	0.934	0.961	0.980
	$\hat{P}(\hat{\tau} - \tau \leq 8)$	0.390	0.732	0.887	0.946	0.967	0.981
	$\hat{P}(\hat{\tau} - \tau \leq 9)$	0.418	0.758	0.904	0.954	0.971	0.983
	$\hat{P}(\hat{\tau} - \tau \leq 10)$	0.442	0.780	0.918	0.960	0.974	0.984
$n=10$	$\hat{P}(\hat{\tau} = \tau)$	0.107	0.294	0.492	0.617	0.706	0.932
	$\hat{P}(\hat{\tau} - \tau \leq 1)$	0.230	0.520	0.728	0.826	0.805	0.975
	$\hat{P}(\hat{\tau} - \tau \leq 2)$	0.327	0.658	0.833	0.901	0.931	0.983
	$\hat{P}(\hat{\tau} - \tau \leq 3)$	0.397	0.739	0.890	0.932	0.950	0.987
	$\hat{P}(\hat{\tau} - \tau \leq 4)$	0.461	0.795	0.922	0.946	0.959	0.989
	$\hat{P}(\hat{\tau} - \tau \leq 5)$	0.513	0.839	0.941	0.956	0.963	0.990
	$\hat{P}(\hat{\tau} - \tau \leq 6)$	0.554	0.869	0.952	0.961	0.967	0.991
	$\hat{P}(\hat{\tau} - \tau \leq 7)$	0.593	0.890	0.959	0.965	0.970	0.991
	$\hat{P}(\hat{\tau} - \tau \leq 8)$	0.626	0.908	0.965	0.968	0.972	0.992
	$\hat{P}(\hat{\tau} - \tau \leq 9)$	0.654	0.922	0.968	0.971	0.973	0.992
	$\hat{P}(\hat{\tau} - \tau \leq 10)$	0.676	0.933	0.972	0.973	0.975	0.993
$n=15$	$\hat{P}(\hat{\tau} = \tau)$	0.164	0.305	0.604	0.739	0.826	0.973
	$\hat{P}(\hat{\tau} - \tau \leq 1)$	0.329	0.533	0.830	0.905	0.938	0.992
	$\hat{P}(\hat{\tau} - \tau \leq 2)$	0.438	0.654	0.904	0.950	0.963	0.995
	$\hat{P}(\hat{\tau} - \tau \leq 3)$	0.516	0.740	0.939	0.965	0.973	0.996
	$\hat{P}(\hat{\tau} - \tau \leq 4)$	0.579	0.801	0.957	0.971	0.976	0.997
	$\hat{P}(\hat{\tau} - \tau \leq 5)$	0.633	0.844	0.968	0.976	0.979	0.997
	$\hat{P}(\hat{\tau} - \tau \leq 6)$	0.677	0.872	0.973	0.978	0.982	0.998
	$\hat{P}(\hat{\tau} - \tau \leq 7)$	0.716	0.894	0.976	0.980	0.984	0.998
	$\hat{P}(\hat{\tau} - \tau \leq 8)$	0.749	0.911	0.979	0.982	0.986	0.998
	$\hat{P}(\hat{\tau} - \tau \leq 9)$	0.772	0.924	0.981	0.983	0.986	0.999
	$\hat{P}(\hat{\tau} - \tau \leq 10)$	0.795	0.933	0.982	0.984	0.987	

Table 2.7 Empirical distribution of $\hat{\tau}$ around τ when σ_x decreases to $\delta_1 \times \sigma_x$ and σ_y decreases to $\delta_2 \times \sigma_y$ ($\delta_1 = \delta_2 = \delta < 1$).

	P/δ	0.9	0.8	0.7	0.6	0.5	0.25
$n=4$	$\hat{P}(\hat{\tau} = \tau)$	0.056	0.225	0.417	0.620	0.767	0.970
	$\hat{P}(\hat{\tau} - \tau \leq 1)$	0.128	0.420	0.674	0.849	0.933	0.994
	$\hat{P}(\hat{\tau} - \tau \leq 2)$	0.194	0.548	0.797	0.927	0.975	0.997
	$\hat{P}(\hat{\tau} - \tau \leq 3)$	0.250	0.632	0.863	0.960	0.989	0.997
	$\hat{P}(\hat{\tau} - \tau \leq 4)$	0.298	0.696	0.908	0.977	0.994	0.997
	$\hat{P}(\hat{\tau} - \tau \leq 5)$	0.342	0.746	0.937	0.987	0.995	0.998
	$\hat{P}(\hat{\tau} - \tau \leq 6)$	0.378	0.781	0.953	0.991	0.996	0.998
	$\hat{P}(\hat{\tau} - \tau \leq 7)$	0.412	0.816	0.965	0.994	0.997	0.998
	$\hat{P}(\hat{\tau} - \tau \leq 8)$	0.445	0.842	0.973	0.996	0.997	0.999
	$\hat{P}(\hat{\tau} - \tau \leq 9)$	0.472	0.862	0.979	0.997	0.998	0.999
	$\hat{P}(\hat{\tau} - \tau \leq 10)$	0.499	0.880	0.984	0.997	0.998	0.999
$n=10$	$\hat{P}(\hat{\tau} = \tau)$	0.107	0.401	0.644	0.825	0.905	0.997
	$\hat{P}(\hat{\tau} - \tau \leq 1)$	0.230	0.649	0.863	0.951	0.969	0.999
	$\hat{P}(\hat{\tau} - \tau \leq 2)$	0.327	0.770	0.932	0.976	0.980	
	$\hat{P}(\hat{\tau} - \tau \leq 3)$	0.397	0.847	0.962	0.983	0.984	
	$\hat{P}(\hat{\tau} - \tau \leq 4)$	0.461	0.890	0.978	0.987	0.986	
	$\hat{P}(\hat{\tau} - \tau \leq 5)$	0.513	0.919	0.986	0.989	0.988	
	$\hat{P}(\hat{\tau} - \tau \leq 6)$	0.554	0.939	0.989	0.990	0.990	
	$\hat{P}(\hat{\tau} - \tau \leq 7)$	0.593	0.954	0.991	0.991	0.991	
	$\hat{P}(\hat{\tau} - \tau \leq 8)$	0.626	0.965	0.992	0.992	0.991	
	$\hat{P}(\hat{\tau} - \tau \leq 9)$	0.654	0.974	0.992	0.993	0.992	
	$\hat{P}(\hat{\tau} - \tau \leq 10)$	0.676	0.980	0.993	0.993	0.992	
$n=15$	$\hat{P}(\hat{\tau} = \tau)$	0.126	0.402	0.721	0.866	0.909	0.999
	$\hat{P}(\hat{\tau} - \tau \leq 1)$	0.272	0.651	0.894	0.943	0.970	
	$\hat{P}(\hat{\tau} - \tau \leq 2)$	0.374	0.771	0.939	0.961	0.981	
	$\hat{P}(\hat{\tau} - \tau \leq 3)$	0.453	0.842	0.955	0.969	0.986	
	$\hat{P}(\hat{\tau} - \tau \leq 4)$	0.515	0.886	0.964	0.973	0.988	
	$\hat{P}(\hat{\tau} - \tau \leq 5)$	0.568	0.916	0.969	0.977	0.989	
	$\hat{P}(\hat{\tau} - \tau \leq 6)$	0.614	0.938	0.972	0.979	0.990	
	$\hat{P}(\hat{\tau} - \tau \leq 7)$	0.648	0.954	0.974	0.980	0.991	
	$\hat{P}(\hat{\tau} - \tau \leq 8)$	0.681	0.965	0.976	0.982	0.992	
	$\hat{P}(\hat{\tau} - \tau \leq 9)$	0.710	0.971	0.977	0.983	0.992	
	$\hat{P}(\hat{\tau} - \tau \leq 10)$	0.737	0.977	0.978	0.984	0.993	

Table 2.8 Empirical distribution of $\hat{\tau}$ around τ when σ_x increases to $\delta_1 \times \sigma_x$ to (or σ_y increases to $\delta_2 \times \sigma_y$) (δ_1 (or δ_2) = $\delta > 1$).

	P/δ	1.1	1.2	1.3	1.4	1.5	2.0
$n=4$	$\hat{P}(\hat{\tau} = \tau)$	0.031	0.101	0.180	0.267	0.339	0.623
	$\hat{P}(\hat{\tau} - \tau \leq 1)$	0.076	0.220	0.357	0.449	0.587	0.850
	$\hat{P}(\hat{\tau} - \tau \leq 2)$	0.114	0.301	0.479	0.617	0.712	0.932
	$\hat{P}(\hat{\tau} - \tau \leq 3)$	0.152	0.376	0.568	0.701	0.792	0.960
	$\hat{P}(\hat{\tau} - \tau \leq 4)$	0.185	0.436	0.638	0.761	0.898	0.976
	$\hat{P}(\hat{\tau} - \tau \leq 5)$	0.211	0.486	0.688	0.811	0.886	0.984
	$\hat{P}(\hat{\tau} - \tau \leq 6)$	0.235	0.529	0.732	0.846	0.912	0.987
	$\hat{P}(\hat{\tau} - \tau \leq 7)$	0.258	0.569	0.767	0.874	0.930	0.990
	$\hat{P}(\hat{\tau} - \tau \leq 8)$	0.284	0.602	0.795	0.894	0.943	0.991
	$\hat{P}(\hat{\tau} - \tau \leq 9)$	0.307	0.631	0.820	0.913	0.953	0.992
	$\hat{P}(\hat{\tau} - \tau \leq 10)$	0.327	0.658	0.842	0.927	0.961	0.993
$n=10$	$\hat{P}(\hat{\tau} = \tau)$	0.076	0.214	0.356	0.483	0.584	0.866
	$\hat{P}(\hat{\tau} - \tau \leq 1)$	0.167	0.406	0.601	0.734	0.817	0.971
	$\hat{P}(\hat{\tau} - \tau \leq 2)$	0.235	0.525	0.727	0.842	0.909	0.988
	$\hat{P}(\hat{\tau} - \tau \leq 3)$	0.293	0.618	0.809	0.902	0.947	0.992
	$\hat{P}(\hat{\tau} - \tau \leq 4)$	0.344	0.685	0.860	0.934	0.966	0.994
	$\hat{P}(\hat{\tau} - \tau \leq 5)$	0.387	0.738	0.896	0.954	0.977	0.995
	$\hat{P}(\hat{\tau} - \tau \leq 6)$	0.424	0.777	0.919	0.967	0.983	0.996
	$\hat{P}(\hat{\tau} - \tau \leq 7)$	0.459	0.811	0.936	0.975	0.987	0.996
	$\hat{P}(\hat{\tau} - \tau \leq 8)$	0.487	0.839	0.950	0.979	0.989	0.997
	$\hat{P}(\hat{\tau} - \tau \leq 9)$	0.514	0.862	0.960	0.983	0.991	0.997
	$\hat{P}(\hat{\tau} - \tau \leq 10)$	0.538	0.880	0.967	0.986	0.991	0.997
$n=15$	$\hat{P}(\hat{\tau} = \tau)$	0.068	0.208	0.465	0.617	0.708	0.937
	$\hat{P}(\hat{\tau} - \tau \leq 1)$	0.156	0.398	0.721	0.841	0.902	0.991
	$\hat{P}(\hat{\tau} - \tau \leq 2)$	0.225	0.520	0.837	0.920	0.959	0.996
	$\hat{P}(\hat{\tau} - \tau \leq 3)$	0.287	0.607	0.895	0.958	0.980	0.997
	$\hat{P}(\hat{\tau} - \tau \leq 4)$	0.339	0.674	0.930	0.975	0.998	0.998
	$\hat{P}(\hat{\tau} - \tau \leq 5)$	0.384	0.727	0.949	0.985	0.992	0.998
	$\hat{P}(\hat{\tau} - \tau \leq 6)$	0.419	0.770	0.964	0.989	0.994	0.999
	$\hat{P}(\hat{\tau} - \tau \leq 7)$	0.455	0.806	0.973	0.992	0.995	0.999
	$\hat{P}(\hat{\tau} - \tau \leq 8)$	0.487	0.834	0.979	0.994	0.996	0.999
	$\hat{P}(\hat{\tau} - \tau \leq 9)$	0.518	0.857	0.983	0.995	0.996	0.999
	$\hat{P}(\hat{\tau} - \tau \leq 10)$	0.543	0.876	0.987	0.995	0.997	0.999

Table 2.9 Empirical distribution of $\hat{\tau}$ around τ when σ_x decreases to $\delta_1 \times \sigma_x$ (or σ_y decreases to $\delta_2 \times \sigma_y$) (δ_1 (OR δ_2) = $\delta < 1$).

	P/δ	0.9	0.8	0.7	0.6	0.5	0.25
$n=4$	$\hat{P}(\hat{\tau} = \tau)$	0.032	0.139	0.285	0.464	0.628	0.934
	$\hat{P}(\hat{\tau} - \tau \leq 1)$	0.086	0.291	0.515	0.720	0.858	0.992
	$\hat{P}(\hat{\tau} - \tau \leq 2)$	0.132	0.398	0.657	0.832	0.938	0.998
	$\hat{P}(\hat{\tau} - \tau \leq 3)$	0.170	0.483	0.739	0.897	0.969	0.999
	$\hat{P}(\hat{\tau} - \tau \leq 4)$	0.204	0.547	0.798	0.935	0.983	0.999
	$\hat{P}(\hat{\tau} - \tau \leq 5)$	0.235	0.605	0.843	0.958	0.990	0.999
	$\hat{P}(\hat{\tau} - \tau \leq 6)$	0.265	0.647	0.877	0.973	0.994	0.999
	$\hat{P}(\hat{\tau} - \tau \leq 7)$	0.292	0.685	0.900	0.982	0.997	
	$\hat{P}(\hat{\tau} - \tau \leq 8)$	0.314	0.716	0.919	0.987	0.998	
	$\hat{P}(\hat{\tau} - \tau \leq 9)$	0.337	0.746	0.933	0.990	0.998	
	$\hat{P}(\hat{\tau} - \tau \leq 10)$	0.359	0.771	0.946	0.993	0.998	
$n=10$	$\hat{P}(\hat{\tau} = \tau)$	0.083	0.284	0.519	0.708	0.855	0.990
	$\hat{P}(\hat{\tau} - \tau \leq 1)$	0.189	0.512	0.814	0.911	0.971	0.997
	$\hat{P}(\hat{\tau} - \tau \leq 2)$	0.267	0.645	0.876	0.965	0.991	0.998
	$\hat{P}(\hat{\tau} - \tau \leq 3)$	0.326	0.731	0.926	0.983	0.995	0.998
	$\hat{P}(\hat{\tau} - \tau \leq 4)$	0.382	0.794	0.954	0.992	0.996	0.998
	$\hat{P}(\hat{\tau} - \tau \leq 5)$	0.433	0.838	0.969	0.995	0.997	0.998
	$\hat{P}(\hat{\tau} - \tau \leq 6)$	0.476	0.868	0.980	0.996	0.997	0.999
	$\hat{P}(\hat{\tau} - \tau \leq 7)$	0.513	0.893	0.987	0.997	0.997	
	$\hat{P}(\hat{\tau} - \tau \leq 8)$	0.546	0.914	0.990	0.998	0.998	
	$\hat{P}(\hat{\tau} - \tau \leq 9)$	0.573	0.929	0.993	0.998	0.998	
	$\hat{P}(\hat{\tau} - \tau \leq 10)$	0.603	0.941	0.995	0.998	0.998	
$n=15$	$\hat{P}(\hat{\tau} = \tau)$	0.106	0.286	0.613	0.806	0.855	0.990
	$\hat{P}(\hat{\tau} - \tau \leq 1)$	0.232	0.509	0.836	0.944	0.975	0.997
	$\hat{P}(\hat{\tau} - \tau \leq 2)$	0.323	0.638	0.920	0.974	0.992	0.998
	$\hat{P}(\hat{\tau} - \tau \leq 3)$	0.398	0.724	0.955	0.982	0.996	0.999
	$\hat{P}(\hat{\tau} - \tau \leq 4)$	0.456	0.784	0.972	0.987	0.997	0.999
	$\hat{P}(\hat{\tau} - \tau \leq 5)$	0.507	0.832	0.980	0.989	0.998	0.999
	$\hat{P}(\hat{\tau} - \tau \leq 6)$	0.550	0.866	0.984	0.990	0.998	0.999
	$\hat{P}(\hat{\tau} - \tau \leq 7)$	0.592	0.892	0.986	0.990	0.998	
	$\hat{P}(\hat{\tau} - \tau \leq 8)$	0.623	0.911	0.988	0.991	0.998	
	$\hat{P}(\hat{\tau} - \tau \leq 9)$	0.652	0.928	0.989	0.992	0.999	
	$\hat{P}(\hat{\tau} - \tau \leq 10)$	0.677	0.939	0.990	0.992	0.999	

Table 2.10 Empirical distribution of $\hat{\tau}$ around τ when σ_x increases to $\delta_1 \times \sigma_x$ ($\delta_1 > 1$) while σ_y decreases to $\delta_2 \times \sigma_y$ ($\delta_2 < 1$).

δ_1		1.1	1.2	1.3	1.4	1.5	2.0
δ_2		0.9	0.8	0.7	0.6	0.5	0.25
$n=4$	$\hat{P}(\hat{\tau} = \tau)$	0.076	0.230	0.415	0.597	0.731	0.966
	$\hat{P}(\hat{\tau} - \tau \leq 1)$	0.172	0.446	0.674	0.833	0.923	0.998
	$\hat{P}(\hat{\tau} - \tau \leq 2)$	0.244	0.575	0.801	0.924	0.974	
	$\hat{P}(\hat{\tau} - \tau \leq 3)$	0.308	0.668	0.874	0.960	0.992	
	$\hat{P}(\hat{\tau} - \tau \leq 4)$	0.359	0.734	0.917	0.980	0.997	
	$\hat{P}(\hat{\tau} - \tau \leq 5)$	0.408	0.785	0.943	0.989	0.998	
	$\hat{P}(\hat{\tau} - \tau \leq 6)$	0.450	0.822	0.959	0.993	0.999	
	$\hat{P}(\hat{\tau} - \tau \leq 7)$	0.483	0.853	0.971	0.995	0.999	
	$\hat{P}(\hat{\tau} - \tau \leq 8)$	0.513	0.875	0.979	0.997		
	$\hat{P}(\hat{\tau} - \tau \leq 9)$	0.543	0.894	0.984	0.998		
	$\hat{P}(\hat{\tau} - \tau \leq 10)$	0.570	0.911	0.989	0.998		
$n=10$	$\hat{P}(\hat{\tau} = \tau)$	0.162	0.460	0.691	0.855	0.942	0.999
	$\hat{P}(\hat{\tau} - \tau \leq 1)$	0.338	0.713	0.902	0.975	0.995	
	$\hat{P}(\hat{\tau} - \tau \leq 2)$	0.450	0.828	0.963	0.994	0.999	
	$\hat{P}(\hat{\tau} - \tau \leq 3)$	0.531	0.890	0.983	0.998		
	$\hat{P}(\hat{\tau} - \tau \leq 4)$	0.599	0.928	0.993	0.999		
	$\hat{P}(\hat{\tau} - \tau \leq 5)$	0.646	0.951	0.996			
	$\hat{P}(\hat{\tau} - \tau \leq 6)$	0.691	0.966	0.998			
	$\hat{P}(\hat{\tau} - \tau \leq 7)$	0.726	0.976	0.999			
	$\hat{P}(\hat{\tau} - \tau \leq 8)$	0.758	0.984				
	$\hat{P}(\hat{\tau} - \tau \leq 9)$	0.782	0.988				
	$\hat{P}(\hat{\tau} - \tau \leq 10)$	0.803	0.991				
$n=15$	$\hat{P}(\hat{\tau} = \tau)$	0.220	0.570	0.807	0.931	0.980	0.999
	$\hat{P}(\hat{\tau} - \tau \leq 1)$	0.419	0.808	0.952	0.991	0.999	
	$\hat{P}(\hat{\tau} - \tau \leq 2)$	0.548	0.902	0.986	0.997	0.999	
	$\hat{P}(\hat{\tau} - \tau \leq 3)$	0.635	0.944	0.995	0.998	0.999	
	$\hat{P}(\hat{\tau} - \tau \leq 4)$	0.701	0.966	0.997	0.999	0.999	
	$\hat{P}(\hat{\tau} - \tau \leq 5)$	0.749	0.979	0.998	0.999		
	$\hat{P}(\hat{\tau} - \tau \leq 6)$	0.790	0.986	0.998	0.999		
	$\hat{P}(\hat{\tau} - \tau \leq 7)$	0.821	0.990	0.998	0.999		
	$\hat{P}(\hat{\tau} - \tau \leq 8)$	0.847	0.992	0.999	0.999		
	$\hat{P}(\hat{\tau} - \tau \leq 9)$	0.877	0.994	0.999	0.999		
	$\hat{P}(\hat{\tau} - \tau \leq 10)$	0.887	0.994	0.999	0.999		

2.5 Illustrative example

We will now give an illustrative example on how to use the proposed estimator in practice. Considering the lumber manufacturing example of Alt (1985), data generated from the in-control mean vector and covariance matrix are given as:

$$\boldsymbol{\mu}_0 = (265, 470)', \text{ and } \boldsymbol{\Sigma}_0 = \begin{bmatrix} 100 & 66 \\ 66 & 121 \end{bmatrix}.$$

The given quality characteristics are stiffness (X_1) and bending strength (X_2) on lumber boards. Each subgroup consists of $n = 10$ lumber boards. Our procedure will be illustrated with generalized variance control chart based on its distributional properties. When the desired Type-I error (α) is 0.0054, then, the upper control limit for this chart is 31,349 and the lower control limit is 512.87. Under the assumption that the process is in-control, the first 15 samples were generated from *iid* $N_2(\boldsymbol{\mu}_0, \boldsymbol{\Sigma}_0)$ and the remaining samples were generated from *iid* $N_2(\boldsymbol{\mu}_0, \boldsymbol{\Sigma}_1)$ until the control chart issued a signal. Here, $\boldsymbol{\Sigma}_1$ denotes the changed covariance matrix where the standard deviations of each quality characteristics have increased by 30 percent:

$$\boldsymbol{\Sigma}_1 = \begin{bmatrix} (1.3)^2 \times 100 & (1.3)^2 \times 66 \\ (1.3)^2 \times 66 & (1.3)^2 \times 121 \end{bmatrix} = \begin{bmatrix} 169.00 & 111.54 \\ 111.54 & 204.49 \end{bmatrix}.$$

When the twentieth subgroup was generated, generalized variance control chart has issued a signal. That means following the signal at $T = 20$, the C statistics can be calculated. Our aim in this procedure is to find the maximum value of C , in other words, to find where the change occurred in the interval of $0 \leq t \leq T - 1$.

According to Table 2.11, the generalized control chart did not issue a signal until the twentieth subgroup was generated. On the other hand, the change point estimator has its maximum value in the sixteenth subgroup. That means, the fifteenth subgroup was the last subgroup obtained from in-control process and the sixteenth

Table 2.11 Subgroup average vectors, generalized variances and C statistics

i	\bar{X}_{i1}	\bar{X}_{i2}	$ S $	t	C_t
1	263.77	469.83	5,673	0	3.77
2	266.33	468.63	4,975.9	1	4.03
3	264.40	470.88	3,418.2	2	3.40
4	265.67	469.07	7,803.5	3	4.05
5	267.91	471.15	2,199.2	4	4.36
6	269.53	470.94	6,442.5	5	4.90
7	270.88	474.23	2,009.3	6	5.15
8	265.66	469.93	8,734.6	7	5.75
9	263.01	471.20	2,982.2	8	5.60
10	261.97	469.06	8,337.8	9	5.88
11	263.01	466.69	6,996.5	10	6.27
12	264.13	469.62	6,583.5	11	6.96
13	266.21	471.76	5,427.5	12	8.12
14	264.69	470.15	6,535.5	13	9.20
15	267.73	475.78	4,500.1	14	10.68
16	263.08	473.58	23,455	15	12.86
17	265.94	469.82	24,666	16	9.60
18	274.40	470.35	6,207.7	17	8.39
19	258.72	464.66	10,628	18	6.12
20	268.59	474.84	41,421	19	5.47

subgroup was the first subgroup of the changed process, as we initially aimed. For the practitioners, investigating the signal issued subgroup is not sufficient to find

out the special cause. As it is occurred in our illustrative example, a step change may exist several subgroups earlier from the signal of the control chart.

2.6 Conclusions

Maximum likelihood estimation of a change point combined with control charts is a practical and considerably rational way of identification of the time of a step change and its special causes in industrial processes. For univariate and multivariate statistical process control, several estimators have been proposed. The certain information of the time of a step change is in great importance in statistical process control, including multivariate cases. Even though, the generalized variance control chart is designed to detect the change in multivariate normal process variance, a considerable delay may exist in issuing a signal after the change occurs. Moreover, the detection performance of the chart decreases, respectively, with small magnitudes of shift in covariance matrix. Using generalized variance control chart with the proposed procedure would be beneficial for detecting changes and identifying special causes for practitioners.

In this section, a change point estimator ($\hat{\tau}$) is proposed which is capable of identifying the change point of a step change in a multivariate normal process covariance. The proposed estimator is assumed to be calculated under the assumption that the mean vector remains the same after the change and only the covariance matrix changes. The estimator indicates the time of the change after a signal is issued by generalized variance control chart. The performance of the estimator is evaluated with Monte Carlo simulation results. For different structural changes in covariance matrix and various sample sizes, it is indicated that our change point estimator is considerably effective in both accuracy and precision. It is shown that, the estimator is respectively effective in estimating the time for the case when one of the standard deviation increases while the other decreases. The simulation runs help us to show that the estimator performs well for various sample sizes and even for small changes (decrease or increase) which yield large run lengths in the control chart. An illustrative example is considered to indicate the practical

use of the change point estimator. This hypothetical example indicates the ease of implementation and interpretation.

CHAPTER THREE
A MULTIVARIATE CHANGE POINT DETECTION PROCEDURE FOR
MONITORING MEAN AND COVARIANCE SIMULTANEOUSLY

3.1 Introduction

Control charts have proven to be effective for improving process performance in addition to the fact that they are easy for practitioners to apply and interpret. There has been an increasing interest in multivariate quality control practices in the industry. Many industrial processes are characterized by several inter-related quality metrics. The efforts to monitor the mean vector started with Hotelling's T^2 control chart in 1947. When the process parameters are known or can be estimated, this chart plots $n(\bar{\mathbf{X}}_i - \boldsymbol{\mu}_0)' \boldsymbol{\Sigma}_0^{-1} (\bar{\mathbf{X}}_i - \boldsymbol{\mu}_0)$ where $\mathbf{X}_i \sim N_p(\boldsymbol{\mu}_0, \boldsymbol{\Sigma}_0)$, $i = 1, 2, \dots, n$. If a point falls beyond the upper control limit $UCL = \chi_{p,1-\alpha}^2$, the process is considered to be out of control. This control chart is also called Phase II X^2 chart or χ^2 chart (Bersimis et al., 2007). As monitoring only the mean vector is not an effective way of controlling the process, many authors focused on developing the methods to monitor dispersion. Alt (1985) and Alt and Smith (1988) proposed different procedures of carrying out multivariate dispersion control and monitoring. They proposed the multivariate analogue of the univariate S -chart. In this chart, $|\mathbf{S}_i|^{1/2}$ values are plotted when the control limits are given in (1.1).

For discussions and reviews of multivariate mean and dispersion control charts, see, for example, Lowry and Montgomery (1995), Alt (1985) and Alt and Smith (1988), Surtihadi et al. (2004), Khoo and Quah (2004), Bersimis et al. (2007), and Vargas and Lagos (2007).

The mean vector monitoring procedures are affected by the shifts in covariance but it is known that a variance chart is not affected by the shifts in mean vector. This leads to an understanding of the importance of joint performance of the mean and variance charts. Since a successful monitoring program requires monitoring both

mean vector and covariance shifts, the importance of simultaneously monitoring process mean and variability has been increased. The traditional way of simultaneous monitoring is done by constructing two charts: one for the mean and one for the variability. In other words, χ^2 and $|\mathbf{S}|$ charts are used simultaneously. If any of them or both of them generates a signal the process is considered to be out-of-control. There are several simultaneous control alternatives to this approach in the literature. Chen et al. (2005) proposed a single multivariate exponentially moving average (MEWMA) control chart to monitor mean vector and covariance matrix simultaneously. Thaga and Gabaitiri (2006) proposed the Multivariate Maximum Control Chart which is capable of jointly monitoring the mean and covariance shifts. The basic idea in these procedures, namely the Max-MEWMA and Max-M charts, is to transform the monitoring statistics for mean and covariance to standardized normal random variables and determining the maximum of these standard normal readings. Machado et al. (2009) proposed the MVMAX chart and the joint use of two charts based on the non-central chi-square statistic. Zhang et al. (2010) proposed a single MEWMA chart based on the generalized likelihood ratio (GLR) test for joint monitoring both the multivariate mean and variability.

Control charts generate a signal when a change in the process distribution is detected and has a potential delay to generate this signal. However, the signal does not indicate that a special cause actually occurred at that particular point in trigger time (Park and Park, 2004). Since accurate and precise estimation of the change point is vital for many processes, using follow-up change point estimation procedures is recommended. Park and Park (2004) applied the univariate joint maximum likelihood estimator (MLE) of the change point for mean and variance. They investigated the performance of their follow-up estimator for $\bar{X} - S$ combination control chart. Lee and Park (2007) proposed the MLEs for the change point to detect the time of a change in process mean and/or variability with both fixed sampling rate and variable sampling rate. They investigated the performance of this estimator for Shewhart, EWMA and CUSUM charts. Sullivan and Woodall (2000) proposed a single multivariate control chart based on GLR for multivariate individual process readings. They also divided the test statistics into a

part for the mean shift and another part for the covariance shift. Their approach was able to detect the location of a shift, the presence of multiple changes and the type of the change (mean shift, covariance shift or combination shift). Zamba and Hawkins (2009) proposed a multivariate change point model through GLR statistics for estimating the change in mean vector and/or covariance structure. Their change point model is able to monitor short runs and unknown or not fully known parameter processes.

In this study, joint estimation of a change point is applied to multivariate normal processes for monitoring both mean and covariance shifts. A follow up change point estimation procedure is proposed for Phase II applications following the work of Samuel et al. (1998a, 1998b), Nedumaran et al. (2000), Pignatiello and Samuel (2001), and Dogu and Deveci-Kocakoc(2011a). The proposed change point estimator is a complementary procedure for multivariate mean and covariance monitoring control charts. Our proposed estimator focuses on estimating the most likely location of the change after a single or combination multivariate control chart issues a signal. This procedure helps process engineers and professionals to find the location of the change when monitoring the mean vector and covariance matrix simultaneously. As many industrial professionals prefer applying χ^2 and $|\mathbf{S}|$ control charts simultaneously for this case, the proposed ‘add-on’ procedure is very useful in practice. When the combination chart generates a signal, they can estimate the change point and investigate the assignable cause(s). Some other alternative multivariate charting techniques including MCUSUMs and MEWMAAs for simultaneous location and dispersion monitoring can be applied to this procedure, but our performance analysis focuses on the change point estimation for χ^2 and $|\mathbf{S}|$ charts.

The remainder of this paper is organized as follows: the next section gives the details of the model assumptions. In the third section, estimation procedure is given. Performance assessment and other performance measurements are provided in the following section. Then an illustrative example for spring manufacturing and conclusions are presented.

3.2 Process model assumptions

It is assumed that the process distribution is p -variate normal with known mean vector $\boldsymbol{\mu}_0$ and known covariance matrix $\boldsymbol{\Sigma}_0$. Suppose that p -critical quality characteristics are monitored with χ^2 and $|\mathbf{S}|$ control charts. Let $\mathbf{X}_{ij} = (X_{ij1}, X_{ij2}, \dots, X_{ijp})'$ be a $p \times 1$ vector which represents the p characteristics of the j^{th} observation ($j = 1, 2, \dots, n$) for the i^{th} subgroup of size n . Suppose further that when the process is in control, the \mathbf{X}_{ij} 's are independent and identically distributed (*iid*) and follow a p -dimensional Normal distribution with mean vector $\boldsymbol{\mu}_0$ and covariance matrix $\boldsymbol{\Sigma}_0$ that is, the \mathbf{X}_{ij} 's are *iid* $N_p(\boldsymbol{\mu}_0, \boldsymbol{\Sigma}_0)$. We let n denote the subgroup size and we let $\bar{\mathbf{X}}_i$ denote the average vector of the i^{th} subgroup. It is assumed that when the multivariate process mean and dispersion changes, there has been a step-change from its in-control value of $\boldsymbol{\mu} = \boldsymbol{\mu}_0$ and $\boldsymbol{\Sigma} = \boldsymbol{\Sigma}_0$ to an unknown value $\boldsymbol{\mu} = \boldsymbol{\mu}_1$ and $\boldsymbol{\Sigma} = \boldsymbol{\Sigma}_1$ where $\boldsymbol{\mu}_0 \neq \boldsymbol{\mu}_1$ and $\boldsymbol{\Sigma}_0 \neq \boldsymbol{\Sigma}_1$. If control chart statistics exceed the control limits, it is concluded that the step-change in the process parameters occurred after some unknown time τ , where $0 \leq \tau \leq T - 1$ and T is the time that the combination chart signals.

3.3 Estimation of the change point

After determining the process model assumptions, we consider the derivation of the maximum likelihood estimator (MLE) of the change point τ when a step change occurs in the process mean vector and/or covariance matrix. It is assumed that the process experiences a change at an unknown time, τ . The change is detected at the time T by the combination control chart. We assume that the subgroup averages $\bar{\mathbf{X}}_1, \bar{\mathbf{X}}_2, \dots, \bar{\mathbf{X}}_\tau$ and subgroup covariances $\mathbf{S}_1, \mathbf{S}_2, \dots, \mathbf{S}_\tau$ come from in-control process and the subgroup averages $\bar{\mathbf{X}}_{\tau+1}, \bar{\mathbf{X}}_{\tau+2}, \dots, \bar{\mathbf{X}}_T$ and the subgroup covariances $\mathbf{S}_{\tau+1}, \mathbf{S}_{\tau+2}, \dots, \mathbf{S}_T$ come from the out-of-control process. It is further assumed that the process mean vector and covariance matrix remains at the new level until the

special cause is identified. The MLE of τ can be the value of t for which the statistic MC attains its maximum; that is,

$$\hat{\tau}_{MC} = \arg \max_t (MC_t), \quad t = 0, 1, \dots, T-1, \quad (3.1)$$

where

$$MC_t = \left[\frac{1}{2} \left(\text{tr} \left(\Sigma_0^{-1} \sum_{i=t+1}^T \sum_{j=1}^n (\mathbf{x}_{ij} - \boldsymbol{\mu}_0)' (\mathbf{x}_{ij} - \boldsymbol{\mu}_0) \right) \right) - \frac{n(T-t)}{2} \log_e \left(\left| \left(\sum_{i=t+1}^T \sum_{j=1}^n (\mathbf{x}_{ij} - \bar{\mathbf{x}}_{T,t}) (\mathbf{x}_{ij} - \bar{\mathbf{x}}_{T,t})' \right) / n(T-t) \right| \Sigma_0 \right) - \frac{np(T-t)}{2} \right], \quad (3.2)$$

and

$$\hat{\boldsymbol{\mu}}_1 = \bar{\mathbf{X}}_{t,T} = \frac{1}{T-t} \sum_{i=t+1}^T \bar{\mathbf{X}}_i \quad \text{and} \quad \hat{\Sigma}_1 = \frac{1}{n(T-t)} \sum_{i=t+1}^T \sum_{j=1}^n (\mathbf{x}_{ij} - \hat{\boldsymbol{\mu}}_1) (\mathbf{x}_{ij} - \hat{\boldsymbol{\mu}}_1)' \quad \text{are the}$$

MLE's of mean vector and covariance matrix of the $(T-t)$ most recent subgroup averages.

Derivation of the MLE of τ , the multivariate joint process change point estimator is as follows:

$$\log L(\tau, \Sigma_1) = \log_e \left(\frac{1}{(2\pi)^{np/2} |\Sigma_0|^{n/2}} \right)^\tau + \log_e \left(\frac{1}{(2\pi)^{np/2} |\Sigma_1|^{n/2}} \right)^{T-\tau} - \frac{1}{2} \left[\sum_{i=1}^{\tau} \sum_{j=1}^n (\mathbf{x}_{ij} - \boldsymbol{\mu}_0)' \Sigma_0^{-1} (\mathbf{x}_{ij} - \boldsymbol{\mu}_0) \right] - \frac{1}{2} \left[\sum_{i=\tau+1}^T \sum_{j=1}^n (\mathbf{x}_{ij} - \boldsymbol{\mu}_1)' \Sigma_1^{-1} (\mathbf{x}_{ij} - \boldsymbol{\mu}_1) \right].$$

The first part of the function can be written as;

$$-\frac{n\tau}{2} \log_e \left((2\pi) |\Sigma_0| \right) - \frac{n(T-\tau)}{2} \log_e \left((2\pi) |\Sigma_1| \right).$$

There are three unknowns in the likelihood function; τ , $\boldsymbol{\mu}_1$ and $\boldsymbol{\Sigma}_1$. If the change point τ would be known, the MLE of $\boldsymbol{\mu}_1$ and $\boldsymbol{\Sigma}_1$ would be;

$$\hat{\boldsymbol{\mu}}_1 = \bar{\bar{\mathbf{X}}}_{t,T} = \frac{1}{T-t} \sum_{i=t+1}^T \bar{\mathbf{X}}_i, \quad \hat{\boldsymbol{\Sigma}}_1 = \frac{1}{n(T-t)} \sum_{i=t+1}^T \sum_{j=1}^n (\mathbf{X}_{ij} - \hat{\boldsymbol{\mu}}_1)(\mathbf{X}_{ij} - \hat{\boldsymbol{\mu}}_1)'$$

Substituting $\hat{\boldsymbol{\mu}}_1$ and $\hat{\boldsymbol{\Sigma}}_1$ into the log likelihood function, then

$$\begin{aligned} \log_e L(\tau, \boldsymbol{\Sigma}_1) &= \frac{1}{2} \sum_{i=t+1}^T \sum_{j=1}^n (\mathbf{X}_{ij} - \boldsymbol{\mu}_0)' \boldsymbol{\Sigma}_0^{-1} (\mathbf{X}_{ij} - \boldsymbol{\mu}_0) \\ &\quad - \frac{n(T-t)}{2} \log_e \left(\left| \left(\sum_{i=t+1}^T \sum_{j=1}^n (\mathbf{X}_{ij} - \bar{\bar{\mathbf{X}}}_{T,t}) (\mathbf{X}_{ij} - \bar{\bar{\mathbf{X}}}_{T,t})' \right) \right| / n(T-t) |\boldsymbol{\Sigma}_0| \right) - \frac{np(T-t)}{2}. \end{aligned}$$

The MLE estimate of τ is the value of t that maximizes the log-likelihood function. So;

$$\begin{aligned} MC_t &= \frac{1}{2} \left(tr \left(\boldsymbol{\Sigma}_0^{-1} \sum_{i=t+1}^T \sum_{j=1}^n (\mathbf{X}_{ij} - \boldsymbol{\mu}_0)' (\mathbf{X}_{ij} - \boldsymbol{\mu}_0) \right) \right) \\ &\quad - \frac{n(T-t)}{2} \log_e \left(\left| \left(\sum_{i=t+1}^T \sum_{j=1}^n (\mathbf{X}_{ij} - \bar{\bar{\mathbf{X}}}_{T,t}) (\mathbf{X}_{ij} - \bar{\bar{\mathbf{X}}}_{T,t})' \right) \right| / n(T-t) |\boldsymbol{\Sigma}_0| \right) - \frac{np(T-t)}{2}, \end{aligned}$$

$$\hat{\tau}_{MC} = \arg \max_{0 < t < T-1} [MC_t]$$

$$\begin{aligned} \hat{\tau}_{MC} &= \arg \max_{0 < t < T-1} \left[\frac{1}{2} \left(tr \left(\boldsymbol{\Sigma}_0^{-1} \sum_{i=t+1}^T \sum_{j=1}^n (\mathbf{X}_{ij} - \boldsymbol{\mu}_0)' (\mathbf{X}_{ij} - \boldsymbol{\mu}_0) \right) \right) \right. \\ &\quad \left. - \frac{n(T-t)}{2} \log_e \left(\left| \left(\sum_{i=t+1}^T \sum_{j=1}^n (\mathbf{X}_{ij} - \bar{\bar{\mathbf{X}}}_{T,t}) (\mathbf{X}_{ij} - \bar{\bar{\mathbf{X}}}_{T,t})' \right) \right| / n(T-t) |\boldsymbol{\Sigma}_0| \right) - \frac{np(T-t)}{2} \right]. \end{aligned}$$

3.4 Performance assessment of the proposed estimator

The performance assessment of our proposed estimator is investigated and evaluated by Monte Carlo simulation. The simulation study is focused on Phase II performance of the proposed estimator. The ‘average change point estimate’ and ‘the empirical distribution of the estimated change point around the actual change point’ were used by Samuel et al. (1998a, 1998b), Nedumaran et al. (2000), Park and Park (2004) and Dogu and Deveci-Kocakoc (2011a) as the performance indicators. The simulation study settings are constructed for bivariate case for simplicity and these performance indicators are investigated.

Observations were randomly generated from a $N_p(\boldsymbol{\mu}_0, \boldsymbol{\Sigma}_0)$ distribution when $i \leq 50$, the on-target mean vector was $\boldsymbol{\mu}_0 = (0,0)'$ and the in-control covariance matrix was selected as follows:

$$\boldsymbol{\Sigma}_0 = \begin{bmatrix} 1 & \rho \\ \rho & 1 \end{bmatrix},$$

where $-1 \leq \rho \leq 1$ is the correlation coefficient between two quality characteristics. In this study, the correlation coefficient was set to 0.0, 0.5 and 0.9 and Type I error probability was set to 0.0027 which is frequently used in SPC applications. While the process is in-control, the observations which exceed the control limits are considered as false alarms. If a false alarm at the i^{th} observation ($i \leq \tau$) occurred, it was treated in the same way that a false alarm would be treated on an actual process. When an actual false alarm is determined in a process, the process professionals consider the process is in control and let the monitoring restart. The same approach is used in the simulation study. If i^{th} observation was a false alarm, then the control chart restarted at $(i+1)^{\text{th}}$ observation and the change point remained in its scheduled point. Starting with subgroup 51, the observations were randomly generated from $N_p(\boldsymbol{\mu}_1, \boldsymbol{\Sigma}_1)$ until the combination control chart issued a signal. The structure of the changed mean vector and covariance matrix are given as:

$$\boldsymbol{\mu}'_1 = \begin{pmatrix} \mu_x + \lambda_1 \\ \mu_y + \lambda_2 \end{pmatrix}, \boldsymbol{\Sigma}_1 = \begin{pmatrix} \delta_1^2 \times \sigma_x^2 & \rho \times \delta_1 \times \delta_2 \times \sigma_x \times \sigma_y \\ \rho \times \delta_1 \times \delta_2 \times \sigma_x \times \sigma_y & \delta_2^2 \times \sigma_y^2 \end{pmatrix}.$$

For every run, when the combination control chart issued a signal, the time of the change was calculated with the proposed estimator. This procedure was repeated a total of 10,000 times for each of the case and different magnitudes, denoted by δ and λ , for the subgroup size of $n = 4$. The average of change point estimates for every simulation run was computed along with its standard error to investigate the accuracy of our estimator. Additionally, the empirical distributions of the estimated change point around the actual change point for all cases and magnitudes of shift were considered in order to evaluate the precision of the estimator.

3.4.1 Accuracy Evaluation

In order to measure the accuracy performance of the change point estimator, the average change point estimation is considered, which is denoted by $E(T)$ of the combination chart. $E(T)$ can be expressed as the sum of Average Run Length (ARL) and exact change point (τ). If the practitioner chose $\alpha_1 = \alpha_2 = \alpha$, then the combination of χ^2 and $|\mathbf{S}|$ charts has a combined Type I error probability of $1 - (1 - \alpha)^2$. As we chose $\alpha = 0.0027$, the ARL of the combination chart was expected to be $1 / (1 - (1 - \alpha)^2) = 1 / 0.0054 \cong 185$ when no shifts of mean vector and covariance matrix were introduced.

Since this simulation study aimed to compute the estimation of τ , the last sample from the in control process, $\bar{\tau}$ should be close to 50.

Table 3.1 Expected time of a signal, average change point estimates and their standard errors after a combination chart signals; $\tau = 50$, $\rho = 0.0$ and 10,000 independent simulation runs

Covariance Shift Setting			Mean Shift Setting						
			1	2	3	4	5	6	7
λ_1			0	0	0	0.5	1	0	2
δ_1	δ_2	λ_2	0	0.5	1	1	1	2	2
1	1	$E(T)$	234.68	107.55	59.20	56.41	53.08	51.32	51.01
		$\bar{\hat{\tau}}$	-	51.19	49.91	49.77	49.67	49.54	49.85
		Std. error	-	0.08	0.04	0.04	0.03	0.03	0.02
1.3	1	$E(T)$	92.12	73.92	56.66	54.88	52.70	52.70	51.02
		$\bar{\hat{\tau}}$	53.19	50.34	49.77	49.75	49.65	49.63	49.84
		Std. error	0.14	0.06	0.04	0.03	0.03	0.03	0.02
1.3	1.3	$E(T)$	65.97	60.55	54.48	53.68	52.36	51.34	51.03
		$\bar{\hat{\tau}}$	50.31	49.89	49.67	49.59	49.56	49.56	49.85
		Std. error	0.09	0.07	0.04	0.04	0.04	0.03	0.02
1.5	1.3	$E(T)$	59.40	57.01	53.72	53.13	53.65	52.20	51.04
		$\bar{\hat{\tau}}$	49.71	49.55	49.51	49.51	49.57	49.54	49.85
		Std. error	0.07	0.06	0.05	0.04	0.05	0.04	0.02
2	2	$E(T)$	52.02	51.91	51.67	51.45	51.47	51.23	51.06
		$\bar{\hat{\tau}}$	49.21	49.28	49.40	49.49	49.45	49.68	49.88
		Std. error	0.05	0.04	0.04	0.04	0.04	0.03	0.01

Table 3.2 Expected time of a signal, average change point estimates and their standard errors after a combination chart signals; $\tau = 50$, $\rho = 0.5$ and 10,000 independent simulation runs

Covariance Shift Setting			Mean Shift Setting						
			1	2	3	4	5	6	7
λ_1			0	0	0	0.5	1	0	2
δ_1	δ_2	λ_2	0	0.5	1	1	1	2	2
1	1	$E(T)$	234.68	93.23	55.73	59.11	55.79	51.11	51.10
		$\bar{\hat{\tau}}$	-	50.61	49.76	49.94	49.78	49.70	49.69
		Std. error	-	0.06	0.04	0.03	0.03	0.02	0.03
1.3	1	$E(T)$	90.22	65.46	54.53	56.74	54.41	51.10	51.13
		$\bar{\hat{\tau}}$	52.53	50.37	49.69	49.85	49.73	49.70	49.67
		Std. error	0.12	0.06	0.04	0.03	0.04	0.03	0.03
1.3	1.3	$E(T)$	59.40	59.19	53.45	54.49	53.46	51.16	51.16
		$\bar{\hat{\tau}}$	49.66	49.72	49.51	49.64	49.64	49.67	49.68
		Std. error	0.07	0.06	0.04	0.04	0.04	0.03	0.03
1.5	1.3	$E(T)$	59.30	56.51	53.01	53.67	52.99	51.15	51.17
		$\bar{\hat{\tau}}$	49.53	49.57	49.56	49.50	49.54	49.67	49.70
		Std. error	0.07	0.05	0.04	0.04	0.04	0.03	0.02
2	2	$E(T)$	52.00	51.88	51.58	51.67	51.59	51.15	51.17
		$\bar{\hat{\tau}}$	49.21	49.26	49.39	49.40	49.47	49.76	49.73
		Std. error	0.05	0.05	0.04	0.04	0.04	0.02	0.02

Table 3.3 Expected time of a signal, average change point estimates and their standard errors after a combination chart signals; $\tau = 50$, $\rho = 0.9$ and 10,000 independent simulation runs

Covariance Shift Setting			Mean Shift Setting						
			1	2	3	4	5	6	7
λ_1			0	0	0	0.5	1	0	2
δ_1	δ_2	λ_2	0	0.5	1	1	1	2	2
1	1	$E(T)$	234.68	55.90	51.11	53.44	58.47	51.00	51.26
		$\bar{\hat{\tau}}$	-	49.77	49.67	49.65	49.81	50.00	49.55
		Std. error	-	0.03	0.02	0.03	0.04	0.00	0.03
1.3	1	$E(T)$	75.02	54.28	51.13	52.85	55.51	51.00	51.00
		$\bar{\hat{\tau}}$	50.49	49.79	49.74	49.74	49.84	50.00	49.99
		Std. error	0.05	0.03	0.02	0.03	0.03	0.00	0.00
1.3	1.3	$E(T)$	66.10	53.51	51.17	52.59	54.32	51.00	51.32
		$\bar{\hat{\tau}}$	50.23	49.56	49.69	49.57	49.59	49.99	49.61
		Std. error	0.09	0.04	0.02	0.04	0.04	0.00	0.03
1.5	1.3	$E(T)$	58.79	52.97	51.16	52.30	53.48	51.00	51.31
		$\bar{\hat{\tau}}$	49.66	49.54	49.71	49.56	49.61	49.99	49.68
		Std. error	0.06	0.04	0.03	0.04	0.04	0.00	0.03
2	2	$E(T)$	52.03	51.59	51.16	51.49	51.65	51.00	51.21
		$\bar{\hat{\tau}}$	49.21	49.42	49.78	49.49	49.41	49.99	49.68
		Std. error	0.05	0.04	0.02	0.04	0.04	0.00	0.03

Analyzing the average of change point estimates ($\bar{\hat{\tau}}$), for all magnitudes of shift, the outputs are fairly close to the actual change point. In general, our proposed change point estimator can be evaluated to be close to the actual change point without considering different magnitudes of shift in mean vector and (or) covariance matrix.

For example, when a shift setting $[\lambda_1, \lambda_2, \delta_1, \delta_2] = [0.0, 0.5, 1.3, 1.0]$ is considered, the average change point estimates are 50.34, 50.37 and 49.79 for different correlation values, respectively. The average run lengths after the signal provided by the combination chart are 23.79, 15.46 and 4.28 from Table 3.1-3.3 respectively. As the correlation between the variables increase, the run length of the combination chart decreases. However, the closest run length to the actual change point is approximately four samples after the change. When the magnitude of shift decreases, the detection performance of the combination chart decreases (See Table 3.1-3.3 and Table 3.8). But the change point estimator has a fairly successful

detection performance for all cases. The most remarkable accuracy results were obtained when the magnitude of shift is small.

3.4.2 Precision Evaluation

Empirical distribution of $\bar{\tau}$ around τ are given in Tables 3.4-3.6. Each table is constructed to show the estimated probability of being in the k^{th} neighborhood of the actual change point for various magnitudes of shift and strengths of correlation.

When a shift setting $[\lambda_1, \lambda_2, \delta_1, \delta_2] = [0.0, 1.0, 1.3, 1.3]$ is considered, the exact detection probabilities are 0.527, 0.643 and 0.884 for different correlation values, respectively. The observed frequencies of the change point estimates which are within a given number of periods (k) of the actual change point are also provided. The detection probabilities for the change point estimator and the control chart are shown in Table 3.4-3.6 and Table 3.9.

Figure 3.1 presents the measures versus various mean shift settings and covariance combinations as a summary of the tables. When $k=5$, at least 60% of the simulation results fall in this interval for all shift settings. As the magnitude of shift increases, the percentage increases to approximately 90% regardless of the level of correlation between the variables.

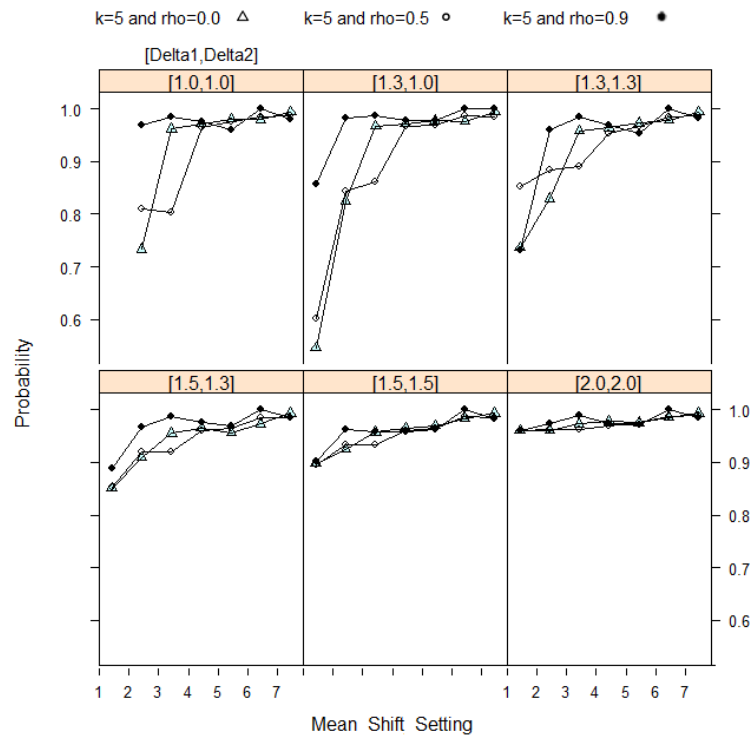
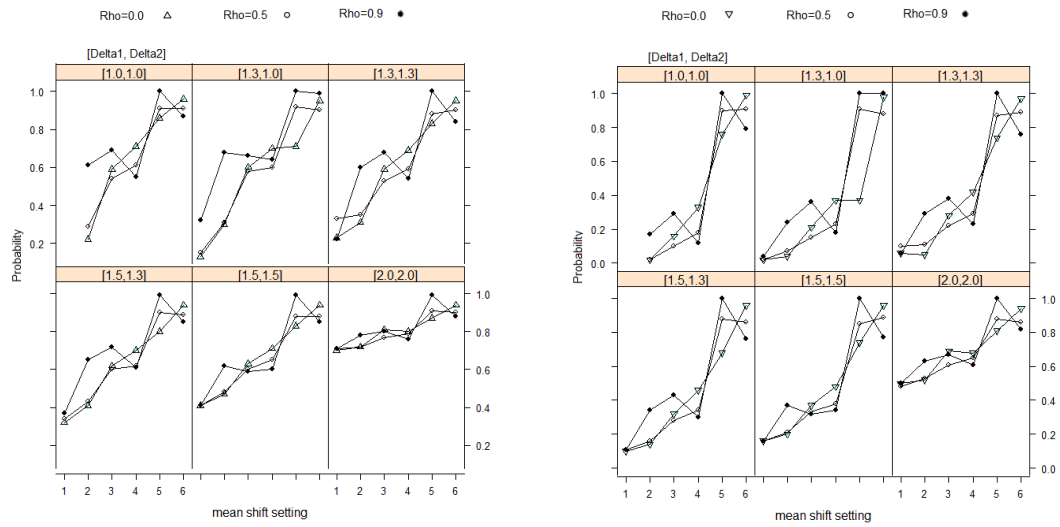


Figure 3.1 Plots of precision measures versus various mean-dispersion shift settings when $|\hat{\tau} - \tau| \leq 5$; $\tau = 50$, $\rho = 0.0, 0.5$ and 0.9 and 10,000 independent simulation runs

The combination chart can give its earliest signal right after the shift is introduced. For our case this happens when $ARL=1$. We defined the cases which had $ARL=1$ as the cases in which the change point is detected exactly by the combination chart. On the other hand, the exact detection performance of the change point estimator can be evaluated. For this purpose, we considered the cases in which $\hat{\tau} = 50$ to compare the performance of the combination chart and our proposed estimator. Table 3.7 indicates that our proposed estimator over-performs the combination chart by means of exact detection performances. Figure 3.2 indicates the exact change point detection ability of the combination chart and the change point estimator.



Change Point Estimator

Combination Chart

Figure 3.2 Plots of exact detection probabilities for change point estimator and combination chart versus various mean-dispersion shift settings; $\tau = 50$, $\rho = 0.0, 0.5$ and 0.9 and 10,000 independent simulation runs

The proposed change point estimator showed a remarkable precision performance. While a simultaneous shift is introduced, the change point estimation procedure detected the change point exactly in at least 30% of the simulation runs for all levels of correlation coefficient tested.

Table 3.4 Empirical distribution of $\hat{\tau}$ around τ after a combination chart signals; $\tau = 50$, $\rho = 0.0$ and 10,000 independent simulation runs

Covariance Shift Setting		λ_1	Mean Shift Setting						
δ_1	δ_2		λ_2	1	2	3	4	5	6
			0	0	0	0.5	1	0	2
			0	0.5	1	1	1	2	2
1	1	$\hat{P}(\hat{\tau} - \tau \leq 0)$		0.220	0.532	0.587	0.706	0.858	0.958
		$\hat{P}(\hat{\tau} - \tau \leq 1)$		0.421	0.768	0.810	0.887	0.945	0.982
		$\hat{P}(\hat{\tau} - \tau \leq 2)$		0.540	0.866	0.900	0.949	0.964	0.988
		$\hat{P}(\hat{\tau} - \tau \leq 5)$		0.733	0.962	0.972	0.981	0.980	0.994
		$\hat{P}(\hat{\tau} - \tau \leq 10)$		0.868	0.987	0.986	0.989	0.987	0.996
1.3	1	$\hat{P}(\hat{\tau} - \tau \leq 0)$	0.128	0.298	0.562	0.602	0.698	0.707	0.955
		$\hat{P}(\hat{\tau} - \tau \leq 1)$	0.266	0.518	0.796	0.825	0.884	0.889	0.985
		$\hat{P}(\hat{\tau} - \tau \leq 2)$	0.358	0.643	0.889	0.908	0.941	0.941	0.991
		$\hat{P}(\hat{\tau} - \tau \leq 5)$	0.546	0.825	0.968	0.972	0.978	0.977	0.995
		$\hat{P}(\hat{\tau} - \tau \leq 10)$	0.724	0.934	0.984	0.985	0.988	0.987	0.996
1.3	1.3	$\hat{P}(\hat{\tau} - \tau \leq 0)$	0.229	0.312	0.527	0.590	0.687	0.833	0.947
		$\hat{P}(\hat{\tau} - \tau \leq 1)$	0.414	0.532	0.762	0.813	0.875	0.941	0.980
		$\hat{P}(\hat{\tau} - \tau \leq 2)$	0.538	0.659	0.864	0.900	0.933	0.962	0.988
		$\hat{P}(\hat{\tau} - \tau \leq 5)$	0.737	0.830	0.959	0.964	0.973	0.979	0.994
		$\hat{P}(\hat{\tau} - \tau \leq 10)$	0.871	0.964	0.981	0.980	0.983	0.988	0.996
1.5	1.3	$\hat{P}(\hat{\tau} - \tau \leq 0)$	0.325	0.412	0.541	0.616	0.554	0.704	0.943
		$\hat{P}(\hat{\tau} - \tau \leq 1)$	0.552	0.650	0.778	0.832	0.784	0.889	0.979
		$\hat{P}(\hat{\tau} - \tau \leq 2)$	0.673	0.766	0.877	0.911	0.876	0.940	0.987
		$\hat{P}(\hat{\tau} - \tau \leq 5)$	0.851	0.909	0.955	0.965	0.957	0.973	0.994
		$\hat{P}(\hat{\tau} - \tau \leq 10)$	0.939	0.964	0.976	0.979	0.978	0.984	0.996
2	2	$\hat{P}(\hat{\tau} - \tau \leq 0)$	0.698	0.722	0.765	0.813	0.804	0.873	0.939
		$\hat{P}(\hat{\tau} - \tau \leq 1)$	0.872	0.886	0.915	0.936	0.930	0.958	0.982
		$\hat{P}(\hat{\tau} - \tau \leq 2)$	0.922	0.931	0.951	0.962	0.957	0.973	0.989
		$\hat{P}(\hat{\tau} - \tau \leq 5)$	0.961	0.961	0.973	0.978	0.976	0.986	0.996
		$\hat{P}(\hat{\tau} - \tau \leq 10)$	0.976	0.977	0.982	0.986	0.984	0.991	0.996

Table 3.6 Empirical distribution of $\hat{\tau}$ around τ after a combination chart signals; $\tau = 50$, $\rho = 0.9$ and 10,000 independent simulation runs

Covariance Shift Setting		λ_1	Mean Shift Setting						
δ_1	δ_2		λ_2	1	2	3	4	5	6
			0	0	0	0.5	1	0	2
			0	0.5	1	1	1	2	2
1	1	$\hat{P}(\hat{\tau} - \tau \leq 0)$		0.613	0.908	0.693	0.546	0.997	0.869
		$\hat{P}(\hat{\tau} - \tau \leq 1)$		0.827	0.962	0.876	0.774	0.999	0.951
		$\hat{P}(\hat{\tau} - \tau \leq 2)$		0.911	0.973	0.939	0.871	1.000	0.965
		$\hat{P}(\hat{\tau} - \tau \leq 5)$		0.970	0.985	0.977	0.960	1.000	0.981
		$\hat{P}(\hat{\tau} - \tau \leq 10)$		0.613	0.908	0.693	0.546	0.997	0.869
1.3	1	$\hat{P}(\hat{\tau} - \tau \leq 0)$	0.320	0.677	0.918	0.661	0.636	0.997	0.995
		$\hat{P}(\hat{\tau} - \tau \leq 1)$	0.556	0.876	0.971	0.863	0.851	1.000	0.999
		$\hat{P}(\hat{\tau} - \tau \leq 2)$	0.679	0.939	0.981	0.932	0.926	1.000	1.000
		$\hat{P}(\hat{\tau} - \tau \leq 5)$	0.856	0.982	0.988	0.979	0.978	1.000	1.000
		$\hat{P}(\hat{\tau} - \tau \leq 10)$	0.953	0.991	0.993	0.988	0.990	1.000	1.000
1.3	1.3	$\hat{P}(\hat{\tau} - \tau \leq 0)$	0.222	0.596	0.884	0.675	0.538	0.995	0.841
		$\hat{P}(\hat{\tau} - \tau \leq 1)$	0.414	0.815	0.959	0.871	0.770	0.999	0.946
		$\hat{P}(\hat{\tau} - \tau \leq 2)$	0.533	0.898	0.973	0.930	0.865	1.000	0.970
		$\hat{P}(\hat{\tau} - \tau \leq 5)$	0.732	0.960	0.986	0.970	0.954	1.000	0.983
		$\hat{P}(\hat{\tau} - \tau \leq 10)$	0.872	0.980	0.992	0.982	0.977	1.000	0.989
1.5	1.3	$\hat{P}(\hat{\tau} - \tau \leq 0)$	0.370	0.645	0.901	0.724	0.615	0.994	0.853
		$\hat{P}(\hat{\tau} - \tau \leq 1)$	0.607	0.856	0.967	0.900	0.829	0.999	0.951
		$\hat{P}(\hat{\tau} - \tau \leq 2)$	0.726	0.923	0.979	0.948	0.907	0.999	0.971
		$\hat{P}(\hat{\tau} - \tau \leq 5)$	0.889	0.968	0.988	0.976	0.969	1.000	0.986
		$\hat{P}(\hat{\tau} - \tau \leq 10)$	0.954	0.981	0.992	0.986	0.982	1.000	0.992
2	2	$\hat{P}(\hat{\tau} - \tau \leq 0)$	0.650	0.772	0.918	0.825	0.767	0.996	0.900
		$\hat{P}(\hat{\tau} - \tau \leq 1)$	0.857	0.922	0.976	0.942	0.921	0.999	0.971
		$\hat{P}(\hat{\tau} - \tau \leq 2)$	0.921	0.957	0.985	0.966	0.959	1.000	0.981
		$\hat{P}(\hat{\tau} - \tau \leq 5)$	0.965	0.979	0.992	0.983	0.979	1.000	0.990
		$\hat{P}(\hat{\tau} - \tau \leq 10)$	0.979	0.987	0.995	0.991	0.986	1.000	0.994

Table 3.7 Exact detection probabilities of the change point estimator and the combination chart;
 $\tau = 50$ and 10,000 independent simulation runs

δ_1	δ_2	λ_1	ρ	0	0	0	0.5	1	0	2
		λ_2		0	0.5	1	1	1	2	2
1	1	$\hat{P}(\hat{\tau} = \tau)$	0.0		0.22	0.53	0.59	0.71	0.86	0.96
		$\hat{P}(E(T) = \tau + 1)$			0.02	0.11	0.16	0.33	0.76	0.99
1.3	1	$\hat{P}(\hat{\tau} = \tau)$		0.13	0.30	0.56	0.60	0.70	0.71	0.95
		$\hat{P}(E(T) = \tau + 1)$		0.02	0.04	0.15	0.21	0.37	0.73	0.98
1.3	1.3	$\hat{P}(\hat{\tau} = \tau)$		0.23	0.31	0.53	0.59	0.69	0.83	0.95
		$\hat{P}(E(T) = \tau + 1)$		0.06	0.05	0.22	0.28	0.42	0.74	0.97
1.5	1.3	$\hat{P}(\hat{\tau} = \tau)$		0.32	0.41	0.54	0.62	0.70	0.80	0.94
		$\hat{P}(E(T) = \tau + 1)$		0.10	0.14	0.27	0.32	0.46	0.68	0.96
2	2	$\hat{P}(\hat{\tau} = \tau)$		0.70	0.72	0.77	0.81	0.80	0.87	0.94
		$\hat{P}(E(T) = \tau + 1)$		0.50	0.52	0.60	0.69	0.68	0.81	0.94
1	1	$\hat{P}(\hat{\tau} = \tau)$	0.5		0.29	0.61	0.54	0.61	0.91	0.91
		$\hat{P}(E(T) = \tau + 1)$			0.02	0.18	0.10	0.18	0.90	0.91
1.3	1	$\hat{P}(\hat{\tau} = \tau)$		0.15	0.31	0.63	0.58	0.60	0.92	0.90
		$\hat{P}(E(T) = \tau + 1)$		0.02	0.07	0.22	0.15	0.23	0.91	0.88
1.3	1.3	$\hat{P}(\hat{\tau} = \tau)$		0.33	0.35	0.64	0.53	0.59	0.88	0.90
		$\hat{P}(E(T) = \tau + 1)$		0.10	0.11	0.24	0.22	0.29	0.87	0.89
1.5	1.3	$\hat{P}(\hat{\tau} = \tau)$		0.34	0.43	0.65	0.60	0.62	0.90	0.89
		$\hat{P}(E(T) = \tau + 1)$		0.11	0.16	0.34	0.28	0.34	0.88	0.86
2	2	$\hat{P}(\hat{\tau} = \tau)$		0.71	0.72	0.79	0.77	0.79	0.91	0.90
		$\hat{P}(E(T) = \tau + 1)$		0.48	0.53	0.62	0.61	0.65	0.88	0.86
1	1	$\hat{P}(\hat{\tau} = \tau)$	0.9		0.61	0.91	0.69	0.55	1.00	0.87
		$\hat{P}(E(T) = \tau + 1)$			0.17	0.90	0.29	0.12	1.00	0.79
1.3	1	$\hat{P}(\hat{\tau} = \tau)$		0.32	0.68	0.92	0.66	0.64	1.00	0.99
		$\hat{P}(E(T) = \tau + 1)$		0.04	0.24	0.88	0.36	0.18	1.00	1.00
1.3	1.3	$\hat{P}(\hat{\tau} = \tau)$		0.22	0.60	0.88	0.68	0.54	1.00	0.84
		$\hat{P}(E(T) = \tau + 1)$		0.06	0.29	0.86	0.38	0.23	1.00	0.76
1.5	1.3	$\hat{P}(\hat{\tau} = \tau)$		0.37	0.65	0.90	0.72	0.61	0.99	0.85
		$\hat{P}(E(T) = \tau + 1)$		0.11	0.34	0.87	0.43	0.30	1.00	0.76
2	2	$\hat{P}(\hat{\tau} = \tau)$		0.71	0.78	0.90	0.80	0.76	0.99	0.88
		$\hat{P}(E(T) = \tau + 1)$		0.50	0.63	0.86	0.67	0.61	1.00	0.82

3.4.3 Comparison with other change point estimators

Under the assumption of the process is jointly being monitored by a combination of χ^2 and $|\mathbf{S}|$ control charts, it is also possible to use a combination of the change point estimators for process mean vector and process covariance matrix. The change point estimator for the mean vector, $\hat{\tau}_M$, was proposed by Nedumaran et al. (2000) given in (1.4) and (2.2).

$\hat{\tau}_M = \arg \max(M_t)$ where $M_t = (T-t)(\bar{\mathbf{X}}_{t,T} - \boldsymbol{\mu}_0)' \boldsymbol{\Sigma}_0^{-1} (\bar{\mathbf{X}}_{t,T} - \boldsymbol{\mu}_0)$ and $t = 0, 1, \dots, T-1$. The change point estimator for the covariance matrix, $\hat{\tau}_C$, was proposed by Dogu and Deveci-Kocakoc (2011a):

$$\hat{\tau}_C = \arg \max(C_t)$$

$$\text{where } C_t = \frac{1}{2} \left(\text{tr} \left(\boldsymbol{\Sigma}_0^{-1} \sum_{i=t+1}^T \sum_{j=1}^n (\mathbf{X}_{ij} - \boldsymbol{\mu}_0)' (\mathbf{X}_{ij} - \boldsymbol{\mu}_0) \right) \right) - \frac{n(T-t)}{2} \log_e \left(\det \left[\sum_{i=t+1}^T \sum_{j=1}^n (\mathbf{X}_{ij} - \boldsymbol{\mu}_0)' (\mathbf{X}_{ij} - \boldsymbol{\mu}_0) \right] / n(T-t) |\boldsymbol{\Sigma}_0| \right) - \frac{np(T-t)}{2},$$

and $t = 0, 1, \dots, T-1$. In order to compare the performance of the proposed joint monitoring procedure with these change point estimators we propose a combination of $\hat{\tau}_M$ and $\hat{\tau}_C$, $\hat{\tau}_{Comb}$. Park and Park (2004) used a similar procedure for univariate joint change point estimation.

$$\hat{\tau}_{Comb} = \begin{cases} \hat{\tau}_M, & \text{if only the } \chi^2 \text{ control chart generates a signal.} \\ \hat{\tau}_C, & \text{if } |\mathbf{S}| \text{ control chart or both charts generate a signal.} \end{cases} \quad (3.3)$$

A simulation study for this comparison was also conducted. Table 3.8-3.9 indicates the accuracy and precision results of this simulation study. Figure 3.3 illustrates the accuracy performance of the proposed change point procedure and

combination change point procedure. From Table 3.8-3.9 it can be concluded that our proposed estimator over-performs the combination change point estimator in terms of accuracy and precision of the estimates. Especially for small magnitudes of shift, the proposed estimator performs far better than the combination estimator. For example, when a shift setting $[\lambda_1, \lambda_2, \delta_1, \delta_2] = [0.0, 0.0, 1.1, 1.3]$ is considered, the average estimation of combination change point estimator is 65.59 and the average estimation of proposed change point estimator is 52.08 ($\tau = 50$). In this case, the exact detection probabilities are 0.099 and 0.156, respectively.

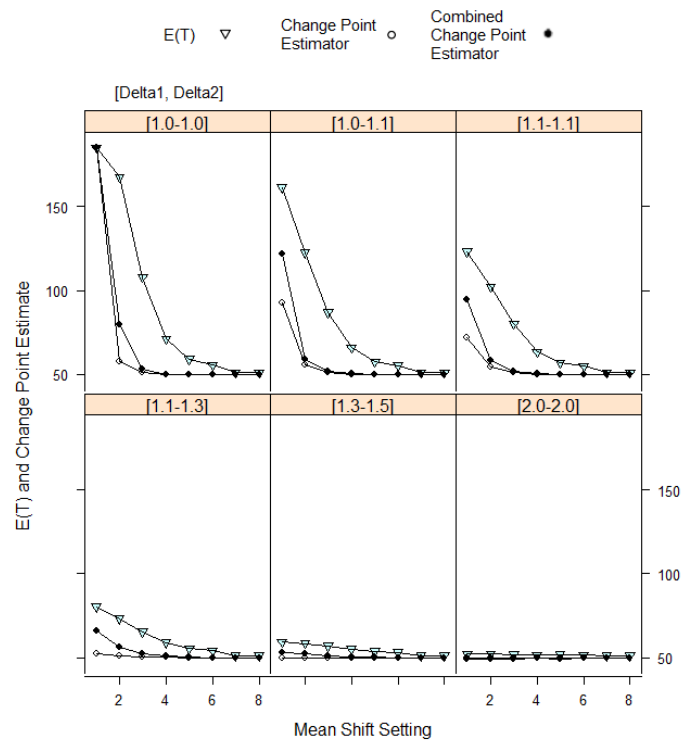


Figure 3.3 Plots of $E(T)$, $\bar{\tau}_{MC}$ and $\bar{\tau}_{Comb}$ versus various mean-dispersion shift settings; $\tau = 50$, $\rho = 0.5$ and 10,000 independent simulation runs

Table 3.8 Expected time of a signal, averages of proposed and combination change point estimates after a combination chart signals; $\tau = 50$, $\rho = 0.5$ and 10,000 independent simulation runs

δ_1	δ_2	λ_1	0	0	0.25	0.5	0.5	1	0	2
		λ_2	0	0.25	0.5	0.75	1	1	2	2
1	1	$E(T)$	234.68	167.72	107.85	71.07	59.28	55.67	51.11	51.11
		$\bar{\tau}_{MC}$		57.42	51.20	50.22	49.93	49.75	49.69	49.68
		$\bar{\tau}_{Comb}$		79.64	53.17	50.12	49.91	49.79	49.86	49.86
1	1.1	$E(T)$	161.56	122.60	87.11	65.98	57.62	55.27	51.13	51.11
		$\bar{\tau}_{MC}$	92.63	55.74	51.47	50.16	49.85	49.73	49.66	49.68
		$\bar{\tau}_{Comb}$	121.74	58.79	51.74	50.25	49.93	49.83	49.85	49.84
1.1	1.1	$E(T)$	123.25	102.36	80.02	63.50	56.97	54.78	51.13	51.13
		$\bar{\tau}_{MC}$	71.98	54.60	51.03	50.17	49.83	49.78	49.65	49.64
		$\bar{\tau}_{Comb}$	94.37	58.13	51.79	50.31	49.93	49.89	49.85	49.86
1.1	1.3	$E(T)$	80.32	73.26	65.53	58.95	55.39	54.11	51.17	51.15
		$\bar{\tau}_{MC}$	52.08	51.08	50.52	50.05	49.84	49.71	49.65	49.68
		$\bar{\tau}_{Comb}$	65.59	56.24	52.05	50.68	50.16	49.94	49.87	49.89
1.3	1.5	$E(T)$	59.39	58.43	56.84	55.01	53.66	53.00	51.19	51.15
		$\bar{\tau}_{MC}$	49.54	49.57	49.59	49.61	49.53	49.52	49.69	49.68
		$\bar{\tau}_{Comb}$	53.01	52.22	51.30	50.57	50.19	49.97	49.87	49.89
2	1.5	$E(T)$	53.10	52.96	52.77	52.45	51.98	52.12	51.12	51.17
		$\bar{\tau}_{MC}$	49.21	49.24	49.24	49.34	49.43	49.48	49.77	49.75
		$\bar{\tau}_{Comb}$	50.20	50.18	49.93	49.97	49.90	49.91	49.85	49.88
2	2	$E(T)$	52.01	51.99	51.92	51.57	51.66	51.57	51.14	51.15
		$\bar{\tau}_{MC}$	49.23	49.23	49.17	49.44	49.32	49.42	49.75	49.77
		$\bar{\tau}_{Comb}$	49.80	49.76	49.72	49.74	49.74	49.76	49.87	49.92

Table 3.9 Precision evaluation for proposed and combination change point estimates after a combination chart signals; $\tau = 50$, $\rho = 0.5$ and 10,000 independent simulation runs

		C-P*	PP**	C-P	P-P	C-P	P-P	C-P	P-P	C-P	P-P
δ_1	λ_1	0		0		0.25		0.5		1	
δ_2	λ_2	0		0.25		0.5		1		1	
1	$\hat{P}(\hat{\tau} - \tau \leq 0)$			0.070	0.086	0.221	0.224	0.594	0.535	0.674	0.612
1	$\hat{P}(\hat{\tau} - \tau \leq 1)$			0.152	0.183	0.403	0.413	0.822	0.770	0.876	0.828
	$\hat{P}(\hat{\tau} - \tau \leq 2)$			0.215	0.260	0.515	0.532	0.908	0.872	0.940	0.909
	$\hat{P}(\hat{\tau} - \tau \leq 5)$			0.344	0.416	0.698	0.729	0.975	0.963	0.982	0.973
	$\hat{P}(\hat{\tau} - \tau \leq 10)$			0.477	0.578	0.827	0.871	0.991	0.988	0.992	0.987
1	$\hat{P}(\hat{\tau} - \tau \leq 0)$	0.017	0.021	0.569	0.636	0.209	0.215	0.559	0.512	0.665	0.605
1.1	$\hat{P}(\hat{\tau} - \tau \leq 1)$	0.038	0.051	0.773	0.840	0.382	0.397	0.794	0.751	0.869	0.819
	$\hat{P}(\hat{\tau} - \tau \leq 2)$	0.060	0.078	0.864	0.907	0.498	0.513	0.891	0.857	0.939	0.907
	$\hat{P}(\hat{\tau} - \tau \leq 5)$	0.119	0.153	0.953	0.959	0.696	0.716	0.971	0.956	0.983	0.971
	$\hat{P}(\hat{\tau} - \tau \leq 10)$	0.198	0.241	0.982	0.974	0.845	0.858	0.990	0.983	0.993	0.986
1.1	$\hat{P}(\hat{\tau} - \tau \leq 0)$	0.028	0.035	0.079	0.106	0.197	0.221	0.561	0.526	0.652	0.587
1.1	$\hat{P}(\hat{\tau} - \tau \leq 1)$	0.066	0.085	0.174	0.226	0.369	0.409	0.792	0.754	0.860	0.810
	$\hat{P}(\hat{\tau} - \tau \leq 2)$	0.099	0.122	0.245	0.312	0.483	0.530	0.883	0.855	0.932	0.899
	$\hat{P}(\hat{\tau} - \tau \leq 5)$	0.169	0.216	0.401	0.488	0.692	0.734	0.968	0.955	0.983	0.970
	$\hat{P}(\hat{\tau} - \tau \leq 10)$	0.268	0.344	0.568	0.661	0.844	0.873	0.988	0.982	0.991	0.987
1.1	$\hat{P}(\hat{\tau} - \tau \leq 0)$	0.099	0.156	0.040	0.110	0.214	0.278	0.513	0.508	0.616	0.592
1.3	$\hat{P}(\hat{\tau} - \tau \leq 1)$	0.198	0.307	0.190	0.280	0.390	0.484	0.746	0.747	0.838	0.816
	$\hat{P}(\hat{\tau} - \tau \leq 2)$	0.267	0.412	0.320	0.470	0.512	0.612	0.853	0.852	0.919	0.898
	$\hat{P}(\hat{\tau} - \tau \leq 5)$	0.404	0.611	0.470	0.670	0.714	0.807	0.960	0.952	0.979	0.967
	$\hat{P}(\hat{\tau} - \tau \leq 10)$	0.544	0.770	0.660	0.860	0.871	0.925	0.987	0.981	0.991	0.984
1.3	$\hat{P}(\hat{\tau} - \tau \leq 0)$	0.250	0.290	0.260	0.320	0.320	0.390	0.520	0.540	0.590	0.622
1.5	$\hat{P}(\hat{\tau} - \tau \leq 1)$	0.410	0.540	0.480	0.650	0.570	0.690	0.770	0.740	0.812	0.835
	$\hat{P}(\hat{\tau} - \tau \leq 2)$	0.480	0.640	0.640	0.770	0.660	0.770	0.870	0.870	0.904	0.911
	$\hat{P}(\hat{\tau} - \tau \leq 5)$	0.670	0.860	0.730	0.850	0.820	0.920	0.970	0.960	0.973	0.966
	$\hat{P}(\hat{\tau} - \tau \leq 10)$	0.860	0.960	0.870	0.970	0.960	0.990	0.990	0.970	0.988	0.980
2	$\hat{P}(\hat{\tau} - \tau \leq 0)$	0.682	0.697	0.690	0.690	0.720	0.690	0.760	0.780	0.750	0.790
2	$\hat{P}(\hat{\tau} - \tau \leq 1)$	0.865	0.874	0.920	0.890	0.880	0.860	0.970	0.930	0.900	0.920
	$\hat{P}(\hat{\tau} - \tau \leq 2)$	0.927	0.925	0.960	0.940	0.940	0.890	0.990	0.950	0.940	0.950
	$\hat{P}(\hat{\tau} - \tau \leq 5)$	0.976	0.960	0.980	0.970	0.970	0.930	1.000	0.970	0.960	0.960
	$\hat{P}(\hat{\tau} - \tau \leq 10)$	0.987	0.976	0.990	0.980	0.980	0.950	1.000	0.980	0.970	0.980

*Combination Procedure, **Proposed Procedure

3.4.4 Confidence Sets Based on the Change Likelihood Function

In this part, the confidence sets on the process change point (τ) are considered. The confidence sets for the time of the process change will provide useful information about the potential change points. The set of candidate change points will help process professionals to focus on quick and correct identification of the special cause and taking appropriate actions. This search window approach can improve quality and reduce special cause identification time.

$$\ln(L(t)) = \frac{1}{2} \left(\text{tr} \left(\Sigma_0^{-1} \times \sum_{i=t+1}^T \sum_{j=1}^n (\mathbf{X}_{ij} - \boldsymbol{\mu}_0)' (\mathbf{X}_{ij} - \boldsymbol{\mu}_0) \right) \right) - \frac{n(T-t)}{2} \log_e \left(\frac{\det \left[\sum_{i=t+1}^T \sum_{j=1}^n (\mathbf{X}_{ij} - \bar{\mathbf{X}}_{T,t}) (\mathbf{X}_{ij} - \bar{\mathbf{X}}_{T,t})' \right]}{n(T-t) |\Sigma_0|} \right) - \frac{np(T-t)}{2}$$

is the value of log likelihood function at t , and D is the reference value to develop a $100(1-\alpha)\%$ confidence set. Box and Cox (1964) proposed using $D = (1/2)\chi_{1,\alpha}^2$ which yields a value of 1.353 for a 90% confidence set. On the other hand, Siegmund(1986) proposed using $D = -\ln(1 - (1-\alpha)^{1/2})$ which yields a value of 2.97 for a 90% confidence set. If $\ln(L(t))$ exceeds the limit of $\ln(L(\hat{\tau})) - D$, then t is a candidate change point. We considered a set of reference values that $D = \{1.353, 1.5, 2.00, 2.5, 2.97\}$ and investigated the coverage probabilities of each shift setting. The coverage probability represents the percentage of the sets which include the exact change point within 10,000 simulation runs. Also the sizes (cardinality) of the sets are recorded (See Table 3.10). It is also possible to investigate the coverage probabilities and expected cardinalities of the sets for different magnitudes of shift and different values of τ . We have chosen five levels of τ ($\tau = 10, 50, 100, 200, 300$). The results are summarized in Table 3.11 for a critical value of $D = 2.97$. The performance results indicate that the coverage probability is approximately 0.85 for a mean shift of $[0.0, 0.5]$ and no shift in covariance matrix. These probabilities are close to this value over the range of τ and increase with the increase of the magnitude of shift. The results are shown

graphically in Figure 3.4-3.5. As the coverage probabilities do not alter for various levels of τ , using $\tau = 50$ seems to be a reasonable choice.

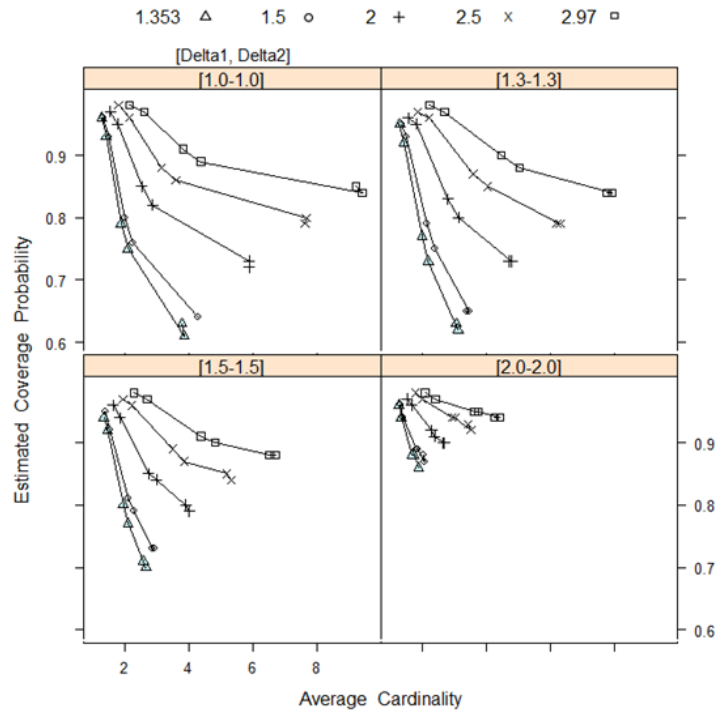


Figure 3.4 Plot of coverage probabilities versus estimated cardinality of confidence sets for various magnitudes of shift following a signal from a combination chart using different critical values of D ; $\tau = 50$ and 10,000 Independent Simulation Runs

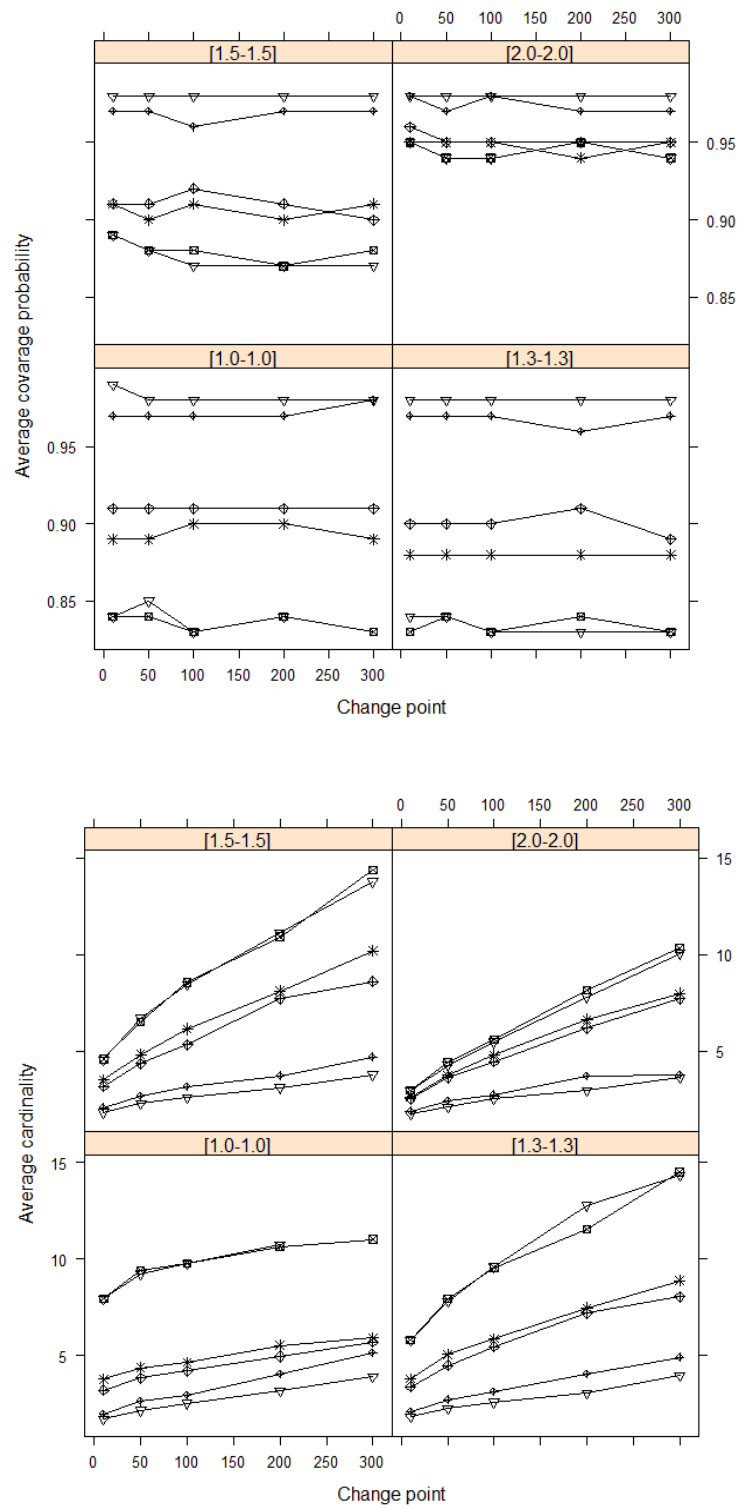


Figure 3.5 Plots of coverage probabilities and average cardinalities versus various change points; $\tau = 50$ and 10,000 independent simulation runs

Table 3.10 Average cardinality and coverage probability values obtained using different critical values (D) after a combination chart signal; $\tau = 50$ and 10,000 independent simulation runs

		λ_1	0					0.5				
		λ_2	0.5					0.5				
δ_1	δ_2	D	1.35	1.50	2.00	2.50	2.97	1.35	1.50	2.00	2.50	2.97
1	1	Average Cardinality	3.78	4.28	5.87	7.61	9.21	3.85	4.28	5.88	7.65	9.40
		Coverage Probability	0.63	0.64	0.72	0.79	0.85	0.61	0.64	0.73	0.80	0.84
1.3	1.3	Average Cardinality	3.07	3.41	4.71	6.21	7.78	3.13	3.49	4.80	6.31	7.93
		Coverage Probability	0.63	0.65	0.73	0.79	0.84	0.62	0.65	0.73	0.79	0.84
1.5	1.5	Average Cardinality	2.65	2.93	4.00	5.30	6.69	2.57	2.84	3.90	5.17	6.51
		Coverage Probability	0.70	0.73	0.79	0.84	0.88	0.71	0.73	0.80	0.85	0.88
2	2	Average Cardinality	1.91	2.05	2.67	3.44	4.27	1.91	2.07	2.71	3.53	4.45
		Coverage Probability	0.86	0.88	0.90	0.93	0.94	0.86	0.87	0.90	0.92	0.94
		λ_1	0.5					1				
		λ_2	1					1				
δ_1	δ_2	D	1.35	1.50	2.00	2.50	2.97	1.35	1.50	2.00	2.50	2.97
1	1	Average Cardinality	2.09	2.25	2.85	3.58	4.36	1.87	2.00	2.51	3.13	3.82
		Coverage Probability	0.75	0.76	0.82	0.86	0.89	0.79	0.80	0.85	0.88	0.91
1.3	1.3	Average Cardinality	2.20	2.40	3.14	4.04	5.04	2.01	2.17	2.81	3.60	4.48
		Coverage Probability	0.73	0.75	0.80	0.85	0.88	0.77	0.79	0.83	0.87	0.90
1.5	1.5	Average Cardinality	2.10	2.28	2.98	3.85	4.82	1.94	2.10	2.73	3.50	4.37
		Coverage Probability	0.77	0.79	0.84	0.87	0.90	0.80	0.81	0.85	0.89	0.91
2	2	Average Cardinality	1.75	1.88	2.40	3.03	3.76	1.70	1.82	2.30	2.94	3.64
		Coverage Probability	0.88	0.89	0.91	0.94	0.95	0.88	0.89	0.92	0.94	0.95
		λ_1	1					2				
		λ_2	2					2				
δ_1	δ_2	D	1.35	1.50	2.00	2.50	2.97	1.35	1.50	2.00	2.50	2.97
1	1	Average Cardinality	1.41	1.48	1.77	2.13	2.60	1.28	1.32	1.53	1.80	2.14
		Coverage Probability	0.93	0.93	0.95	0.96	0.97	0.96	0.96	0.97	0.98	0.98
1.3	1.3	Average Cardinality	1.45	1.52	1.82	2.23	2.71	1.31	1.37	1.58	1.88	2.24
		Coverage Probability	0.92	0.93	0.95	0.96	0.97	0.95	0.95	0.96	0.97	0.98
1.5	1.5	Average Cardinality	1.45	1.52	1.83	2.21	2.68	1.34	1.39	1.62	1.93	2.28
		Coverage Probability	0.92	0.92	0.94	0.96	0.97	0.94	0.95	0.96	0.97	0.98
2	2	Average Cardinality	1.36	1.42	1.68	2.01	2.42	1.29	1.34	1.54	1.81	2.11
		Coverage Probability	0.94	0.94	0.96	0.97	0.97	0.96	0.96	0.97	0.98	0.98

Table 3.11 Average cardinality and coverage probability values various change points; $\tau = 50$ and 10,000 independent simulation runs

		λ_1	0					0.5				
		λ_2	0.5					0.5				
δ_1	δ_2	D	10	50	100	200	300	10	50	100	200	300
1	1	Average Cardinality	7.92	9.21	9.74	10.72	10.97	7.92	9.40	9.74	10.63	11.00
		Coverage Probability	0.84	0.85	0.83	0.84	0.83	0.84	0.84	0.83	0.84	0.83
1.3	1.3	Average Cardinality	5.78	7.78	9.58	12.75	14.33	5.80	7.93	9.54	11.54	14.49
		Coverage Probability	0.84	0.84	0.83	0.83	0.83	0.83	0.84	0.83	0.84	0.83
1.5	1.5	Average Cardinality	4.54	6.69	8.44	11.11	13.79	4.59	6.51	8.55	10.92	14.37
		Coverage Probability	0.89	0.88	0.87	0.87	0.87	0.89	0.88	0.88	0.87	0.88
2	2	Average Cardinality	2.97	4.27	5.48	7.81	10.06	2.97	4.45	5.59	8.15	10.32
		Coverage Probability	0.95	0.94	0.94	0.95	0.94	0.95	0.94	0.94	0.95	0.94
		λ_1	0.5					1				
		λ_2	1					1				
δ_1	δ_2	D	10	50	100	200	300	10	50	100	200	300
1	1	Average Cardinality	3.76	4.36	4.63	5.51	5.89	3.19	3.82	4.20	4.94	5.68
		Coverage Probability	0.89	0.89	0.90	0.90	0.89	0.91	0.91	0.91	0.91	0.91
1.3	1.3	Average Cardinality	3.78	5.04	5.84	7.44	8.87	3.36	4.48	5.44	7.18	8.04
		Coverage Probability	0.88	0.88	0.88	0.88	0.88	0.90	0.90	0.90	0.91	0.89
1.5	1.5	Average Cardinality	3.50	4.82	6.14	8.11	10.19	3.18	4.37	5.32	7.72	8.59
		Coverage Probability	0.91	0.90	0.91	0.90	0.91	0.91	0.91	0.92	0.91	0.90
2	2	Average Cardinality	2.63	3.76	4.81	6.64	7.98	2.52	3.64	4.46	6.20	7.72
		Coverage Probability	0.95	0.95	0.95	0.94	0.95	0.96	0.95	0.95	0.95	0.95
		λ_1	1					2				
		λ_2	2					2				
δ_1	δ_2	D	10	50	100	200	300	10	50	100	200	300
1	1	Average Cardinality	1.96	2.60	2.90	4.01	5.11	1.70	2.14	2.52	3.15	3.88
		Coverage Probability	0.97	0.97	0.97	0.97	0.98	0.99	0.98	0.98	0.98	0.98
1.3	1.3	Average Cardinality	2.09	2.71	3.11	4.04	4.90	1.82	2.24	2.58	3.05	3.94
		Coverage Probability	0.97	0.97	0.97	0.96	0.97	0.98	0.98	0.98	0.98	0.98
1.5	1.5	Average Cardinality	2.08	2.68	3.17	3.73	4.70	1.82	2.28	2.60	3.10	3.78
		Coverage Probability	0.97	0.97	0.96	0.97	0.97	0.98	0.98	0.98	0.98	0.98
2	2	Average Cardinality	1.90	2.42	2.75	3.69	3.76	1.73	2.11	2.52	2.97	3.62
		Coverage Probability	0.98	0.97	0.98	0.97	0.97	0.98	0.98	0.98	0.98	0.98

In Figure 3.4 the lines represent each critical value, the symbols represent different mean shift settings and each panel represents a covariance shift setting. Following the lines the biggest critical value ($D=2.97$) satisfies approximately 90% confidence region for each simulation settings. The choice of τ has an impact on the expected cardinalities. As the change point τ increases, the size of the confidence sets increase.

3.5 Illustrative example

The following illustrative example is considered in order to show the practical usage of our estimator. The illustrative example is from spring manufacturing. Two critical quality characteristics are considered: spring inner diameter (X_1) with a specification of 28.30 ± 0.10 and spring elasticity (X_2) with a specification of 46.00 ± 0.50 . The first ten observations are from Chen et al. (2005) and the historical mean and covariance are as follows:

$$\boldsymbol{\mu}_0 = (28.29 \ 45.85)' \text{ and, } \boldsymbol{\Sigma}_0 = \begin{bmatrix} 0.0035 & -0.0046 \\ -0.0046 & 0.0226 \end{bmatrix}.$$

After the 10th process reading a combination of mean and covariance shift ($[\lambda_1, \lambda_2, \delta_1, \delta_2] = [0.5, 0.5, 1.3, 1.0]$) is introduced. When the 20th subgroup was generated, the combination chart has issued a signal. That means following the signal at $T=20$, the MC_t statistics can be calculated. Our aim in this procedure is to find the maximum value of MC_t , in other words, to find where the change occurred in the interval of $0 \leq t \leq T-1$.

According to Table 3.12, the combination chart did not issue a signal until the 20th subgroup was generated. On the other hand, the change point estimator has its maximum value in the 11th subgroup. That means, the 10th subgroup was the last subgroup obtained from in-control process and the 11th subgroup was the first subgroup of the changed process, as we initially aimed. For the practitioners, investigating the point at which a signal issued is not sufficient to find out the

special cause because of the potential delay. As it has occurred in our illustrative example, a step change may exist several subgroups earlier from the signal of the control chart.

Table 3.12 Spring data, chi-squares, generalized variances, M_t , C_t and MC_t statistics

i	t	\bar{X}_{i1}	\bar{X}_{i2}	χ^2	$ \mathbf{S} \times 10^4$	M_t	C_t	MC_t
1	0	28.236	45.934	4.217	0.529	5.005	7.525	15.777
2	1	28.334	45.880	5.096	0.292	5.937	8.014	17.781
3	2	28.310	45.686	6.300	0.135	5.134	5.397	14.707
4	3	28.260	45.890	1.286	0.060	5.982	5.913	16.328
5	4	28.310	45.838	0.633	0.243	6.818	6.532	18.289
6	5	28.282	45.886	0.288	0.051	6.832	6.977	18.440
7	6	28.328	45.784	2.141	0.156	7.265	8.252	19.933
8	7	28.314	45.776	1.367	0.198	7.258	8.991	20.236
9	8	28.324	45.800	1.660	0.825	7.813	9.547	21.463
10	9	28.316	45.804	1.008	0.035	7.945	7.118	20.864
11	10	28.361	45.840	9.447	0.691	8.387	8.251	22.596
12	11	28.364	45.777	8.242	0.624	7.013	6.316	18.703
13	12	28.317	45.830	1.152	0.496	6.439	5.487	16.937
14	13	28.333	45.849	3.676	0.558	6.769	6.225	17.526
15	14	28.276	46.034	8.672	0.539	6.487	6.538	16.966
16	15	28.309	45.897	2.101	0.602	5.156	5.656	13.552
17	16	28.311	45.994	9.647	2.000	4.921	6.071	13.182
18	17	28.345	45.826	5.124	0.468	3.114	3.283	8.9689
19	18	28.271	45.985	4.234	0.865	2.986	2.441	8.5846
20	19	28.323	46.006	13.870	0.191	2.774	3.506	8.5871

In order to construct the confidence set on the change point, the points satisfy $\max(MC) - (MC_t) < 2.97$ are considered as candidate change points. In other words, the log likelihood values exceed 19.63 were considered to be the potential change points. The corresponding group for our example was $CS_{MC} = \{7, 8, 9, 10, 11\}$ and the cardinality of the confidence set was 5 subgroups. Confidence set construction is presented in Figure 3.7. The points over the threshold are the candidate change points.

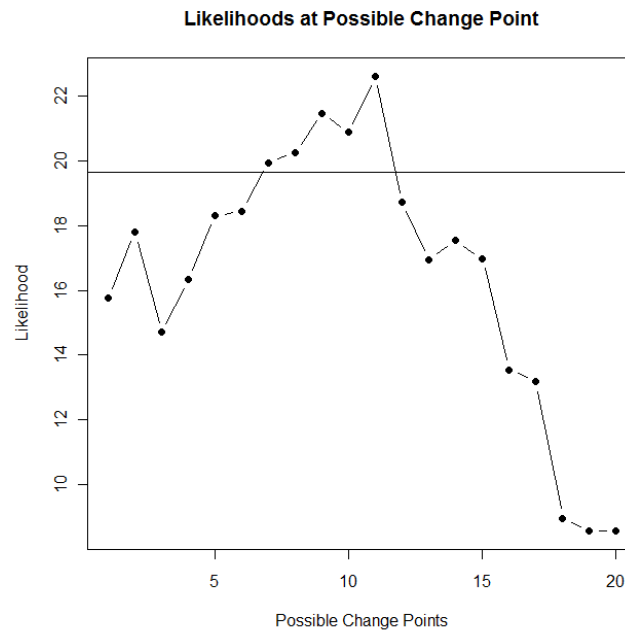


Figure 3.6 Plot of likelihood values at possible change points and the threshold for spring data.

3.6 Conclusions

A follow-up change point estimation procedure for jointly monitoring the mean and covariance of a p -variate process is proposed. The proposed estimator is capable of detecting the step change successfully. We compared the performance of our estimator under the assumption that the process is monitored with a combination of χ^2 and $|\mathbf{S}|$ charts as the most widely used joint multivariate monitoring tool. The main advantage of the proposed estimator is to use one statistic for all the complex process information to detect the change point.

The performance evaluation has shown that the change point formulation has high detection ability. The performance evaluation also has the comparison with a combination of the beforehand proposed change point estimators. Our simultaneous estimation procedure performs better than the combination estimator by means of accuracy and precision. An illustrative example is considered to indicate the practical use of the change point estimator. This hypothetical example indicates the ease of implementation and interpretation. While the change point estimation

procedure achieves the goal of detecting the shifts in the process, it is also important to identify whether it is a mean shift, covariance shift or both. So we recommend using diagnostic tools in order to improve the identification ability of the method.

CHAPTER FOUR

CHANGE POINT ESTIMATION FOR MULTIVARIATE SINGLE CONTROL CHARTS

4.1 Introduction

Shewhart control charts are effective tools to improve quality of a product or process. The basic practice is to determine the quality of an item with a single quality characteristic. However, many industrial processes are characterized by more than one inter-related quality metrics. Several monitoring approaches are proposed in the literature for these multi-dimensional processes. Hotelling's T^2 control chart (1947) started the efforts for multivariate quality control of the mean vector. Alt (1985) and Alt and Smith (1988) proposed different procedures of multivariate dispersion control and monitoring. Recently, the researchers mostly focused on developing multivariate control charts which are able to detect small shifts. For discussions and reviews of multivariate mean and dispersion control charts, see, Alt (1985), Alt Smith (1988), Lowry and Montgomery (1995), and Bersimis et al. (2007).

The multivariate monitoring effort includes monitoring the central tendency and dispersion of the process. In multivariate quality control, traditionally separate control charts were used to monitor the process mean and dispersion. Alt (1985) noted the importance of the need to develop a single control chart for simultaneous monitoring of both mean and dispersion. Cheng and Thaga (2006) also concluded that this practice needs more resources such as quality professionals and time. The simultaneous monitoring approaches are scarce in the literature. The existing studies are as follows: the traditional combination of the χ^2 and $|S|$ control charts, Max-MEWMA chart proposed by Chen et al. (2005), Multivariate Maximum Control Chart proposed by Thaga and Gabaitiri (2006), Multivariate Max-CUSUM control chart proposed by Cheng and Thaga (2005) and MELR chart by Zhang et al. (2010). The basic idea in the max procedures, namely the Max-M, Max-MEWMA and

Max-CUSUM charts, is to transform the monitoring statistics for mean and covariance into standardized normal random variables and determine the maximum of these standard normal readings, and then apply a multivariate Shewhart procedure. According to Thaga and Gabaitiri (2006), these control charts are practical because the complex multivariate readings are transformed into standardized univariate scores and monitoring can proceed using the existing charts for univariate processes. Also the practitioners can monitor both the mean and the variability using only a single control chart. The superiority of these monitoring schemes is their ability of giving diagnostic aids along with the control chart statistic. A recent remarkable multivariate single control chart was proposed by Zhang et al. (2010). They proposed using the generalized likelihood ratio test statistic differently from the above work flow.

A signal generated from the monitoring procedure does not always mean that the assignable cause actually occurred at that point. Finding the actual change point has been in great importance for many industries. For multivariate processes, Nedumaran et al. (2000) proposed an add-on change point estimation procedure when only mean shift is considered and Dogu and Deveci-Kocakoc (2011a) proposed an add-on change point estimator when only covariance shift is considered. Dogu and Deveci-Kocakoc (2011b) proposed a change point estimation procedure for χ^2 and $|\mathbf{S}|$ combination chart emphasising the simultaneous monitoring of mean and variability for multivariate normal processes. The estimator ($\hat{\tau}$) focuses on estimating the most likely location of the change after a single or combination multivariate control chart issues a signal. The performance assessment of the estimator can be found in Dogu and Deveci-Kocakoc (2011b). Their assumption was that the χ^2 and $|\mathbf{S}|$ combination chart should generate a signal in order to start the follow-up procedure. However, the ARL performance of χ^2 and $|\mathbf{S}|$ combination chart may be inadequate for many industrial processes. The pressure to have high quality and yield processes forces organizations to improve their monitoring tools. Recently, only small shifts are tolerable for many implementations and industries. Exponentially weighted moving average (EWMA) based control

charts like Max-MEWMA and MELR are proper tools for these cases. Although, Zhang et al. (2010) showed that their procedure over-performs other alternatives in terms of run length results, we used Max-MEWMA and MELR control charts with the follow up change point estimator and summarized the simulation results in Section 4.4.

The monitoring approaches generally should have good special cause detection and identification abilities. The change point estimation procedures enhance the detection ability of the monitoring procedure. The estimator ($\hat{\tau}$) when used with a multivariate joint monitoring scheme helps practitioners to find the actual time of a step change. Therefore, it improves the detection ability of the monitoring system. For multivariate single charts, it is not always easy to distinguish the actual responsible of the special cause between mean and variability. So when using a change point estimator along with the multivariate control charts, we recommend using some diagnostic tools to find out if the change is a mean shift, a covariance shift or both. As Max-MEWMA procedure provides diagnostic aids along with the chart statistics, some practitioners may prefer using this approach. In section 4.5, an illustrative example is provided to show the practice of the add-on change point estimation procedure. Our aim here is to investigate the detection performance of the change point estimator with various alternative monitoring tools such as: Max-MEWMA and MELR control charts. We believe that change point detection performance of a monitoring tool is as important as its quick response ability to a shift.

The remainder of this paper is organized as follows: the next section provides the details of the Max-MEWMA and MELR control charts. The third section gives the details of the change point model. In the fourth section, performance assessment and other performance measurements are provided. Then an illustrative example and conclusions are presented.

4.2 Maximum Multivariate Exponentially Weighted Moving Average (Max-MEWMA) and Multivariate Exponentially Weighted Likelihood Ratio Charts (MELR)

In order to show the performance of the follow-up change point estimator with multivariate single control charts, we will consider Max-MEWMA control chart proposed by Chen et al. (2005) and MELR chart proposed by Zhang et al. (2010). These control charts are the competing procedures for multivariate simultaneous monitoring. Zhang et al. (2010) showed that MELR chart performs better than Max-MEWMA chart in terms of ARL performances. However, Max-MEWMA control chart provides diagnostics while MELR does not. When an out-of-control signal is generated by the Max-MEWMA control chart, the chart indicates whether it is a mean shift, covariance shift or both. We will show the performance of the change point estimator with both procedures.

The Max-MEWMA chart simply plots the maximum absolute values of mean and dispersion control chart statistics. It is capable of monitoring mean vector and covariance matrix simultaneously with a single control chart. Consider $\mathbf{Z}_t = \omega(\bar{\mathbf{X}}_t - \boldsymbol{\mu}_0) + (1-\omega)\mathbf{Z}_{t-1}$ where $\mathbf{Z}_0 = \mathbf{0}_p$, ω is a smoothing factor satisfying $0 < \omega < 1$ and $T_t = \frac{n(2-\omega)}{\omega(1-(1-\omega)^{2t})} \mathbf{Z}_t' \boldsymbol{\Sigma}_0^{-1} \mathbf{Z}_t$, then define the monitoring statistic for the mean vector as $U_t = \Phi^{-1} \left[H_p \left(\frac{n(2-\omega)}{\omega(1-(1-\omega)^{2t})} \mathbf{Z}_t' \boldsymbol{\Sigma}_0^{-1} \mathbf{Z}_t \right) \right]$ where $H_p(\cdot)$ is the chi-square distribution function with p degrees of freedom and Φ^{-1} is the inverse standard normal distribution.

In order to obtain a monitoring statistic for the variability define $W_t = \sum_{j=1}^n (\mathbf{X}_{tj} - \bar{\mathbf{X}}_t)' \boldsymbol{\Sigma}_0^{-1} (\mathbf{X}_{tj} - \bar{\mathbf{X}}_t)$ and $W_t \sim \chi_{p(n-1)}^2$. If a transformation $\Phi^{-1} \{ H_{p(n-1)}(W_t) \}$ is applied then $Y_t = \omega \Phi^{-1} \{ H_{p(n-1)}(W_t) \} + (1-\omega)Y_{t-1}$. When the process is in control and the starting point is $Y_0 = 0$, then define

$V_t = \sqrt{\frac{n(2-\omega)}{\omega(1-(1-\omega)^{2t})}} Y_t$. As U_t and V_t are independent and follow standard normal distribution when the process is in-control, a combination of U_t and V_t is determined as the single charting statistic:

$$\text{Max-MEWMA}_t = \max(|U_t|, |V_t|). \quad (4.1)$$

If $\text{Max-MEWMA}_t > h_1$, then the process is considered to be out-of-control, where $h_1 > 0$ is the upper control limit which achieves a specific significance level and some values of h_1 can be obtained from Chen et al. (2005).

MELR control chart is a single MEWMA control chart based on the generalized likelihood ratio (GLR) test for joint monitoring both the multivariate mean and variability. The run length results for various magnitudes of shift showed that MELR control chart over performs the competing single and combination charts. The following hypotheses are considered in MELR procedure.

The null hypothesis is $H_0 : \mu = \mathbf{0}$ and $\Sigma = \mathbf{I}_p$ and the alternative hypothesis is $H_1 : \mu \neq \mathbf{0}$ and $\Sigma \neq \mathbf{I}_p$. The GLR statistic is obtained as follows:

$$\text{MELR}_t = \text{tr}(\mathbf{v}_t) - \log|\mathbf{v}_t| + p\|\mathbf{u}_t\|^2. \quad (4.2)$$

Here, $\mathbf{u}_t = \omega \bar{\mathbf{X}}_t + (1-\omega)\mathbf{u}_{t-1}$, $\mathbf{v}_t = \omega \mathbf{S}_t + (1-\omega)\mathbf{v}_{t-1}$, $\mathbf{S}_t^* = \sum_{j=1}^n (\mathbf{X}_{tj} - \mathbf{u}_t)' (\mathbf{X}_{tj} - \mathbf{u}_t) / n$, $\mathbf{u}_0 = \mathbf{0}_p$, and $\mathbf{v}_0 = \mathbf{I}_p$. ω is a smoothing factor satisfying $0 < \omega < 1$. $\text{MELR}_t > h_2$, then the process is considered to be out-of-control, where $h_2 > 0$ is a threshold to achieve a specified IC ARL. The MELR does not provide diagnostics and Zhang et al. (2010) stated that this omnibus procedure may be problematic in diagnosing which parameter or parameters have shifted.

4.3 Multivariate Joint Change Point Estimation for Single Control Charts

A very important issue of simultaneous multivariate process monitoring is the identification of the location or time of a special cause. While the single control charts provide a stopping time for the process professionals after a shift, this signal does not always mean that the assignable cause occurred at that particular time. In other words, the control charts have a potential delay to detect the change point. The change point analysis provides a solution to this setback of the control charts. Nedumaran et al. (2000) and Dogu and Deveci-Kocakoc (2011a) proposed add-on change point estimators for multivariate processes. Nedumaran et al. (2000) focused on the mean shift only model while Dogu and Deveci-Kocakoc (2011a) proposed a change point estimator for covariance shift only model. Dogu and Deveci-Kocakoc (2011b) proposed a multivariate change point procedure in order to detect step changes of mean and dispersion simultaneously and showed that their estimator works better than a combination change point estimator to find the most likely time of the special cause. The idea of the follow-up estimation of the change point based on backward CUSUMs started with the work of Samuel et al. (1998a, 1998b) for Phase II analysis. The MLE of change point is performed after a control chart generates a signal.

Dogu and Deveci-Kocakoc(2011b) provided the accuracy and precision evaluation for the follow-up change point estimator when the process is monitored with χ^2 and $|\mathbf{S}|$ combination chart. In order to show the consistency of this estimator we considered the estimation procedure for the same magnitudes of shift when the process is monitored with the Max-MEWMA and the MELR and compared the results with the case when the process is monitored with χ^2 and $|\mathbf{S}|$ combination chart.

Let $\mathbf{X}_{ij} = (X_{ij1}, X_{ij2}, \dots, X_{ijp})'$ be a $p \times 1$ vector which represents the p characteristics of the j th observation ($j = 1, 2, \dots, n$) for the i^{th} subgroup of size n . Suppose further that when the process is in-control, the \mathbf{X}_{ij} 's are *iid* $N_p(\boldsymbol{\mu}_0, \boldsymbol{\Sigma}_0)$.

We let n denote the subgroup size and we let $\bar{\mathbf{X}}_i$ denote the average vector of the i^{th} subgroup. It is assumed that when the multivariate process mean and dispersion changes, there has been a step-change from its in-control value of $\boldsymbol{\mu} = \boldsymbol{\mu}_0$ and $\boldsymbol{\Sigma} = \boldsymbol{\Sigma}_0$ to an unknown value $\boldsymbol{\mu} = \boldsymbol{\mu}_1$ and $\boldsymbol{\Sigma} = \boldsymbol{\Sigma}_1$ where $\boldsymbol{\mu}_0 \neq \boldsymbol{\mu}_1$ and $\boldsymbol{\Sigma}_0 \neq \boldsymbol{\Sigma}_1$. If control chart statistics exceed the control limits, it is concluded that the step-change in the process parameters occurred after some unknown time τ , where $0 \leq \tau \leq T-1$ and T is the time that the combination chart signals.

The maximum likelihood estimator of τ can be the value of t for which the statistic MC attains its maximum; that is,

$$\hat{\tau}_{MC} = \arg \max_t (MC_t), \quad t = 0, 1, \dots, T-1,$$

where

$$\hat{\tau}_{MC} = \arg \max_{0 < t < T-1} \left[\frac{1}{2} \left(tr \left(\boldsymbol{\Sigma}_0^{-1} \times \sum_{i=t+1}^T \sum_{j=1}^n (\mathbf{X}_{ij} - \boldsymbol{\mu}_0)' (\mathbf{X}_{ij} - \boldsymbol{\mu}_0) \right) \right) - \frac{n(T-t)}{2} \log_e \left(\det \left[\sum_{i=t+1}^T \sum_{j=1}^n (\mathbf{X}_{ij} - \bar{\bar{\mathbf{X}}}_{T,t}) (\mathbf{X}_{ij} - \bar{\bar{\mathbf{X}}}_{T,t})' \right] / n(T-t) |\boldsymbol{\Sigma}_0| \right) - \frac{np(T-t)}{2} \right],$$

where $\hat{\boldsymbol{\mu}}_1 = \bar{\bar{\mathbf{X}}}_{t,T} = \frac{1}{T-t} \sum_{i=t+1}^T \bar{\mathbf{X}}_i$ and $\hat{\boldsymbol{\Sigma}}_1 = \frac{1}{n(T-t)} \sum_{i=t+1}^T \sum_{j=1}^n (\mathbf{X}_{ij} - \hat{\boldsymbol{\mu}}_1)' (\mathbf{X}_{ij} - \hat{\boldsymbol{\mu}}_1)$ are the MLE's of mean vector and covariance matrix of the $(T-t)$ most recent subgroup averages.

4.4 Performance assessment

The add-on change point estimation procedure provides additional benefits such as the estimation of the time of a step change. We now investigate the combination and single charts' detection performance along with the change point estimator. We specifically calculate the 'average change point estimate' and 'the empirical distribution of the estimated change point around the actual change point' for each monitoring procedure. These performance indicators were used by Samuel et al.

(1998a, 1998b), Nedumaran et al. (2000), Park and Park (2004) and Dogu and Devenci-Kocakoc (2011a, 2011b). The simulation study settings are constructed for bivariate case for simplicity and the performance comparison was conducted under the assumption that a step change of magnitude $[\lambda_1, \lambda_2, \delta_1, \delta_2]$ occurs following the τ^{th} observation vector.

Observations were randomly generated from an in-control $N_p(\boldsymbol{\mu}_0, \boldsymbol{\Sigma}_0)$ distribution when $i \leq 50$, the on-target mean vector was $\boldsymbol{\mu}_0 = (0,0)'$ and the in-control covariance matrix was selected as follows:

$$\boldsymbol{\Sigma}_0 = \begin{bmatrix} 1 & \rho \\ \rho & 1 \end{bmatrix},$$

where $-1 \leq \rho \leq 1$ is the correlation coefficient between two quality characteristics. In this study, the correlation coefficient was set to 0.0, 0.5 and 0.9. While the process is in-control, the observations which exceed the control limits are considered as false alarms. If a false alarm at the i^{th} observation ($i \leq \tau$) occurred, it was treated in the same way that a false alarm would be treated on an actual process. When an actual false alarm is determined in a process, the process professionals consider the process is in control and let the monitoring restart. The same approach is used in the simulation study. If the i^{th} observation is a false alarm, then the control chart restarted at $(i+1)^{\text{th}}$ observation and the change point remained in its scheduled point. Starting with subgroup 51, the observations are randomly generated from $N_p(\boldsymbol{\mu}_1, \boldsymbol{\Sigma}_1)$ until the combination control chart issued a signal. The structure of the changed mean vector and covariance matrix are given as:

$$\boldsymbol{\mu}'_1 = \begin{pmatrix} \mu_x + \lambda_1 \\ \mu_y + \lambda_2 \end{pmatrix}, \quad \boldsymbol{\Sigma}_1 = \begin{pmatrix} \delta_1^2 \times \sigma_x^2 & \rho_1 \times \delta_1 \times \delta_2 \times \sigma_x \times \sigma_y \\ \rho_1 \times \delta_1 \times \delta_2 \times \sigma_x \times \sigma_y & \delta_2^2 \times \sigma_y^2 \end{pmatrix}.$$

For every run, when the control chart issued a signal, the time of the signal and the time of the change were calculated with the proposed estimator. This procedure was repeated a total of 10,000 times for each of the case and different magnitudes, denoted by δ and λ , for the subgroup size of $n = 4$.

A calibration procedure was used for each control chart so that they all had the same in-control ARL. If the practitioner chose $\alpha_{\chi^2} = \alpha_{|\mathbf{S}|} = \alpha$, then the combination of χ^2 and $|\mathbf{S}|$ charts has a combined Type I error probability of $1 - (1 - \alpha)^2$. As we choose $\alpha = 0.0027$, the ARL of the combination chart is expected to be $1 / (1 - (1 - \alpha)^2) = 1 / 0.0054 \cong 185$ when no shifts of mean vector and covariance matrix are introduced. In order to be consistent in the comparison, the ARL of the Max-MEWMA and MELR control charts are calibrated to 185. The smoothing constant for these control charts is 0.2 and upper control limits are calculated to achieve this specified in-control run length.

4.4.1 Accuracy Evaluation

In order to measure the accuracy performance of the change point estimator, the average change point estimation is considered with the expected signal point, which is denoted by $E(T)$. $E(T)$ can be considered as the sum of Average Run Length (ARL) and exact change point (τ).

Table 4.1 Expected time of a signal, average change point estimates and their standard errors after $\chi^2 - |\mathbf{S}|$, Max-MEWMA and MELR control charts signal; $\tau = 50$, $\rho_1 = 0.0$ and 10,000 independent simulation runs

				Mean Shift Setting							
				1	2	3	4	5	6		
Covariance Shift Setting		λ_1		0	0	0.25	0.5	0.5	1		
δ_1	δ_2	λ_2		0	0.25	0.5	0.75	1	1		
1	1	$\chi^2 - \mathbf{S} $	$E(T)$		181.19	95.07	62.72	56.47	53.07		
			$\bar{\hat{\tau}}$		62.06	50.83	49.99	49.83	49.66		
			Std. error		0.23	0.09	0.03	0.03	0.04		
		Max-MEWMA	$E(T)$		110.85	61.18	55.07	53.83	52.91		
			$\bar{\hat{\tau}}$		60.55	50.40	49.34	49.43	49.56		
			Std. error		0.26	0.08	0.06	0.04	0.03		
		MELR	$E(T)$		79.55	60.31	54.87	53.66	52.67		
			$\bar{\hat{\tau}}$		57.55	50.67	49.41	49.38	49.40		
			Std. error		0.18	0.08	0.05	0.04	0.04		
		1.1	1.1	$\chi^2 - \mathbf{S} $	$E(T)$	122.51	105.62	75.17	59.23	55.23	52.80
					$\bar{\hat{\tau}}$	71.74	56.35	50.91	49.88	49.74	49.59
					Std. error	0.39	0.19	0.09	0.04	0.06	0.02
Max-MEWMA	$E(T)$			104.01	81.10	60.03	54.98	53.76	52.86		
	$\bar{\hat{\tau}}$			66.36	55.50	50.23	49.59	49.44	49.58		
	Std. error			0.33	0.18	0.08	0.05	0.04	0.03		
MELR	$E(T)$			117.84	79.55	59.19	54.64	53.50	52.62		
	$\bar{\hat{\tau}}$			75.75	57.55	50.40	49.40	49.31	49.52		
	Std. error			0.39	0.18	0.08	0.06	0.05	0.03		
1.1	1.3			$\chi^2 - \mathbf{S} $	$E(T)$	80.72	75.48	64.36	56.75	54.45	52.59
					$\bar{\hat{\tau}}$	52.28	51.47	50.34	49.88	49.72	49.62
					Std. error	0.21	0.13	0.06	0.05	0.04	0.04
		Max-MEWMA	$E(T)$	67.10	64.00	58.06	54.67	53.68	52.84		
			$\bar{\hat{\tau}}$	51.12	50.50	49.82	49.47	49.51	49.59		
			Std. error	0.12	0.11	0.07	0.05	0.04	0.03		
		MELR	$E(T)$	66.77	62.69	56.90	54.12	53.22	52.47		
			$\bar{\hat{\tau}}$	53.10	52.02	50.11	49.39	49.47	49.48		
			Std. error	0.12	0.10	0.07	0.05	0.04	0.04		
		1.3	1.5	$\chi^2 - \mathbf{S} $	$E(T)$	59.56	58.67	56.47	54.09	53.18	52.20
					$\bar{\hat{\tau}}$	49.62	49.59	49.44	49.48	49.50	49.57
					Std. error	0.09	0.06	0.06	0.03	0.04	0.03
Max-MEWMA	$E(T)$			56.20	55.87	54.98	53.85	53.28	52.68		
	$\bar{\hat{\tau}}$			49.04	49.11	49.40	49.48	49.51	49.64		
	Std. error			0.08	0.07	0.06	0.04	0.04	0.03		
MELR	$E(T)$			55.87	55.46	54.30	53.23	52.66	52.18		
	$\bar{\hat{\tau}}$			49.54	49.74	49.52	49.48	49.44	49.48		
	Std. error			0.07	0.06	0.06	0.05	0.04	0.04		

Table 4.2 Expected time of a signal, average change point estimates and their standard errors after $\chi^2 - |\mathbf{S}|$, Max-MEWMA and MELR control charts signal; $\tau = 50$, $\rho_1 = 0.5$ and 10,000 independent simulation runs

				Mean Shift Setting							
				1	2	3	4	5	6		
Covariance Shift Setting		λ_1		0	0	0.25	0.5	0.5	1		
δ_1	δ_2	λ_2		0	0.25	0.5	0.75	1	1		
1	1	$\chi^2 - \mathbf{S} $	$E(T)$		138.73	79.44	59.62	55.65	53.06		
			$\bar{\hat{\tau}}$		50.36	50.27	50.04	49.85	49.77		
			Std. error		0.06	0.05	0.03	0.03	0.02		
		Max-MEWMA	$E(T)$		101.44	60.91	55.17	53.87	52.97		
			$\bar{\hat{\tau}}$		49.97	49.87	49.61	49.69	49.70		
			Std. error		0.05	0.05	0.04	0.03	0.03		
		MELR	$E(T)$		60.00	56.30	54.06	53.27	52.50		
			$\bar{\hat{\tau}}$		50.24	49.47	49.42	49.48	49.52		
			Std. error		0.07	0.06	0.05	0.04	0.03		
		1.1	1.1	$\chi^2 - \mathbf{S} $	$E(T)$	109.49	82.23	69.50	57.79	54.98	52.84
					$\bar{\hat{\tau}}$	50.78	50.23	50.30	50.04	49.87	49.71
					Std. error	0.07	0.06	0.04	0.04	0.03	0.03
Max-MEWMA	$E(T)$			91.80	77.93	59.70	55.08	53.88	52.95		
	$\bar{\hat{\tau}}$			50.07	50.03	49.89	49.72	49.66	49.67		
	Std. error			0.07	0.06	0.05	0.04	0.04	0.03		
MELR	$E(T)$			60.21	58.86	55.85	53.83	53.12	52.42		
	$\bar{\hat{\tau}}$			50.61	50.15	49.67	49.36	49.37	49.47		
	Std. error			0.08	0.08	0.06	0.05	0.05	0.04		
1.1	1.3			$\chi^2 - \mathbf{S} $	$E(T)$	80.15	75.52	63.26	56.37	54.21	52.68
					$\bar{\hat{\tau}}$	50.56	50.34	50.24	49.97	49.86	49.72
					Std. error	0.07	0.06	0.04	0.04	0.04	0.02
		Max-MEWMA	$E(T)$	66.05	63.65	57.87	54.75	53.78	52.92		
			$\bar{\hat{\tau}}$	49.99	49.90	49.81	49.64	49.67	49.73		
			Std. error	0.06	0.06	0.05	0.04	0.04	0.03		
		MELR	$E(T)$	57.45	56.73	54.99	53.48	52.91	52.31		
			$\bar{\hat{\tau}}$	50.11	50.09	49.68	49.39	49.50	49.56		
			Std. error	0.07	0.07	0.06	0.05	0.04	0.03		
		1.3	1.5	$\chi^2 - \mathbf{S} $	$E(T)$	61.09	60.29	57.11	54.43	53.41	52.41
					$\bar{\hat{\tau}}$	49.95	50.01	49.87	49.86	49.69	49.66
					Std. error	0.07	0.05	0.05	0.04	0.04	0.03
Max-MEWMA	$E(T)$			56.25	55.97	55.05	55.02	53.35	52.75		
	$\bar{\hat{\tau}}$			49.50	49.54	49.63	49.42	49.62	49.78		
	Std. error			0.06	0.05	0.05	0.06	0.04	0.03		
MELR	$E(T)$			54.49	54.26	53.63	52.89	52.50	52.11		
	$\bar{\hat{\tau}}$			49.59	49.58	49.43	49.46	49.51	49.47		
	Std. error			0.06	0.06	0.06	0.05	0.04	0.04		

As this particular study aimed to show the accuracy performance of the change point estimator with various alternative charting schemes, $\bar{\hat{\tau}}$ should be close to 50. Table 4.1-4.3 show the accuracy results for different values of ρ_1 . The average of change point estimates ($\bar{\hat{\tau}}$), for all magnitudes of shift, are fairly close to the actual change point.

For example, when a shift setting $[\lambda_1, \lambda_2, \delta_1, \delta_2] = [0.25, 0.5, 1.3, 1.5]$ and $\rho_1 = 0.5$ are considered, the average change point estimates are 49.87, 49.63 and 49.43 for different control chart alternatives, from Table 4.2 respectively. The average run lengths after the signal provided by the control charts are 7.11, 5.05 and 3.63, respectively. If the magnitude of shift is relatively large, then the change point estimator gives similar results for every control chart alternative. The best ARL performance was mostly obtained with the MELR chart. However, if the magnitude of shift is small, then the change point estimation surprisingly differs. The procedures with the MELR charts produce the farthest change point estimation to the actual change point. For instance, when a shift setting $[\lambda_1, \lambda_2, \delta_1, \delta_2] = [0.0, 0.0, 1.1, 1.1]$ and $\rho_1 = 0.0$ are considered, the average change point estimates are 71.74, 66.36 and 75.75 for different control chart alternatives, respectively. This is most likely because there is more information available to estimate the change point when ARL is larger. For example in this case the ARL of the combination chart is 72.51 while the ARL of the MELR is 67.84. As the correlation between the variables increase, the run lengths of the control charts decrease and the accuracy performance increases for all procedures.

4.4.2 Precision Evaluation

The precision performance of the estimator with various control charts is also investigated. The three control chart options are considered and the results are compared for different magnitudes of shift settings. Generally, the precision performance of the change point estimator with the combination and Max-MEWMA charts are higher than the MELR chart scheme. This is probably because the MELR

chart has lower run length results than the others. As an alternative single multivariate control chart to the combination chart, Max-MEWMA has similar precision performance with the combination chart.

For example, when a shift setting $[\lambda_1, \lambda_2, \delta_1, \delta_2] = [1.0, 1.0, 1.3, 1.5]$ and $\rho_1 = 0.5$ are considered, the exact detection probabilities are 0.67, 0.67 and 0.64 for different monitoring procedures, respectively. The observed frequencies of the change point estimates which are within a given number of periods (k) of the actual change point are also obtained. The detection probabilities for the change point estimator for various control charts are shown in Table 4.4-4.6. When the magnitudes of shift for mean vector, covariance matrix and correlation coefficient increase, then the detection performances increase and the difference between them becomes unapparent.

Table 4.4 Empirical distribution of $\hat{\tau}$ around τ after $\chi^2 - |\mathbf{S}|$, Max-MEWMA and MELR control charts signal; $\tau = 50$, $\rho_1 = 0.0$ and 10,000 independent simulation runs

Covariance Shift Setting				Mean Shift Setting					
δ_1	δ_2	λ_1	λ_2	1	2	3	4	5	6
1	1	$\hat{P}(\hat{\tau} - \tau \leq 0)$	$\chi^2 - \mathbf{S} $	0.067	0.264	0.486	0.586	0.712	
			Max-MEWMA	0.056	0.220	0.437	0.550	0.705	
			MELR	0.052	0.215	0.428	0.557	0.686	
		$\hat{P}(\hat{\tau} - \tau \leq 1)$		0.146	0.467	0.717	0.816	0.895	
				0.136	0.407	0.671	0.766	0.876	
				0.122	0.398	0.656	0.774	0.871	
		$\hat{P}(\hat{\tau} - \tau \leq 5)$		0.349	0.782	0.947	0.970	0.980	
				0.333	0.726	0.911	0.951	0.972	
				0.297	0.724	0.914	0.950	0.964	
1.1	1.1	$\hat{P}(\hat{\tau} - \tau \leq 0)$	$\chi^2 - \mathbf{S} $	0.038	0.088	0.252	0.460	0.568	0.686
			Max-MEWMA	0.038	0.080	0.225	0.433	0.551	0.685
			MELR	0.031	0.077	0.218	0.417	0.535	0.675
		$\hat{P}(\hat{\tau} - \tau \leq 1)$		0.089	0.192	0.462	0.698	0.797	0.881
				0.090	0.182	0.415	0.660	0.763	0.868
				0.080	0.169	0.407	0.646	0.759	0.861
		$\hat{P}(\hat{\tau} - \tau \leq 5)$		0.231	0.432	0.778	0.939	0.967	0.974
				0.245	0.425	0.739	0.919	0.951	0.973
				0.211	0.398	0.740	0.909	0.949	0.968
1.1	1.3	$\hat{P}(\hat{\tau} - \tau \leq 0)$	$\chi^2 - \mathbf{S} $	0.140	0.182	0.302	0.463	0.592	0.688
			Max-MEWMA	0.137	0.163	0.273	0.453	0.550	0.682
			MELR	0.120	0.149	0.256	0.431	0.525	0.671
		$\hat{P}(\hat{\tau} - \tau \leq 1)$		0.281	0.344	0.520	0.710	0.812	0.881
				0.275	0.325	0.484	0.680	0.779	0.869
				0.253	0.294	0.464	0.665	0.752	0.862
		$\hat{P}(\hat{\tau} - \tau \leq 5)$		0.582	0.661	0.831	0.940	0.967	0.975
				0.572	0.632	0.804	0.922	0.953	0.970
				0.545	0.619	0.801	0.917	0.945	0.968
1.3	1.5	$\hat{P}(\hat{\tau} - \tau \leq 0)$	$\chi^2 - \mathbf{S} $	0.316	0.347	0.414	0.525	0.616	0.701
			Max-MEWMA	0.306	0.328	0.399	0.520	0.591	0.703
			MELR	0.293	0.306	0.376	0.499	0.571	0.676
		$\hat{P}(\hat{\tau} - \tau \leq 1)$		0.547	0.584	0.652	0.761	0.832	0.885
				0.526	0.552	0.633	0.752	0.807	0.886
				0.517	0.531	0.616	0.731	0.796	0.868
		$\hat{P}(\hat{\tau} - \tau \leq 5)$		0.851	0.872	0.911	0.949	0.964	0.974
				0.838	0.857	0.906	0.946	0.959	0.973
				0.834	0.857	0.905	0.941	0.954	0.967

Table 4.5 Empirical distribution of $\hat{\tau}$ around τ after $\chi^2 - |\mathbf{S}|$, Max-MEWMA and MELR control charts signal; $\tau = 50$, $\rho_1 = 0.5$ and 10,000 independent simulation runs

Covariance Shift Setting				Mean Shift Setting					
δ_1	δ_2	λ_1	λ_2	1	2	3	4	5	6
1	1	$\hat{P}(\hat{\tau} - \tau \leq 0)$	$\chi^2 - \mathbf{S} $	0.323	0.404	0.537	0.615	0.703	
			Max-MEWMA	0.317	0.384	0.505	0.599	0.699	
			MELR	0.250	0.335	0.477	0.572	0.675	
		$\hat{P}(\hat{\tau} - \tau \leq 1)$		0.552	0.645	0.775	0.836	0.895	
				0.544	0.621	0.737	0.818	0.882	
				0.451	0.558	0.709	0.793	0.866	
		$\hat{P}(\hat{\tau} - \tau \leq 5)$		0.853	0.919	0.968	0.979	0.982	
				0.849	0.895	0.950	0.969	0.978	
				0.775	0.859	0.932	0.958	0.968	
1.1	1.1	$\hat{P}(\hat{\tau} - \tau \leq 0)$	$\chi^2 - \mathbf{S} $	0.261	0.398	0.368	0.504	0.593	0.678
			Max-MEWMA	0.257	0.293	0.356	0.476	0.575	0.676
			MELR	0.209	0.234	0.317	0.452	0.552	0.648
		$\hat{P}(\hat{\tau} - \tau \leq 1)$		0.474	0.633	0.606	0.745	0.819	0.881
				0.471	0.526	0.592	0.713	0.797	0.868
				0.391	0.432	0.540	0.688	0.780	0.842
		$\hat{P}(\hat{\tau} - \tau \leq 5)$		0.798	0.908	0.897	0.961	0.972	0.980
				0.798	0.836	0.885	0.942	0.96	0.974
				0.719	0.770	0.858	0.928	0.952	0.962
1.1	1.3	$\hat{P}(\hat{\tau} - \tau \leq 0)$	$\chi^2 - \mathbf{S} $	0.297	0.316	0.392	0.392	0.499	0.670
			Max-MEWMA	0.286	0.306	0.372	0.486	0.560	0.667
			MELR	0.242	0.271	0.338	0.457	0.542	0.651
		$\hat{P}(\hat{\tau} - \tau \leq 1)$		0.510	0.546	0.625	0.627	0.739	0.873
				0.510	0.532	0.6035	0.721	0.794	0.866
				0.447	0.480	0.569	0.694	0.773	0.858
		$\hat{P}(\hat{\tau} - \tau \leq 5)$		0.834	0.858	0.904	0.908	0.955	0.978
				0.829	0.852	0.891	0.944	0.963	0.977
				0.782	0.821	0.875	0.931	0.953	0.968
1.3	1.5	$\hat{P}(\hat{\tau} - \tau \leq 0)$	$\chi^2 - \mathbf{S} $	0.384	0.414	0.466	0.535	0.611	0.676
			Max-MEWMA	0.377	0.399	0.441	0.444	0.585	0.675
			MELR	0.342	0.360	0.414	0.495	0.565	0.640
		$\hat{P}(\hat{\tau} - \tau \leq 1)$		0.639	0.656	0.709	0.779	0.830	0.874
				0.617	0.637	0.679	0.666	0.811	0.870
				0.579	0.597	0.654	0.740	0.800	0.849
		$\hat{P}(\hat{\tau} - \tau \leq 5)$		0.917	0.922	0.944	0.963	0.969	0.976
				0.893	0.909	0.925	0.917	0.963	0.978
				0.880	0.892	0.915	0.946	0.959	0.963

Table 4.6 Empirical distribution of $\hat{\tau}$ around τ after $\chi^2 - |\mathbf{S}|$, Max-MEWMA and MELR control charts signal; $\tau = 50$, $\rho_1 = 0.9$ and 10,000 independent simulation runs

Covariance Shift Setting				Mean Shift Setting					
δ_1	δ_2	λ_1	λ_2	1	2	3	4	5	6
1	1	$\hat{P}(\hat{\tau} - \tau \leq 0)$	$\chi^2 - \mathbf{S} $	0.844	0.843	0.846	0.863	0.863	
			Max-MEWMA	0.849	0.843	0.850	0.867	0.882	
			MELR	0.790	0.794	0.807	0.834	0.857	
		$\hat{P}(\hat{\tau} - \tau \leq 1)$		0.964	0.962	0.963	0.972	0.974	
				0.966	0.968	0.966	0.970	0.973	
				0.925	0.924	0.939	0.951	0.960	
		$\hat{P}(\hat{\tau} - \tau \leq 5)$		0.999	0.998	0.997	0.998	0.998	
				0.997	0.996	0.995	0.995	0.995	
				0.984	0.983	0.986	0.989	0.990	
1.1	1.1	$\hat{P}(\hat{\tau} - \tau \leq 0)$	$\chi^2 - \mathbf{S} $	0.822	0.826	0.814	0.830	0.845	0.857
			Max-MEWMA	0.824	0.833	0.825	0.832	0.849	0.863
			MELR	0.745	0.753	0.760	0.776	0.813	0.830
		$\hat{P}(\hat{\tau} - \tau \leq 1)$		0.957	0.956	0.956	0.961	0.967	0.970
				0.961	0.963	0.957	0.960	0.963	0.969
				0.901	0.911	0.912	0.925	0.942	0.952
		$\hat{P}(\hat{\tau} - \tau \leq 5)$		0.999	0.999	0.998	0.998	0.998	0.996
				0.996	0.996	0.995	0.995	0.995	0.996
				0.980	0.981	0.983	0.984	0.986	0.988
1.1	1.3	$\hat{P}(\hat{\tau} - \tau \leq 0)$	$\chi^2 - \mathbf{S} $	0.794	0.803	0.801	0.809	0.822	0.837
			Max-MEWMA	0.797	0.803	0.805	0.805	0.832	0.850
			MELR	0.729	0.729	0.733	0.762	0.793	0.814
		$\hat{P}(\hat{\tau} - \tau \leq 1)$		0.946	0.949	0.953	0.952	0.958	0.963
				0.944	0.949	0.949	0.948	0.959	0.962
				0.888	0.900	0.901	0.916	0.936	0.947
		$\hat{P}(\hat{\tau} - \tau \leq 5)$		0.997	0.998	0.998	0.997	0.996	0.996
				0.995	0.995	0.994	0.993	0.995	0.995
				0.976	0.980	0.980	0.981	0.985	0.988
1.3	1.5	$\hat{P}(\hat{\tau} - \tau \leq 0)$	$\chi^2 - \mathbf{S} $	0.760	0.409	0.774	0.782	0.800	0.819
			Max-MEWMA	0.755	0.759	0.762	0.789	0.806	0.825
			MELR	0.685	0.705	0.713	0.745	0.767	0.787
		$\hat{P}(\hat{\tau} - \tau \leq 1)$		0.935	0.653	0.938	0.943	0.952	0.957
				0.928	0.930	0.931	0.939	0.948	0.956
				0.881	0.890	0.890	0.910	0.922	0.935
		$\hat{P}(\hat{\tau} - \tau \leq 5)$		0.997	0.923	0.997	0.997	0.995	0.996
				0.992	0.992	0.994	0.994	0.995	0.995
				0.976	0.977	0.974	0.977	0.980	0.985

4.4.3 Confidence Sets Based on the Change Likelihood Function

The accuracy and precision evaluations showed that there is no best in our three monitoring approaches. If the process professionals target to detect small shifts quickly, then they would choose the MEWMA based control charts. As a result, they may not have better change point estimation performance. A solution to this problem can be the construction of some confidence region for the change point estimation. This way, the practitioners may investigate an interval or a set of possible change points. An empirical confidence interval can be constructed using the simulation result in part 4.4 as well. Constructing confidence sets for change point estimates were first introduced by Pignatiello and Samuel (2001). The confidence set of the multivariate joint change point estimator was constructed for the $\chi^2 - |\mathbf{S}|$ combination chart scheme by Dogu and Deveci-Kocakoc (2011b). The set of potential change points will help process professionals to focus on quick and correct identification of the special cause and taking appropriate actions when they use any control chart in order to obtain a signal of the change.

$$\ln(L(t)) = \frac{1}{2} \left(\text{tr} \left(\Sigma_0^{-1} \times \sum_{i=t+1}^T \sum_{j=1}^n (\mathbf{X}_{ij} - \boldsymbol{\mu}_0)' (\mathbf{X}_{ij} - \boldsymbol{\mu}_0) \right) \right) - \frac{n(T-t)}{2} \log_e \left(\frac{\det \left[\sum_{i=t+1}^T \sum_{j=1}^n (\mathbf{X}_{ij} - \bar{\mathbf{X}}_{T,t}) (\mathbf{X}_{ij} - \bar{\mathbf{X}}_{T,t})' \right]}{n(T-t) |\Sigma_0|} \right) - \frac{np(T-t)}{2}$$

is the value of log likelihood function at t , and D is the reference value to develop a $100(1-\alpha)\%$ confidence set. Pignatiello and Samuel (2001) used an interval of reference value where the lower limit is Box and Cox's (1964) proposal and the upper limit is Siegmund's (1986) proposal for a 90% confidence set.

If $\ln(L(t))$ exceeds the limit of $\ln(L(\hat{\tau})) - D$, then t is a candidate change point. We considered a set of reference values as $D = \{1.353, 1.5, 2.00, 2.5, 2.97\}$ and investigated the coverage probabilities of each shift setting for each control chart option we used. The coverage probability represents the percentage of the sets which

include the exact change point within 10,000 simulation runs. Also the sizes (cardinality) of the sets are recorded (See Table 4.7-4.8).

We noted that, however, the ARL for the combination chart is larger than the other single charts, the cardinalities and coverage probabilities of confidence sets are generally smaller. This situation is more obvious when the magnitude of shift is small. When the magnitude of shift is greater than 0.5 for mean vector and covariance matrix, the results for different monitoring schemes become similar. Considering the tables, the largest critical value ($D=2.97$) satisfies approximately 90% confidence region for mean shifts greater than 0.5 (for any covariance shift).

Table 4.7 Average cardinality and coverage probability values obtained using different critical Values (D) after $\chi^2 - |\mathbf{S}|$, Max-MEWMA and MELR control charts signal; $\tau = 50$, mean shift setting 3 and 4 and 10,000 independent simulation runs

δ_1	δ_2	D		λ_1					λ_2				
				1.35	1.50	2.00	2.50	2.97	1.35	1.50	2.00	2.50	2.97
1	1	A. Cardinality	$\chi^2 - \mathbf{S} $	2.80	3.05	3.96	4.92	5.90	2.05	2.20	2.76	3.40	4.08
				0.70	0.73	0.79	0.84	0.88	0.75	0.77	0.82	0.86	0.89
		C. Probability	Max-MEWMA	2.98	3.27	4.33	5.54	6.77	2.28	2.48	3.20	4.03	4.92
				0.68	0.71	0.78	0.84	0.88	0.73	0.75	0.81	0.86	0.89
			MELR	3.02	3.34	4.54	6.01	7.58	2.38	2.59	3.41	4.37	5.46
				0.61	0.63	0.71	0.78	0.83	0.70	0.72	0.78	0.83	0.87
1.1	1.1	A. Cardinality	$\chi^2 - \mathbf{S} $	2.94	3.22	4.22	5.33	6.48	2.17	2.34	2.99	3.73	4.54
				0.66	0.69	0.76	0.82	0.86	0.72	0.74	0.80	0.85	0.88
		C. Probability	Max-MEWMA	3.13	3.45	4.64	5.97	7.33	2.36	2.56	3.36	4.27	5.25
				0.65	0.68	0.76	0.82	0.86	0.70	0.72	0.79	0.84	0.88
			MELR	3.09	3.42	4.70	6.20	7.83	2.46	2.68	3.57	4.63	5.79
				0.59	0.61	0.69	0.76	0.81	0.68	0.70	0.76	0.81	0.86
1.1	1.3	A. Cardinality	$\chi^2 - \mathbf{S} $	2.78	3.05	4.03	5.15	6.28	2.19	2.36	3.05	3.83	4.68
				0.67	0.69	0.76	0.82	0.86	0.71	0.73	0.79	0.83	0.87
		C. Probability	Max-MEWMA	3.03	3.34	4.49	5.82	7.19	2.39	2.60	3.42	4.36	5.37
				0.66	0.68	0.76	0.81	0.86	0.71	0.73	0.80	0.84	0.88
			MELR	3.00	3.31	4.55	6.00	7.58	2.43	2.65	3.53	4.57	5.72
				0.59	0.62	0.69	0.76	0.81	0.67	0.69	0.75	0.81	0.85
1.3	1.5	A. Cardinality	$\chi^2 - \mathbf{S} $	2.51	2.74	3.66	4.70	5.81	2.12	2.29	2.98	3.80	4.68
				0.70	0.72	0.78	0.83	0.87	0.73	0.75	0.80	0.85	0.88
		C. Probability	Max-MEWMA	2.68	2.94	3.99	5.18	6.44	2.56	2.82	3.83	5.03	6.36
				0.69	0.71	0.78	0.83	0.87	0.68	0.71	0.77	0.83	0.87
			MELR	2.63	2.90	3.93	5.17	6.50	2.28	2.49	3.32	4.30	5.38
				0.65	0.67	0.74	0.80	0.84	0.69	0.70	0.76	0.82	0.86

Table 4.8 Average Cardinality and Coverage Probability Values Obtained Using Different Critical Values (D) after $\chi^2 - |\mathbf{S}|$, Max-MEWMA and MELR control charts signal; $\tau = 50$, mean shift setting 5 and 6 and 10,000 Independent Simulation Runs

		λ_1	0.5					1							
		λ_2	1					1							
δ_1	δ_2	D	1.35	1.50	2.00	2.50	2.97	1.35	1.50	2.00	2.50	2.97			
1	1	A. Cardinality	$\chi^2 - \mathbf{S} $	1.80	1.91	2.34	2.86	3.41	1.62	1.72	2.07	2.52	3.04		
		C. Probability		0.79	0.81	0.85	0.88	0.91	0.84	0.86	0.89	0.91	0.93		
			Max-MEWMA	1.93	2.07	2.61	3.25	3.95	1.68	1.78	2.17	2.65	3.17		
				0.78	0.80	0.84	0.88	0.91	0.84	0.85	0.89	0.91	0.93		
			MELR	2.03	2.19	2.81	3.56	4.40	1.75	1.87	2.31	2.85	3.46		
				0.76	0.78	0.83	0.86	0.90	0.82	0.83	0.87	0.90	0.92		
		1.1	1.1	A. Cardinality	$\chi^2 - \mathbf{S} $	1.97	2.04	2.55	3.14	3.80	1.71	1.82	2.23	2.75	3.32
				C. Probability		0.78	0.79	0.84	0.87	0.90	0.83	0.84	0.87	0.90	0.92
					Max-MEWMA	2.04	2.20	2.79	3.49	4.27	1.75	1.86	2.30	2.83	3.42
						0.77	0.79	0.84	0.88	0.91	0.82	0.83	0.87	0.90	0.92
	MELR			2.10	2.28	2.94	3.75	4.66	1.85	1.98	2.50	3.12	3.81		
				0.74	0.76	0.81	0.85	0.89	0.80	0.81	0.85	0.88	0.91		
1.1	1.3			A. Cardinality	$\chi^2 - \mathbf{S} $	1.93	2.06	2.60	3.24	3.94	1.72	1.83	2.23	2.76	3.37
				C. Probability		0.77	0.78	0.83	0.87	0.89	0.82	0.83	0.87	0.90	0.92
					Max-MEWMA	2.05	2.21	2.84	3.58	4.37	1.76	1.87	2.31	2.85	3.42
						0.76	0.77	0.82	0.86	0.89	0.82	0.83	0.87	0.90	0.92
			MELR	2.10	2.28	2.96	3.77	4.68	1.82	1.95	2.45	3.05	3.70		
				0.73	0.75	0.80	0.84	0.88	0.80	0.81	0.85	0.88	0.91		
		1.3	1.5	A. Cardinality	$\chi^2 - \mathbf{S} $	1.93	2.07	2.66	3.36	4.11	1.72	1.84	2.31	2.88	3.52
				C. Probability		0.77	0.79	0.84	0.87	0.90	0.81	0.83	0.86	0.89	0.92
					Max-MEWMA	2.00	2.16	2.77	3.50	4.28	1.71	1.82	2.25	2.77	3.35
						0.77	0.78	0.84	0.88	0.90	0.81	0.83	0.86	0.89	0.92
	MELR			2.06	2.24	2.90	3.72	4.61	1.87	2.01	2.54	3.18	3.91		
				0.75	0.77	0.81	0.85	0.88	0.79	0.81	0.85	0.88	0.91		

4.4.4 Comparison with Generalized Likelihood Ratio Test Statistics based Change Point Estimator

Another most widely used change point estimation procedure is to perform sequential likelihood ratio tests and find the maximum of these statistics. The problem of simultaneous changes in the mean vector and covariance matrix of a Gaussian model was studied by Chen and Gupta (2000). They noted that instead of using the usual GLR test statistic, one can use the log likelihood statistic:

$$\hat{\tau}_{GLR} = \left(\max_{0 < t < T} \left(\log \frac{|\hat{\Sigma}|^T}{|\hat{\Sigma}_0|^t |\hat{\Sigma}_1|^{T-t}} \right) \right)^{\frac{1}{2}}, \quad (4.3)$$

$$\text{where } \hat{\boldsymbol{\mu}}_0 = \bar{\bar{\mathbf{X}}}_{0,t} = \frac{1}{t} \sum_{i=1}^t \bar{\mathbf{X}}_{i,j}, \quad \hat{\boldsymbol{\mu}}_1 = \bar{\bar{\mathbf{X}}}_{t,T} = \frac{1}{T-t} \sum_{i=t+1}^T \bar{\mathbf{X}}_i,$$

$$\hat{\Sigma}_0 = \frac{1}{n(t)} \sum_{i=1}^t \sum_{j=1}^n (\mathbf{x}_{ij} - \hat{\boldsymbol{\mu}}_0)' (\mathbf{x}_{ij} - \hat{\boldsymbol{\mu}}_0), \quad \hat{\Sigma}_1 = \frac{1}{n(T-t)} \sum_{i=t+1}^T \sum_{j=1}^n (\mathbf{x}_{ij} - \hat{\boldsymbol{\mu}}_1)' (\mathbf{x}_{ij} - \hat{\boldsymbol{\mu}}_1),$$

$$\hat{\boldsymbol{\mu}} = \frac{1}{n} \sum_{i=1}^n \mathbf{X}_i, \quad \text{and} \quad \hat{\Sigma} = \frac{1}{n} \sum_{j=1}^n (\mathbf{x}_{ij} - \hat{\boldsymbol{\mu}})' (\mathbf{x}_{ij} - \hat{\boldsymbol{\mu}})$$

are the MLE's of mean vector and covariance matrix. The location of the change is estimated by $\hat{\tau}$, where $\hat{\tau}$ is the value of t such that $\hat{\tau}_{GLR}$ has its maximum. In our case, we will use this estimator in order to find out the special cause when a MELR chart generates a signal. The in-control ARL is set to 185 and the smoothing constant is chosen to as 0.2. As our focus is Phase II analysis of the processes, we use the known parameters of central tendency and dispersion. Here in our simulation study, the known parameters are $\boldsymbol{\mu}_0 = \mathbf{0}$ and $\boldsymbol{\Sigma}_0 = \mathbf{I}_p$.

Table 4.9 shows the accuracy results of these two estimators. Since GLR based estimator has similarities with the likelihood based estimation procedure in formulation, the results are fairly close. The MLE based procedure has a slightly better performance when the small covariance shifts are introduced. On the other hand, the GLR based procedure has a slightly better performance for small mean shifts. For the other cases, the two procedures have high detection capabilities. Table 4.10 shows the empirical distributions of these estimators around τ . The MLE based estimation procedure performs slightly better than the GLR based method, but this difference is less obvious when the magnitude of shift and correlation between variables increase. With pure statistical perspective, natural logarithm of likelihood ratio test statistics gives us a function which includes overall, pre and post shift covariances. The MLE of the change point simply contains pre and post shift probability distributions. The MLE based procedure may be criticized as the traditional distributional results of the change-point theory may not be applicable.

However, the distributional assumptions are enough to run these procedures for many applications of special cause identification.

Table 4.9 Expected time of a signal, average change point estimates for MLE and GLR and their standard errors after MELR control charts signal; $\tau = 50$, $\rho_1 = 0.0$ and 0.5 , 10,000 independent simulation runs

λ_1	λ_2	δ_1	δ_2	$\rho_1 = 0.0$			$\rho_1 = 0.5$		
				$E(T)$	$\bar{\tau}_{MC}$	$\bar{\tau}_{GLR}$	$E(T)$	$\bar{\tau}_{MC}$	$\bar{\tau}_{GLR}$
0.25	0	1	1	116.58	63.41	59.17	61.82	50.33	50.24
				0.60	0.27	0.28	0.07	0.07	0.09
0	0	1.25	1	83.50	57.03	63.62	59.94	50.45	50.38
				0.30	0.17	0.28	0.06	0.07	0.09
0.25	0.50	1	1	62.09	50.79	49.73	57.11	49.89	49.38
				0.08	0.07	0.10	0.04	0.05	0.07
0.5	1	1	1	53.99	49.51	49.14	53.50	49.54	49.22
				0.02	0.04	0.06	0.01	0.04	0.05
1	1	1	1	52.89	49.60	49.34	52.67	49.56	49.37
				0.01	0.03	0.04	0.01	0.03	0.04
0.25	0.50	1.30	1.50	54.69	49.83	49.31	53.93	49.71	49.20
				0.03	0.05	0.07	0.02	0.05	0.07
0.50	1	1.50	2	52.02	49.62	49.40	52.00	49.67	49.36
				0.01	0.03	0.04	0.01	0.03	0.05
0	0	1.30	1.50	56.50	49.98	49.41	54.89	49.75	49.31
				0.04	0.06	0.09	0.03	0.06	0.08
0	0	1.50	2	52.62	49.53	49.16	52.49	49.65	49.31
				0.01	0.04	0.06	0.01	0.04	0.05

A control chart also can be developed from the likelihood ratio test statistic. Sullivan and Woodall (2000) proposed a single multivariate control chart based on GLR for multivariate individual process readings. They used a similar statistic with Chen and Gupta (2000). They also divided the test statistics into a part for the mean shift and another part for the covariance shift. Their approach was able to detect the location of a shift, the presence of multiple changes and the type of the change (mean shift, covariance shift or combination shift). Zamba and Hawkins (2009) proposed a multivariate change point model through GLR statistics for estimating the change in mean vector and/or covariance structure. Their change point model is able to monitor short runs and unknown or not fully known parameter processes. A similar statistic also was used by Zamba and Hawkins (2009) and if the maximum of this statistic exceeds a threshold then a signal of the change is considered to be

generated. The point (t) such yields the maximum is diagnosed as the change point. This approach of change point detection may be criticized because of the computational work load. In this approach, the critical value or the threshold depends on the number of observations. Therefore, the threshold has to be recalculated as each new observation enters the monitoring system along with the control chart statistics and MLE of the change point.

Table 4.10 Empirical distributions of $\bar{\tau}_{MC}$ and $\bar{\tau}_{GLR}$ around τ after MELR chart signals; $\tau = 50$, $\rho_1 = 0.0$ and 0.5 , 10,000 independent simulation runs

λ_1	λ_2	δ_1	δ_2		$\rho_1 = 0.0$		$\rho_1 = 0.5$	
					$\bar{\tau}_{MC}$	$\bar{\tau}_{GLR}$	$\bar{\tau}_{MC}$	$\bar{\tau}_{GLR}$
0.25	0	1	1	$\hat{P}(\hat{\tau} - \tau \leq 0)$	0.051	0.049	0.259	0.237
				$\hat{P}(\hat{\tau} - \tau \leq 1)$	0.122	0.116	0.460	0.430
				$\hat{P}(\hat{\tau} - \tau \leq 5)$	0.306	0.288	0.784	0.746
				$\hat{P}(\hat{\tau} - \tau \leq 10)$	0.452	0.429	0.916	0.888
0.25	0.5	1	1	$\hat{P}(\hat{\tau} - \tau \leq 0)$	0.223	0.217	0.351	0.338
				$\hat{P}(\hat{\tau} - \tau \leq 1)$	0.417	0.402	0.578	0.558
				$\hat{P}(\hat{\tau} - \tau \leq 5)$	0.736	0.719	0.879	0.853
				$\hat{P}(\hat{\tau} - \tau \leq 10)$	0.894	0.871	0.959	0.942
0.5	1	1	1	$\hat{P}(\hat{\tau} - \tau \leq 0)$	0.563	0.556	0.576	0.568
				$\hat{P}(\hat{\tau} - \tau \leq 1)$	0.783	0.772	0.789	0.779
				$\hat{P}(\hat{\tau} - \tau \leq 5)$	0.955	0.946	0.960	0.951
				$\hat{P}(\hat{\tau} - \tau \leq 10)$	0.979	0.969	0.981	0.973
0.25	0.50	1.30	1.50	$\hat{P}(\hat{\tau} - \tau \leq 0)$	0.392	0.377	0.420	0.400
				$\hat{P}(\hat{\tau} - \tau \leq 1)$	0.627	0.601	0.663	0.638
				$\hat{P}(\hat{\tau} - \tau \leq 5)$	0.908	0.884	0.926	0.908
				$\hat{P}(\hat{\tau} - \tau \leq 10)$	0.968	0.951	0.971	0.956
0	0	1.25	1	$\hat{P}(\hat{\tau} - \tau \leq 0)$	0.083	0.064	0.241	0.218
				$\hat{P}(\hat{\tau} - \tau \leq 1)$	0.192	0.148	0.446	0.411
				$\hat{P}(\hat{\tau} - \tau \leq 5)$	0.438	0.348	0.770	0.721
				$\hat{P}(\hat{\tau} - \tau \leq 10)$	0.614	0.496	0.905	0.868
0	0	1.3	1.5	$\hat{P}(\hat{\tau} - \tau \leq 0)$	0.309	0.285	0.356	0.336
				$\hat{P}(\hat{\tau} - \tau \leq 1)$	0.528	0.490	0.592	0.562
				$\hat{P}(\hat{\tau} - \tau \leq 5)$	0.845	0.802	0.886	0.859
				$\hat{P}(\hat{\tau} - \tau \leq 10)$	0.942	0.914	0.959	0.942

4.5 Illustrative example

The change point estimation procedure is applied to a simulated data set to illustrate the practical use of control charts and the change point estimator. The change point estimation procedure is used under the assumption that the parameters are known. The illustration is for a bivariate data set and $n=4$. The in-control

parameters are $\boldsymbol{\mu}_0 = (0, 0)'$ and $\boldsymbol{\Sigma}_0 = \mathbf{I}_2$. The out-of-control parameters are $\boldsymbol{\mu}_1 = (0.5, 0)'$ and $\boldsymbol{\Sigma}_1 = [1.0 \ 0.5; 0.5 \ 1.0]$. In this example, a combination shift is introduced after the 50th observation vector. Data generation process stopped when the combination chart issued a signal. The combination chart issued its first signal at the 61st observation. We used this 61 process readings with the investigated control charts and change point estimators. $\chi^2 - |\mathbf{S}|$ combination chart is given in Figure 4.1.

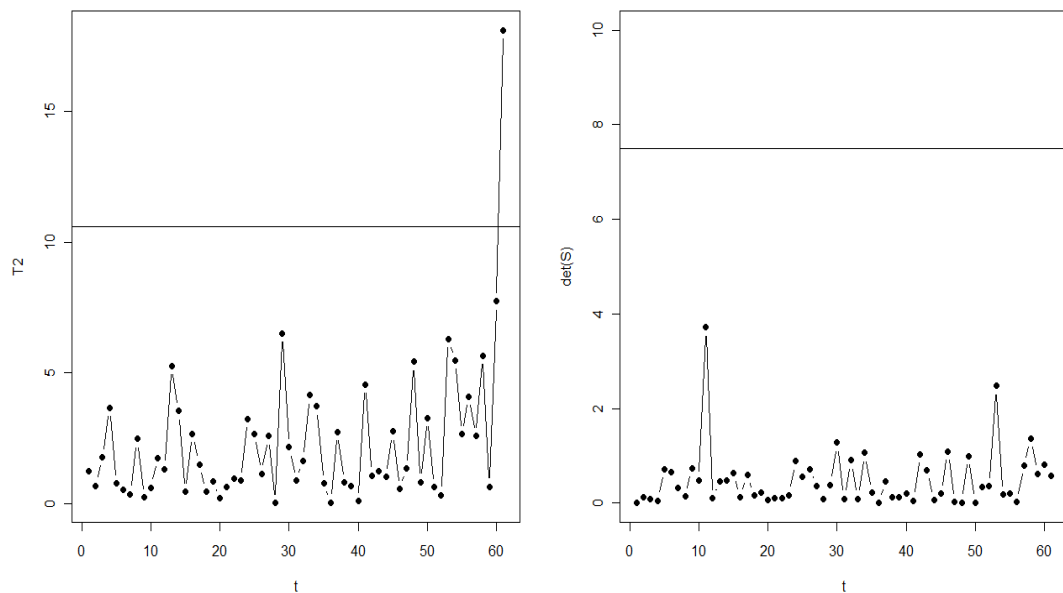


Figure 4.1 $\chi^2 - |\mathbf{S}|$ combination charts for the illustrative example

Figure 4.1 shows that the χ^2 control chart generated a signal at the 61st observation. After generating the first signal, the process was considered to be out-of-control and the time of the shift was investigated. Max-MEWMA control chart was also drawn for the same data set from (4.1). The Max-MEWMA control chart produced its first signal at the 58th process reading. Figure 4.2 shows diagnostic outputs (U and V) along with the Max-MEWMA control chart. After obtaining the signal we run the change point procedure with the Max-MEWMA control chart for the first 58 observations. Lastly, we used the same data set in order to show the

performance under the assumption that the signal was issued with the MELR control chart using (4.2). Figure 4.3 shows the MELR chart for the simulated data set.

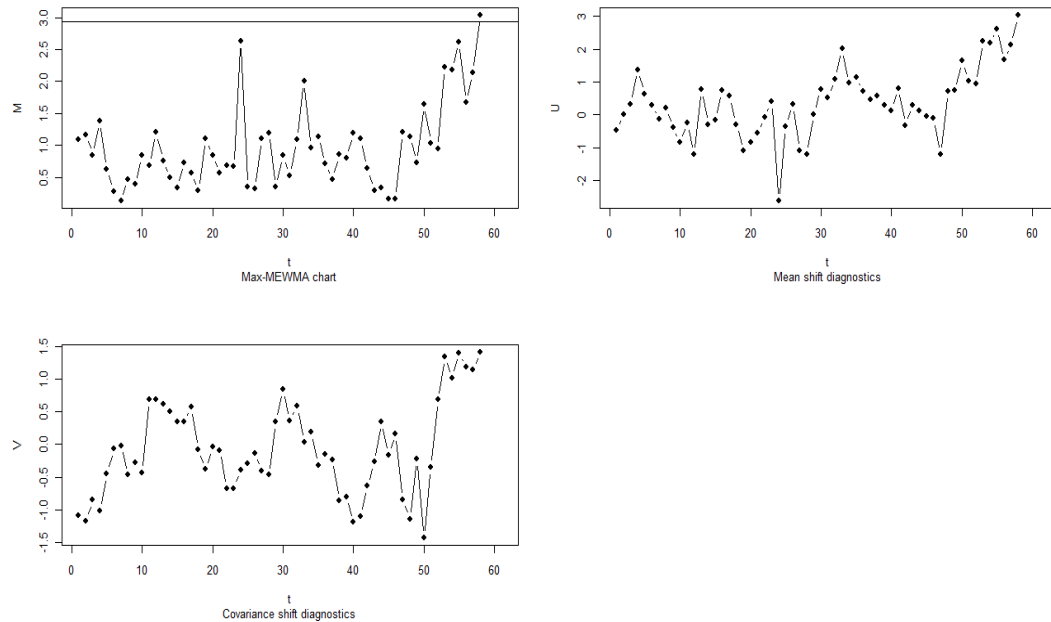


Figure 4.2 The Max-MEWMA control chart, mean shift and covariance shift monitoring statistics for the illustrative example

In Figure 4.3, like the Max-MEWMA control chart the first signal is issued after the 57th process reading. The add-on procedure was run and additionally GLR based estimation procedure was run for the first 58 observation vectors. Figure 4.4 shows the change point estimation results for $\chi^2 - |S|$ combination chart, the Max-MEWMA and the MELR control charts.

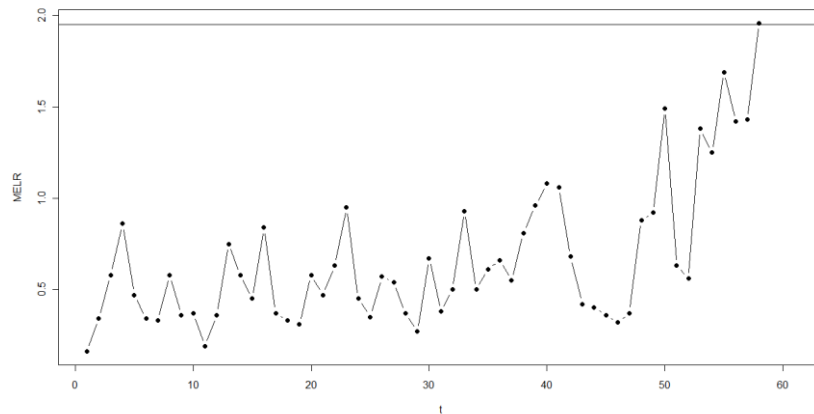


Figure 4.3 The MELR control chart, mean shift and covariance shift monitoring statistics for the illustrative example

Figure 4.4 includes the four versions of change point estimation. Looking closely to the results, one can easily interpret that the time where the likelihoods are maximum is around 50. Using the add-on procedure with the combination chart, the change was estimated to occur after the 50th observation. The same result was obtained with the procedure of the Max-MEWMA control chart. On the other hand, the procedure with the MELR control chart and the GLR based estimation procedure calculated with (4.3) showed that the change was after the 49th observation. As the information gathered from the process during applying different monitoring approaches is approximate, the plots are barely different. But the actual change point was estimated when using the combination chart and the Max-MEWMA control cart. While the MELR control chart provides no insight about the responsible of the shift, the combination and the Max-MEWMA control charts provided helpful diagnostics. The Max-MEWMA control chart diagnostics (U and V) shows a shift in mean vector and a slight shift in covariance matrix while the combination chart only showed a shift in mean vector. The Max-MEWMA reflected the actual case successfully and gave quick response to the shift.

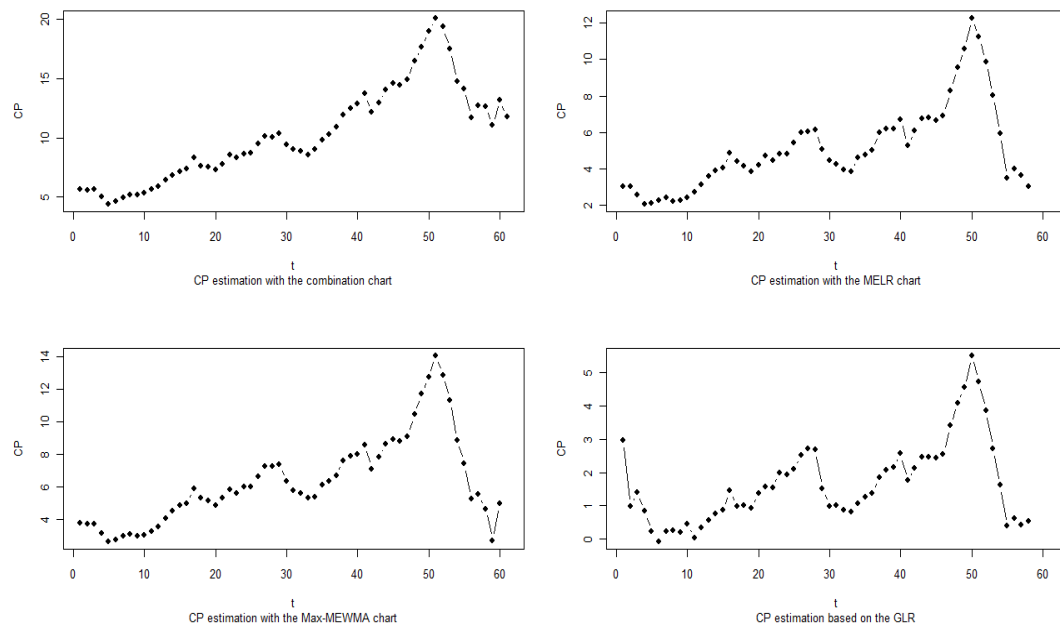


Figure 4.4 Plots of likelihood values at possible change points $\chi^2 - |\mathbf{S}|$ combination chart, the Max-MEWMA and the MELR control charts

4.6 Conclusions

Today, industrial processes produce huge amounts of data and joint assessment of multivariate process quality is needed for most of the cases. Since, there is an increasing pressure to produce high quality products and services, the practitioners need help to find out special causes of variability and identify the time of a small, moderate or large shift in mean and/or variability. The change point analysis with existing monitoring tools is a highly effective technique to investigate the special causes.

A follow-up change point estimation procedure for jointly monitoring the mean and covariance of a p -variate process is proposed by Dogu and Devenci-Kocakoc (2011b). In this study, we examined the performance of this estimation procedure under the assumption that the process is monitored with the $\chi^2 - |S|$ combination chart or multivariate single control charts. Since the performance with the combination chart is shown previously, we focused on the performance with the

multivariate single control chart alternatives and compared them. The single charts are easy to apply and visually attractive because one control chart is enough to jointly monitor the mean and variability. The two competing control charts are used in this study. These are the Max-MEWMA and the MELR control charts.

The proposed estimator is capable of detecting the step change successfully with all of the above control charts. The performance evaluation has shown that the change point formulation has high detection ability independently from control chart type. However, the performance is satisfactory for each monitoring approach, the combination chart has slightly better performance for small magnitudes of shift. This result raised here because the run length of the combination chart is greater than the others. This means that the change point procedure would run with a longer series of process readings. As the information gathered from the process increases, the better estimates are obtained. The change point procedure with multivariate single control charts does not have a better performance for small magnitudes of shift but they have their own advantages. Not estimating the change point for very small magnitudes of shift as accurate as the procedure with the combination chart is a result of the quick detection ability of the multivariate single control charts. Thus, the practitioner may spend effort to construct confidence sets for the change point and investigate this search window for the change point instead of inspecting more products or services. This approach obviously would save time, and man-power for inspection.

We used the likelihood functions of the pre and post shift distributions and followed the work of Pignatiello and Samuel (2001) to find the estimator. In the literature, change point theory widely uses the likelihood ratio test statistics. Thus, we compared the two approaches of change point estimation. Even though, the two estimators have similar accuracies, MLE based change point estimation procedure is slightly more precise than the GLR based approach. An illustrative example is given to indicate the practical use of the change point estimator with multivariate single control charts. This hypothetical example indicates the ease of implementation and

interpretation of the control charts with the change point procedure for jointly monitoring mean and variability.

CHAPTER FIVE

CONCLUSIONS

The primary objective of this research was to develop new change point procedures for multivariate processes. Traditional way of looking for the special cause after a signal does not always work for many processes. More sophisticated tools are needed for better identification of the time of a special cause. The change point analysis as an add-on procedure in SPC has been shown to be effective and successful for this purpose (see for example Samuel et al. (1998a, 1998b), Pignatiello and Samuel (2001), Nedumaran et al. (2000)). We focused on the multivariate frame and proposed change point procedures for well-known multivariate monitoring approaches in this research. After a signal is generated from a multivariate control chart, our proposed procedures are capable of detecting the time of a step change accurately and precisely.

Our first change point proposal was for the $|\mathbf{S}|$ control chart. Following the work of Nedumaran et al. (2000), we developed a multivariate change point procedure for only covariance shift assuming no mean shift. Our assumption here was that the shift occurred only in covariance matrix. We showed that our proposed procedure correctly detects a step change for small, moderate and large magnitudes of shift. The performance analysis was conducted under the assumption that the process was being monitored with a $|\mathbf{S}|$ control chart.

Another main objective in our study was to propose a procedure for simultaneous monitoring of mean vector and covariance matrix. Since the most widely used monitoring approach is a χ^2 and $|\mathbf{S}|$ combination chart, we developed a procedure for χ^2 and $|\mathbf{S}|$ combination chart. We showed that this procedure performs satisfactory in terms of accuracy and precision. The MLE of the process change point allows the construction of a confidence set on the true change point. This confidence set provides valuable knowledge and a search window to

process professionals in order to start looking for the exact time of the change. This set of possible candidates of change point helps the practitioner to identify the special cause easily. We constructed confidence sets for various reference values and showed that this approach is practical for joint estimation of a step change in multivariate setting.

Since a successful monitoring program requires monitoring mean and covariance shifts, the importance of simultaneously monitoring process mean and variability has been increased. On the other hand, the practice of combining existing control charts for mean and variability has been discussed to be unproductive and various multivariate single control charts proposed by Chen et al. (2005), Cheng and Thaga (2005), Thaga and Gabaitiri (2006) and Zhang et al. (2010). As this control charts have better performances than the traditional combination chart, our concern was to show the performance of the joint estimation procedure under the assumption that the process is being monitored with a multivariate single control chart. After conducting simulation studies for various shift combinations and magnitudes, we noted that the proposed joint estimator is capable of detecting the step change successfully with all the single charts. However the performance is satisfactory for each monitoring approach, the traditional combination chart has slightly better performance for small magnitudes of shift. The reason for this result was the better estimation of the parameters obtained from the data gathered from the procedure of combination chart. As the combination chart has long run lengths compared to the single charts, longer series of process readings are available. This surprising performance loss can be easily repaired using the confidence set along with the change point estimation. We conducted a simulation study and showed examples of the confidence sets and coverage probabilities for all the monitoring approaches.

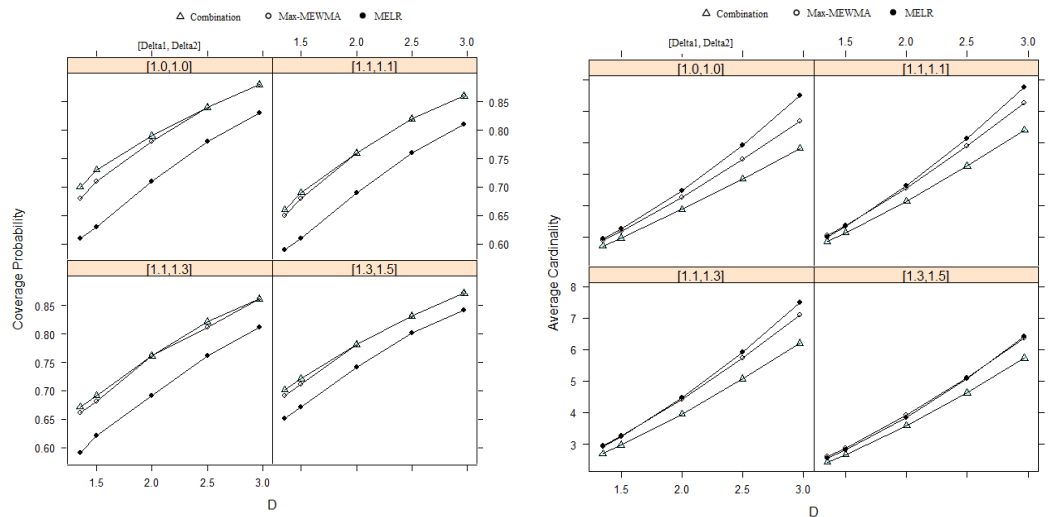


Figure 5.1 Plots of coverage probabilities and average cardinalities versus various references (D) for mean shift setting $\lambda = (0.25, 0.5)$; $\tau = 50$, $\rho = 0.5$ and 10,000 independent simulation runs

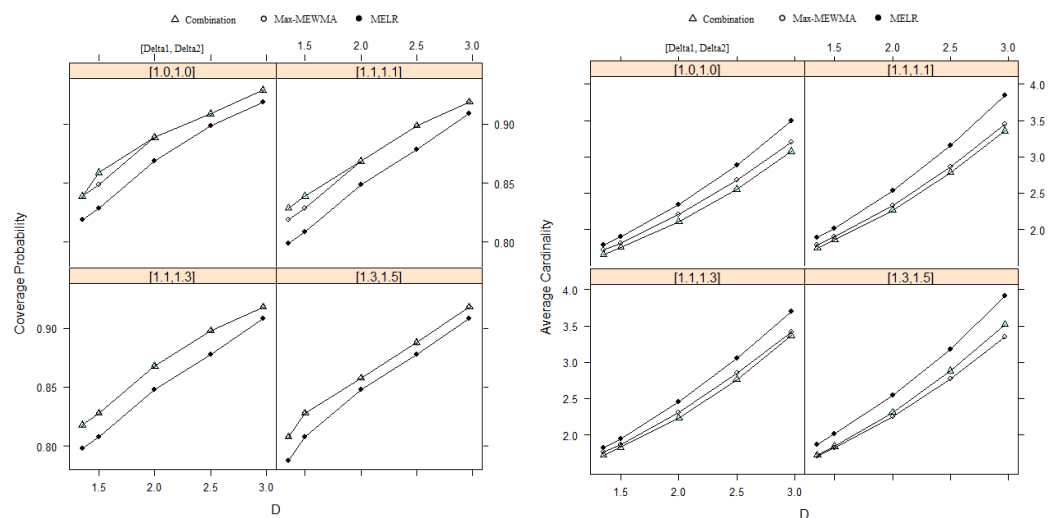


Figure 5.2 Plots of coverage probabilities and average cardinalities versus various references (D) for mean shift setting $\lambda = (1, 1)$; $\tau = 50$, $\rho = 0.5$ and 10,000 independent simulation runs

Figure 5.1 and 5.2 shows the average cardinality and coverage probability for each simulation setting and reference. If the reference value is chosen as 2.97, proposed by Siegmund (1986), then all of the procedures produce at least 80% coverage, and coverage probabilities are fairly similar. But this preference causes the cardinalities to get larger. The largest set lengths and the lowest coverage

probabilities were obtained when the procedure was run under the assumption that the monitoring tool was a MELR chart. Even though MELR chart quickly detects the change, this property affects the identification performance of the change point estimator. As a result, if process professionals prefer quick detection for small shifts, then they need to put more effort for exact special cause identification. In other words, they will have a wider search window to look for the special cause.

The procedure with χ^2 and $|\mathbf{S}|$ combination chart provides the shortest set lengths and highest coverage probabilities. This means that the change point estimator work best with the combination chart among these monitoring tools. The professionals will have a narrow search window and higher caption ability. On the other hand, combination charts have their own disadvantages. They are good at detecting large magnitudes of shift. In contrast, when the magnitude is small, then they could not respond quickly. The other disadvantage is that they need more resources such as professionals and time. If the process is stable then the professionals will have to run two separate control charts for a long period of time.

Another alternative monitoring tool is using the Max procedures. Max-MEWMA chart based procedure provides shorter set lengths and higher coverage probabilities compared to the procedure with MELR. If the assumption is that the monitoring tool is a Max-MEWMA chart, the results are similar to the one with the combination chart. While Max-MEWMA chart produces shorter run lengths than the combination chart, it also provides acceptable set lengths and coverage probabilities. This results show that if the practitioners are trying to detect small and moderate shifts, then using a Max-MEWMA chart with an add-on change point procedure is a preferable choice. Max-MEWMA based procedure practically gives quick signals and better change point detection performances. Moreover, it can provide diagnostics about the change. The control chart statistic can be partitioned and the user can figure out whether it is a mean shift, covariance shift or both. So the need for traditionally proposed approach of investigating separate univariate control charts for mean and variability becomes unnecessary.

Since our research problem was developing new multivariate change point schemes for SPC, we proposed two change point estimators. The first one was the covariance change only model and the second is the simultaneous change of mean vector and/or covariance matrix model. We showed that these estimators perform quite accurate and precise estimations for various magnitudes of shift. As our assumption is that the procedure starts after the control chart issues a signal, we investigated the performance of the joint estimation procedure for several control chart alternatives. We noted their advantages and disadvantages. The main performance criteria are the run lengths for control charts. The literature is rich in run length comparisons of various control charts for univariate and multivariate observations. Our study showed that looking only ARL may result in misleading control chart selection. We showed that the practitioner should evaluate the control charts via change detection, special cause identification, providing helpful diagnostics abilities rather than only detection ability. Strong quick detection ability may result in weak ability of assignable cause identification.

Our change point procedure was under the assumption that the process experiences a step change. Many industrial processes may experience a linear trend or more generally monotonic type changes. Future research can include an investigation for other types of change in multivariate setting. Here in this study, the application area was restricted to typical industrial processes, such as steel manufacturing. Recently many other areas of implementation are available. The application of these methods can be adapted to these areas such as health care delivery and financial analysis. The results of this research have been published in Dogu and Deveci-Kocakoc (2011a, 2011b).

Our estimation procedures are using pure statistical sense. Advanced estimation techniques to determine the change point can also be used. An increasing number of researches have been done about heuristic, neural network based or clustering based estimators (see Ghazanfari et al. (2008), Alaeddini et al. (2009), and Atashgar and Noorossana (2011)). Another interesting future research could be to propose new estimators and compare them with the existing methods.

One of our assumptions was that the process readings follow a multivariate normal distribution. For many industrial processes, this assumption may fail and the distribution may follow an unknown distribution or even we may not be able to define a distribution. In this case, a new future research area emerges. Dealing with distribution free change point detection methods for SPC can be a very attractive further research.

In order to construct a successful monitoring program, the process professional has to decide on many aspects and think about many process parameters. For example, in Six Sigma logic the main target is to reduce variability and the acceptable range of a quality characteristic is $\mu \pm 6\sigma$ while classical approach is to use $\mu \pm 3\sigma$ limits. Thus, the pressure to produce high quality products forces organizations to use more aggressive tolerance and specification limits. Nowadays, quickly eliminating the large shifts, quickly detecting small and moderate shifts and higher identification performance of the time of a shift, or in other words; correctly identifying the time of an assignable cause are vital. We believe that the change point estimation procedures, our investigation, and the results will be helpful for the practitioners for their process monitoring decisions.

REFERENCES

- Alaeddini, A., Ghazanfari, M. & Nayeri, M. A. (2009). A hybrid fuzzy-statistical clustering approach for estimating the time of changes in fixed and variable sampling control charts. *Information Sciences*, 179, 1769-1784.
- Alt, F. B. & Smith, N. D. (1988). Multivariate process control. In: P. R. Krishnaiah and C. R. Rao, eds. *Handbook of Statistics: Quality and Reliability*, 7, Amsterdam: North Holland, 333–351.
- Alt, F. B. (1985). Multivariate quality control. In: S. Kotz and N. L. Johnson, eds. *The Encyclopedia of Statistical Sciences*, 6, New York: Wiley, 110–122.
- Aparisi, F., Jabaloyes, J. & Carrion, A. (1999). Statistical properties of the $|S|$ multivariate control chart. *Communications in Statistics: Theory and Methods*, 28(11), 2671-2686.
- Aparisi, F., Jabaloyes, J. & Carrion, A. (2001). Generalized variance chart design with adaptive sample sizes: The bivariate case. *Communications in Statistics: Simulation and Computation*, 30(4), 931-948.
- Atashgar, K. and Noorossana, R. (2011). An integrating approach to root cause analysis of a bivariate mean vector with linear trend disturbance. *International Journal of Advanced Manufacturing Technology*, 52, 407-420.
- Bersimis, S., Psarakis, S. & Panaretos, J. (2007). Multivariate statistical process control charts: an overview. *Quality and Reliability Engineering International*, 23, 517-543.
- Chen, G., Cheng, S. W. & Xie, H. (2005). A new multivariate control chart for monitoring both location and dispersion. *Communications in Statistics - Simulation and Computation*, 33, 203–217.

- Chen, J. & Gupta, A. K. (2000). *Parametric Statistical Change Point Analysis*. Boston, Birkhauser, 86–95.
- Cheng, S. & Thaga, K. (2005). Multivariate Max-CUSUM chart. *Quality Technology and Quantitative Management*, 2(2), 221–235.
- Cheng, S. & Thaga, K. (2006). Single variables control charts: an overview. *Quality and Reliability Engineering International*, 22, 811–820.
- Costa, A. F. B. & Machado, M. A. G. (2009). A new chart based on sample variances for monitoring the covariance matrix of multivariate processes. *International Journal of Advanced Manufacturing Technology*, 41, 770-779.
- Djauhari, M. (2005). Improved monitoring of multivariate variability. *Journal of Quality Technology*, 37(1), 32–39.
- Djauhari, M., Mashuri, M. & Herwindiati, D. E. (2008). Multivariate process variability monitoring. *Communications in Statistics: Theory and Methods*, 37, 1742–1754.
- Dogu, E. & Deveci-Kocakoc, I. (2011a). Estimation of change point in generalized variance control chart. *Communications in Statistics - Simulation and Computation*, 40, 345–363.
- Dogu, E. & Deveci-Kocakoc, I. (2011b). A Multivariate Change Point Detection Procedure for Monitoring Mean and Covariance Simultaneously. (*Submitted to Communications in Statistics - Simulation and Computation*)
- Ghazanfari, M., Alaeddini, A., Niaki, S. T. A. & Aryanezhad M. B. (2008). A clustering approach to identify the time of a step change in Shewhart control charts. *Quality and Reliability Engineering International*, 24, 765–778.

- Hawkins, D. M. & Olwell, D. H. (1998). *Cumulative sum charts and charting for quality improvement*. Springer-Verlag: New-York, USA.
- Hinkley, D. V. (1970). Inference about the change point in a sequence of random variables. *Biometrika*, 57(1), 1-17.
- Khoo, M. B. C. & Quah, S. H. (2004). Alternatives to the multivariate control charts for process dispersion. *Quality Engineering*, 15(4), 639-642.
- Lee, J. & Park, C. (2007). Estimation of the change point in monitoring the process mean and variance. *Communications in Statistics - Simulation and Computation*, 36, 1333-1345.
- Levinson, W. A., Holmes, D. S., & Mergen, A. E. (2002). Variation chart for multivariate processes. *Quality Engineering*, 14(4), 539-545.
- Lowry, C. A. & Montgomery, D. C. (1995). A review of multivariate control charts. *IIE Transactions in IIE Research*, 27, 800-810.
- Machado, M. A. G., Costa, A. F. B. & Marins, F. A. S., 2009. Control charts for monitoring the mean vector and covariance matrix of bivariate processes. *International Journal of Advanced Manufacturing Technology*, 45, 772-785.
- Montgomery, D. C. (2009). *Introduction to statistical quality control* (6th edn). Wiley: New York, USA.
- Nedumaran, G., Pignatiello, J. J. JR. & Calvin, J. A. (2000). Identifying the time of a step-change with χ^2 control charts. *Quality Engineering*, 13(2), 153-159.
- Noorossana R., Saghaei A., Paynabar K. & Abdi S. (2009). Identifying the period of a step change in high-yield processes. *Quality and Reliability Engineering International*; 25,875-883.

- Park, J. & Park, S. (2004). Estimation of the change point in the \bar{X} and S control charts. *Communications in Statistics - Simulation and Computation*, 33(4), 1115–1132.
- Perry, M. B., Pignatiello J. J. JR & Simpson J. R. (2007). Change point estimation for monotonically changing Poisson rates in SPC. *International Journal of Production Research*, 45(8), 1791–1813.
- Perry, M. B., Pignatiello J. J. JR & Simpson J. R. (2007). Estimating the change-point of the process fraction nonconforming with a monotonic change disturbance in SPC. *Quality and Reliability Engineering International*, 23, 327–339.
- Perry, M. B., Pignatiello J. J. JR and Simpson J. R. (2005). Estimation of the change point of a Poisson rate parameter with a linear trend disturbance. *Quality and Reliability Engineering International*, 22(4), 371–384.
- Perry, M. B. & Pignatiello J. J. JR (2006). Estimation of the change point of a normal process mean with a linear trend disturbance. *Quality Technology and Quantitative Management*, 3(3), 325–334.
- Perry, M. B. & Pignatiello J. J. JR (2005). Estimation of the change point of the process fraction nonconforming in SPC applications. *International Journal of Reliability, Quality and Safety Engineering*, 12(2), 95–110.
- Perry M. B. (2010). Identifying the time of polynomial drift in the mean of autocorrelated processes. *Quality and Reliability Engineering International*, 26, 399–415.
- Pignatiello, J. J. JR. & Simpson, J. R (2002). A magnitude-robust control chart for monitoring and estimating step changes for normal process means. *Quality and Reliability Engineering International*, 18(6), 429–441.

- Pignatiello, J. J. JR. & Samuel, T. R. (2001). Estimation of the change point of a normal process mean in SPC applications. *Journal of Quality Technology*, 33(1), 82–95.
- Samuel, T. R., Pignatiello, J. J. JR. & Calvin, J. A. (1998a). Identifying the time of a step change with \bar{X} control charts. *Quality Engineering*, 10(3), 521–527.
- Samuel, T. R., Pignatiello, J. J. JR. & Calvin, J. A. (1998b). Identifying the time of a step change in a normal process variance, *Quality Engineering*, 10(3), 529–538.
- Samuel, T. R., Pignatiello, J. J. JR. & Calvin, J. A. (1998c). Identifying the time of a step change in a Poisson rate parameter, *Quality Engineering*, 10(3), 673–681.
- Sullivan, J. H. & Woodall, W. H. (2000). Change point detection of mean vector or covariance shifts using multivariate individual observations. *IIE Transactions*, 32, 537–549.
- Sullivan, J. H., Stoumbos, Z. G., Mason, R. L., & Young, J. C. (2007). Step-down analysis for changes in the covariance matrix and other parameters. *Journal of Quality Technology*, 39(1), 66–84.
- Surtihadi, J., Raghavachari, M. & Runger, G. (2004). Multivariate control charts for process dispersion. *International Journal of Production Research*, 42(15), 2993–3009.
- Thaga, K. & Gabaitiri, L. (2006). Multivariate Max-Chart. *Economic Quality Control*, 21(1), 113–125.
- Timmer, D. H. & Pignatiello J. J. JR (2003). Change point estimates for the parameters of an AR(1) process. *Quality and Reliability Engineering International*, 19(4), 355–369.

- Vargas, N. J. A. & Lagos C. J. (2007). Comparison of multivariate control charts for process dispersion. *Quality Engineering*, 19, 191–196.
- Woodall, H. W. (2000). Controversies and contractions in statistical process control. *Journal of Quality Technology*, 32(4), 341-350.
- Zamba, K. D. & Hawkins, D. M. (2006). A multivariate change point model for statistical process control. *Technometrics*, 48(4), 539-549.
- Zamba, K. D. & Hawkins, D. M. (2009). A multivariate change point model for change in mean vector and/or covariance structure. *Journal of Quality Technology*, 41(3), 285–303.
- Zhang, J., Li, Z. & Wang, Z. (2010). A multivariate control chart for simultaneously monitoring process mean and variability. *Computational Statistics and Data Analysis*, 54, 2244–2252.